STATISTICAL MECHANICS OF BIOLOGICAL MEMBRANES: PROTEIN AGGREGATION AND LIPID ORDERING

Thesis by

Jay Edelman

In Partial Fulfillment of the Requirements

for the Degree of

Doctor of Philosophy

California Institute of Technology

Pasadena, California

1978

(Submitted May 8, 1978)

ACKNOWLEDGEMENT

Many thanks to Sunney Chan for allowing me time to play with myriad incorrect models before stumbling into a worthwhile one, for suffering through innumerable versions of this thesis until I learned to write fluently, and for provoking me to connect my theoretical games to nature. Thanks also to Jean-Paul Revel for discussions about freeze-fracture microscopy, Michael Shantz for turning me on to the computer graphics, and Valerie Hu for unpublished data concerning protein effects on lipid phase transitions. Computer facilities were provided by the Bioinformation Systems Group, funded by NIH grants N503627 and E401822 and NSF grant MCS76-24562. I was supported primarily by USPHS fellowships.

ABSTRACT

It is known that membrane proteins are surrounded by a halo of perturbed lipids. When two protein particles approach one another, their effects are superimposed. This produces a force between them. We construct a Landau model of the membrane order parameter, and use it to calculate the interaction potential. Protein aggregation is predicted to be inherently favorable, though sometimes opposed by a barrier. Because experiments can be done only in large populations of particles, the theory is generalized to that situation. This allows us to calculate the protein chemical potential, and to study how the interaction between two given particles is modified by proximity to others. The protein diffusion equation predicts when the lipid-mediated forces lead to protein precipitation rather than a slight clustering tendency.

Next we turn to experimental tests, based on the protein pair correlation function. We describe its relation to the potential and develop a method for measuring it. We find a repulsion between protein particles, extending several nm beyond their apparent edges, and an attraction, extending 10 to 20 nm. The prediction of when precipitation occurs is shown to be at least qualitatively accurate.

The preceding analysis is primarily thermodynamic, and thus neglects molecular details. We next study them,

discovering that the behavior of our order parameter coincides with that of membrane thickness. On a molecular level, it can be controlled by either lipid conformation or tilt. After deriving the model from statistical mechanics, we find the former to be implausible, suggesting that tilt mediates protein interactions.

Lastly, the model is supplemented with a general description of lipid phase transitions. We find that it correctly predicts the phase behavior of protein-lipid systems. It also reveals that the usual analysis underestimates the amount of lipid perturbed by each protein particle. Furthermore, we demonstrate that those lipids are usually constrained between the disordered and ordered states, closer to the former.

CONTENTS

FREQUENTLY USED NOTATION

D	as a subscript, indicates value in disordered phase
D_s	$-2\ K_{2,0}/g'$
d_{ik}	separation between lipid molecules i and k
E_1	protein self energy, roughly $\pi K_1 \Delta^2$
$E^{(2)}$	see equation V.B.19 (page 164)
F	fraction of the phase transition remaining after proteins are incorporated into membrane
G	see equation II.B.6 (page 96)
g(R)	pair correlation function
g	Gibbs free energy density
g^o	g when $\varphi = \varphi_o$
g'	$\partial g_t / \partial T$ at T_t
g_t	$g_D^o - g_0^o$
H	see equation II.B.10 (page 96)
h	membrane thickness
h_o	equilibrium value of h
K_1	lipid elastic constant, see equation II.A.1 (page 67)
K_2	lipid elastic constant, see equation II.A.1 (page 67)
k_B	Boltzmann's constant
M_2	order parameter variance, see page 163
N	number of protein particles
n	see page 164
O	as a subscript, indicates value in ordered phase

OP order parameter

P_t probability that a C-C bond has trans conformation

R gas constant

$\vec{r}$ position in membrane

$\vec{r}_i$ location of protein particle i

r_o radius of protein particle

S_α conformational order parameter, see page 159

S_γ tilt order parameter, see page 159

T temperature

T_p transition temperature in protein-containing membrane

T_t transition temperature in protein-free membrane

t time

V potential energy

V_d see page 164

W see page 161

Y Young modulus, see page 157

Z partition function, see page 162

Δ $\bar{\Phi}-\Phi_o$

δ see equation VI.B.4 (page 181)

ε OP energy density, $g-g^o$, see equation II.A.1 (page 67)

$\langle\varepsilon\rangle$ mean of ε in protein-containing membrane

η reciprocal correlation length, $(K_2/K_1)^{\frac{1}{2}}$

λ matrix of λ_{ij}'s

λ_i $\exp(-\eta|\vec{r}-\vec{r}_i|)$

λ_{ij} $\exp(-\eta|\vec{r}_i-\vec{r}_j|)$

ρ number density of protein particles

ρ_e	ρ within protein precipitate
φ	order parameter
$\overline{\varphi}$	φ adjacent to protein
φ_D	φ_o in disordered phase
φ_0	φ_o in ordered phase
φ_o	equilibrium value of φ
φ_t	$\varphi_D - \varphi_0$
φ_p	$\langle\varphi\rangle_D - \langle\varphi\rangle_0$
$\langle\varphi\rangle$	mean of φ in protein-containing membrane

Note on Equation Numbering:

Equations are consecutively numbered within principal sections of each chapter. The section letter and usually the chapter number are appended to equation numbers when cited in other sections.

LIST OF FIGURES

I. INTRODUCTION

A. SIGNIFICANCE OF MEMBRANE PROTEIN INTERACTIONS

In the past few years, crosslinking[1-4] and electron microscopic[5] studies of membranes have provided a wealth of information about the organization of their proteins. Most analysis has been limited to small scale features, such as polypeptide folding and oligomer formation,[6,7] or to long range structure, such as the distribution of proteins between coexisting lipid phases.[8,9] The arrangement of protein particles among their neighbors has remained poorly characterized. Though they are known to form clusters,[10-13] the origin of their binding tendency has remained obscure. This stickiness should affect the morphology and elasticity of membranes, and the rate of collisions between membrane proteins. Lack of information about the forces between particles has hindered study of these issues. It is also unclear if the interactions of proteins with one another are related to those with lipids.[14-19] This paper shows that they are intimately connected. We predict that proteins which perturb lipids also tend to aggregate.

Though this attraction between proteins is an inevitable consequence of lipid perturbation, there is no guarantee that it is significant. Its influence will be suppressed by thermal motion if it is too weak. On the

other hand, it will be buried under the direct interactions between proteins when its range is too short. Our measurements clearly show that there is an attraction between proteins, whose range exceeds that of any previously known force between them. A basic question is whether it is correctly described by the model.

Unfortunately, there is presently no direct way to measure this force. We can observe only its consequences, most obviously, protein precipitation. After calculating when it occurs, we can compare our predictions with experiment. It will be seen that the model is at least qualitatively accurate.

Our techniques are probably unfamiliar to most readers, since the phenomena we study are generally considered insignificant. It may help to motivate the discussion by describing some possible biological applications of the model.

Membrane proteins are rearranged during many developmental processes: gap and tight junction formation,[18] thylakoid stacking,[19] the acrosome reaction,[20] and cilium formation.[21] The distribution of proteins between different membrane regions alters during various cellular shape changes, such as the discocyte to echinocyte transformation of red blood cells[22] and nerve growth cone formation.[23] The causes of these effects have remained mysterious. Our analysis of protein aggregation suggests

possible mechanisms.

Protein association is also important in membrane biochemistry. The negative cooperativity in the binding of many hormones to their membrane-linked receptors has been attributed to ligand-induced changes in the coupling of receptors to each other[24] or to adenylate cyclase.[25] Lack of information about protein clustering has complicated study of how hormones change it. Another example is hepatic cytochromes P450, whose pre-steady state kinetics have a fast phase followed by a slow one.[26,27] The former is ascribed to the interaction of P450 with initially nearby P450 reductase molecules, and the latter, with initially remote ones. "Nearby" has different meanings, depending on whether the proteins are clustered or randomly dispersed. It is unclear which is relevant. Micrococcus lysodeikticus NADH reductase also exhibits biphasic kinetics.[28] Here, the fast phase is assigned to the reaction of NADH with initially oxidized dehydrogenase molecules, and the slow phase, with ones that have diffused to and been reoxidized by cytochrome b_{556}. Ignorance about protein interactions has prevented interpretation of the rate constants. It is unknown whether the rate limiting step is protein collision or some subsequent redox reaction. Our model predicts that the binding of membrane proteins is inherently favorable, though retarded by a barrier. The rate and equilibrium of aggregation are calculable from the model.

Studies on the mechanics of the erythrocyte membrane have shown it to be a rubberlike solid.[29-33] This is so surprising in view of the fluid mosaic model[34,35] that lipids have been assumed to play a minor role in the mechanics of this membrane.[36-38] A protein network composed of spectrin[39] has instead been regarded as the source of its elasticity. However, spectrin is known to greatly affect the aggregation tendency of other membrane proteins.[40,41] We suggest that lipid-mediated interactions between proteins also can solidify membranes. Though there is no doubt that spectrin is important in the mechanics of the red cell membrane,[42,43] there is no evidence that the spectrin network itself supports external stresses.[44,45] The present model raises the possibility that the mechanical effects of spectrin arise from its interference with protein precipitation.

B. PROTEIN-LIPID INTERACTIONS

1. EXPERIMENTAL STUDIES

Recently, a variety of evidence has accumulated which shows that membrane proteins are surrounded by a "halo" or "annulus" of lipids which differ from those in the bulk of the membrane.[46] The best data have been gleaned from calorimetric studies of the lipid order-disorder transition. Usually, it becomes broader and its enthalpy linearly decreases with increasing protein concentration.[47] A new transition sometimes appears near the original one.[48,49] Fluorescent probe studies yield a similar picture.[50] These results show that proteins eliminate or modify the transition in the annulus.

The dependence of the transition enthalpy on the amount of protein can be used to estimate the area of the annulus. After making assumptions about the shape of the protein and its disposition in the membrane, one finds the number of layers of lipid molecules in the annulus, typically one to four. A similar analysis of protein effects on the phase boundaries of multicomponent membranes shows that some lipids are preferentially included in or excluded from the annulus.[51] Additional information about the halo is provided by membrane enzyme kinetics. Arrhenius plots often reveal a kink near, but not at, the transition temperature of the bulk lipids.[52-56] This too shows that the transition

temperature is shifted in the annulus. Studies of spin labels show that their orientational order parameters and correlation times are affected by proximity to proteins.[57-59]

The interpretation of these results has suggested that the perturbation is limited to the annulus. However, other evidence shows this to be unjustified. Freeze-fracture pictures of many membranes, including most where the annulus has been studied, reveal that the proteins usually precipitate when slowly cooled through the transition.[8,59-64] The lipids are thus divided between two phases. The "unperturbed" lipids are actually those of the protein-poor phase, while the annular lipids are those of the protein-rich one. The usual view of the halo incorrectly estimates its size. Furthermore, calorimetric studies show that the shape of the "unperturbed" transition is in fact changed by proteins.[47-49] Thus even the lipids in the protein-poor phase before melting are perturbed when the proteins are dispersed. The "width of the annulus" is hence only a lower bound.

2. THEORETICAL STUDIES

Since the configurational statistics of each hydrocarbon chain depend on those of its neighbors,[65-71] it is not likely that there is a sharp border between the perturbed lipids and the rest of the membrane. Instead, the effect gradually diminishes with increasing remoteness from each protein. In principle, one could find its distance dependence by a statistical mechanical analysis of the lipids. This is very difficult in practice, though. The problem is that the interaction between two molecules depends on the conformations of both. The total energy cannot be separated into a sum of single molecule energies. The number of states to be summed over thus rises exponentially with the number of molecules. Tractability requires limiting this sum to states of a single molecule, or approximating the interaction so that the summation can be done analytically. This has usually been done by absorbing the interactions into effective trans-gauche energy differences,[72-74] with mean field approximations,[75-77] or via highly simplified lattice models.[78-82] These methods require generalization when the lipid statistics are position dependent.

The most detailed analysis is that of Marčelja, based on the mean field approximation.[83] When summing over the states of each molecule, one guesses the average of its interactions with the others: the mean field. This

decouples the molecules from one another, so that their statistics can be studied individually. One then computes the mean interaction. Self consistency requires it to agree with the guess. The calculation is repeated until this is achieved. That is taken as the approximation to the interaction, or if there are several, the one that leads to the lowest total energy is taken.

In protein-free membranes, every molecule has the same mean field. Proteins change the configurational potential of neighboring lipids, however. The self consistent field is then different for each molecule. Calculating it yields the distance dependence of the protein effect. One finally computes the lipid-mediated interaction,[84] much as in the present model.

Although this approach is useful for studying particular microscopic models of protein-lipid interactions, it is inconvenient for getting a macroscopic picture of their consequences. Limitations of computer time prevent calculation of the protein chemical potential. Furthermore, it is still controversial which lipid degrees of freedom are most significantly influenced by proteins. It would be useful to have a thermodynamic model of the lipids not requiring such knowledge. We could then study the

macroscopic behavior of proteins. In chapter V we determine when the statistical model can be approximated by our thermodynamic one. In effect, we solve the self consistency equation, rather than guess its solution. This also leads to formulas expressing our empirical constants in terms of the more fundamental ones describing the interactions between lipid molecules. This will reveal the molecular basis of the model.

C. OVERVIEW OF THE MODEL

1. GOALS

When two protein particles approach one another, their influences on the lipids are superimposed. This restricts the perturbation to a smaller portion of the membrane, but may also augment it there. The former effect produces an attraction between the proteins; and the latter, a repulsion. We need to formulate the model more precisely before comparing them. A major goal of chapters II and III is development of theoretical and experimental methods for studying this interaction.

Depending on what questions one is asking, there are several levels on which protein-lipid interactions can be studied. Most fundamental is the use of statistical mechanics to describe both the lipids and proteins. Though necessary for a complete understanding of their interactions, this approach is inconvenient when analyzing their macroscopic behavior. We thus usually resort to a thermodynamic description of the lipids. This allows us to study protein statistical mechanics, approximating the lipid-mediated force with its expectation value. Our analysis begins at this level. We examine the validity of its assumptions in chapter V, when we derive this picture from its predecessor. However, even this scheme is too complicated for many purposes. We need a thermodynamic

description of the proteins to study their distribution within the membrane. In particular, we derive a diffusion equation for them, thus leading to predictions about when they precipitate.

2. ASSUMPTIONS

We first assume that the lipids have a degree of freedom, the order parameter (OP), which can be taken to represent their state. Its deviation from unconstrained equilibrium is a measure of how much they have been affected by proteins. There is no general reason to believe that a single order parameter suffices. We assume it does, though, since there is no evidence to the contrary. Possible candidates for the OP are membrane thickness, spectroscopic order parameters, and composition. However, it is described in primarily thermodynamic terms until chapter V. Its identity need not concern us here.

We next suppose that the lipids can be viewed as a continuum. This is reasonable when the OP is roughly constant over distances much larger than molecular spacings.

Finally, we need a formula for the dependence of the energy on the OP. Once we have that, the problem reduces to finding the OP which minimizes the energy, subject to the protein-imposed boundary conditions. We proceed in the spirit of the Landau theory of phase transitions.[85,86] This means that we approximate the energy density as a polynomial in the OP and its derivatives. While Taylor's theorem tells us that this is reasonable for sufficiently

small perturbations, there is no guarantee that it is for the ones actually encountered. Justifying it requires experimental tests.

This paper demonstrates that the simplest plausible implementation of these ideas is indeed useful as a membrane description. Though much of the theory has not yet been definitively tested, it will be seen useful at least as a first order description.

3. CONSEQUENCES

A basic quantity controlling protein behavior is the OP energy. It is the difference in Gibbs free energy between an actual membrane and one which is identical, except that its OP is unperturbed by proteins. Since we are concerned only with differences in OP energy, it does not matter if such a membrane really exists.

A simple measure of how much each protein particle affects the lipids is the self energy, the OP energy of a membrane containing a single particle. It is usually the only needed description of protein-lipid interactions.

The protein influence on the OP has a crucial consequence. Apposition of proteins merges their effects, thus shifting the energy because of its nonlinear dependence on the OP. The result is a force between them. The OP energy is the sum of their self energies when they are far apart. We take that as the reference state, so that the potential energy of any configuration is the OP energy minus the self energies. This choice is made purely for convenience, because only differences in potential are significant.

Ultimately, definitive testing of the model requires direct examination of the OP. Because it is controlled by the lipids, much of the information provided by this analysis is independent of the proteins.

However, many predictions are made about them too. The most basic concern their interactions, the subject of section II.A. There we consider membranes with only one or two protein particles. This is misleading though. Experiments can be done only in large populations of particles. Most measurable quantities depend on the protein chemical potential, rather than the interaction potential. Furthermore, the force between any two particles is modified when others are near them. Sections II.B.2 and 3 are devoted to these issues.

Though the lipid-mediated interaction usually produces protein clustering, only sometimes does it cause formation of a precipitate. In section II.B.4 we determine when that is.

Before making any specific predictions, we need to solve many theoretical problems. Chapter II is concerned mainly with mathematical consequences of the basic model. Experiments are mentioned only to the extent that their gross features show the model to bear at least some resemblance to nature. In chapter III we develop a technique needed to characterize protein clustering. It will be seen that there is a short range repulsion between proteins, in addition to the lipid-mediated attraction. In chapter IV we describe how the effects of these two

forces can be separated. We then measure the empirical constants in the theory, and test its predictions about protein precipitation.

In chapter V we present evidence suggesting that our OP is membrane thickness. We also derive the model from lipid statistical mechanics, thus revealing its molecular basis. We will find that lipid tilt, rather than conformation, controls the lipid-mediated force.

Much information about protein-lipid interactions has been obtained by studying how proteins affect the lipid phase transition, and how it influences their aggregation. In chapter VI, we successfully calculate these results, starting from data derived primarily from measurements of membrane elasticity. This further supports our identification of the OP with thickness. This analysis also reveals some errors in the usual notions concerning the size and structure of the halo of perturbed lipids.

Because our theoretical techniques are probably unfamiliar to most readers, we present some background in sections I.D and I.E. Rather than giving an abstract discussion, we study the appications of analogous methods to other problems in membrane biophysics.

Our measurements of protein clustering require observation of protein particles. This is done with freeze-fracture microscopy, which is described in section I.F.

D. MEMBRANE ELASTICITY THEORY

The previous applications of field theory to membrane biophysics have remained obscure, so that it is useful to review them. We consider only the chief features, using them to illustrate the motives for chosing field theory, and to introduce some necessary background. The discussion is limited to membrane bending, since that topic has been especially well studied. The history of this work also suggests how our model may eventually be definitively tested.

1. EQUILIBRIUM BENDING

We start with the static theory of membrane bending, which has been extensively studied by Helfrich.[88] In this model, shape is controlled by the curvature-dependence of the energy. Two approaches can be used to find this dependence: symmetry and stress-strain relations. Though both methods yield the same result, it is instructive to compare them. We can then study the shapes of actual membranes. In particular, we will see that the model correctly predicts the shape of red blood cells. It also suggests mechanisms for membrane shape changes. We consider only equilibrium shapes in this section. However, a slight generalization allows us to study nonequilibrium ones too. That is done in section I.D.2.

i. Bending Energy

The basic assumption is that the curvature energy can be expressed as the integral over the membrane of some energy density which, at each point, depends on the curvature there, and only there. This assumption is violated in some models[89-91] where the forces generating curvature arise outside the membrane. Its only real justification is that the theory agrees with experiment.

We next need a formula for the curvature energy density, w_c. Our goal is to find the simplest plausible one. We can then calculate its consequences and test them.

Consider some point in the membrane. Call $\vec{n}$ the unit vector normal to the membrane there. We define a local coordinate system by taking the z axis along $\vec{n}$, and x and y axes perpendicular to it and each other. Also set $n_{ij} = \partial n_i / \partial j$, where i=x, y, or z, and j=x or y. The reciprocal of n_{jj} is the radius of curvature in the j direction.

We are trying to express w_c in terms of the n_{ij}'s. We note the following simplifications. $\vec{n}$ specifies only the membrane orientation. The energy must not depend on it if the surrounding media are isotropic. w_c can thus depend on $\vec{n}$ only via its derivatives. Also, $\vec{n}$ is a unit vector, so that $n_{zj} = -n_{xj} - n_{yj}$ and we need not explicitly include the n_{zj}'s. Finally, w_c must be unchanged by

rotations around $\vec{n}$ if the membrane is uniaxial. Thus we need consider only combinations of n_{ij}'s which have this symmetry.

If w_c depends only on the first derivatives of $\vec{n}$, then it can be constructed only from the following:

$$n_{xx} + n_{yy} \qquad (1$$

$$n_{xy} - n_{yx} \qquad (2$$

$$n_{xx}n_{yy} - n_{xy}n_{yx} \qquad (3$$

However, n is perpendicular to the membrane. Expression 2 is thus everywhere zero because of Stokes theorem. It can be shown that the contribution of expression 3 to the total energy is shape-independent in closed vescicles.[88] It too can thus be ignored.

These arguments leave only expression 1. w_c must be at least a quadratic function of it: w_c needs to be minimized by some finite $n_{xx}+n_{yy}$ if there is to be an equilibrium state. The simplest plausible form for w_c is thus:

$$w_c = \tfrac{1}{2} K_c (n_{xx} + n_{yy} - C_o)^2 \qquad (4$$

The factor of $\frac{1}{2}$ is included only for later convenience. K_c is an elastic constant defined by this equation, and C_o is the equilibrium curvature. Addition of an arbitrary constant would have no significance: we care only about changes in w_c.

To find the curvature energy, E_c, of any membrane

configuration, one calculates w_c and integrates it over the membrane. The equilibrium shape is that which minimizes E_c. Finding it is simplified by guessing that it belongs to some family of functions characterized by a parameter, say s_2. The equilibrium can then be gotten by minimizing E_c with respect to s_2, provided that the guess is correct. This ignores the question of whether the arbitrary family includes the actual equilibrium, a complicated issue we will return to later.

A simple collection of membrane shapes consists of "ellipsoids" of revolution. We can specify them as follows. Let Θ be the angle between the symmetry axis and some line segment connecting the center of the ellipsoid to its surface. Then $r(\Theta)$, the length of the segment, is:

$$r(\theta) = r_o + \tfrac{1}{2} s_2 (3 \cos^2\Theta - 1) \qquad (5$$

s_2 is a measure of the eccentricity. To keep the surface area independent of s_2 we set:

$$r_o = r_o^* + \frac{1}{20} \frac{s_2^2}{r_o^*} + \ldots \qquad (6$$

where r_o^* is the radius of a sphere having the same surface area as the ellipsoid. We introduce the constant area condition because membrane dilation is energetically less favorable than bending. Unless geometric constraints require bending to cause stretching, diffusion of solvent across and of lipids within the

membrane relieves the stretching.

After calculating $\vec{n}$ from equation 5, we substitute it into the formula for w_c, and find E_c by integrating over the membrane. This yields:[88]

$$E_c = \frac{8\pi}{5} (6 - r_o C_o) K_c \left(\frac{s_2}{r_o} \right)^2 \qquad (7$$

We note that E_c is minimized by $s_2=0$ when $r_o C_o < 6$: the equilibrium shape is then spherical. On the other hand, no ellipsoid is stable when $r_o C_o > 6$: the membrane assumes some other shape.

By coupling the membrane to its environment, we can study external influences on its shape. One possibility is a pressure difference, ΔP, across it. The deformations occur with constant surface area, so that solvent must permeate the membrane. The free energy change is $V\Delta P \equiv E_V$ when a volume V is transferred. After calculating V, we find the bending energy in this case:[88]

$$E_c + E_V = \frac{4\pi}{5} (\Delta P_c - \Delta P) r_o s_2^2 \qquad (8$$

where:

$$P_c = \frac{2K_c}{r_o^3} (6 - C_o r_o) \qquad (9$$

The equilibrium shape is spherical if $\Delta P < \Delta P_c$. Otherwise, no ellipsoid is stable. One can use a similar analysis to study the effects of external magnetic[92] or electric[93] fields on the vescicle. They deform it, but do not destroy

the stability of ellipsoidal shapes.

Our assumption about the shape is usually only an approximation, seriously wrong for certain values of C_o and ΔP. We need the actual equilibrium shape for experimental tests. The preceding analysis is useful for illustrating the model, though. In particular, it shows that C_o, K_c, and ΔP are important determinants of membrane shape. Before describing the experiments which make the model credible, it is useful to reformulate it, emphasizing different features than before.

ii. Thermodynamic Significance

C_o must be zero in a symmetric membrane, one where both monolayers are the same and face identical solutions. Any asymmetry in the membrane or its environment can make C_o nonzero, thus potentially affecting membrane shape. The following thermodynamic analysis allows us to study this and to rederive equation 4 very differently than before.

We picture the membrane as two apposed slabs of continuous material. We assume they cannot slide over one another: the analysis becomes more complicated when they can, but yields a comparable result.[94] When an originally flat membrane bends, the outer surface area of each slab changes by some factor, say $1+\alpha$. This deformation changes the membrane energy. We want to know how much. If the interface between the slabs remains constant in area, straightforward geometry shows:

$$\alpha^u = h^u (n_{xx} + n_{yy}) \qquad (10$$

$$\alpha^l = -h^l (n_{xx} + n_{yy}) \qquad (11$$

The superscripts "u" and "l" refer to the two slabs, where $\vec{n}$ is directed towards the "u" side. h^u and h^l are the thicknesses of the slabs. We have assumed that the h's are much smaller than the radius of curvature. We can thus

expand the tension, T, in each slab as a Taylor series in α:

$$T^q = \gamma^q + \alpha^q K^q + \ldots \quad (q="u","l") \qquad (12$$

γ is the interfacial tension, and K, the compression modulus. We ignore shear deformations, so that T is isotropic.

The difference in bending energy between any two configurations, "i" and "f" is:[95]

$$\Delta w_c = \int_i^f \left[T^u \, d\alpha^u + T^l \, d\alpha^l \right] \qquad (13$$

A more careful analysis than we have done here shows that[94] $h^u/h^l = K^l/K^u$. Combining this with equations 10 through 13, we recover equation 4 and find:

$$C_o = \left(\frac{\gamma^u}{K^u} - \frac{\gamma^l}{K^l} \right)/h \qquad (14$$

and

$$K_c = h^2 \left(\frac{K^u K^l}{K^u + K^l} \right) \qquad (15$$

where $h = h^u + h^l$ is the membrane thickness.

In a symmetric membrane, $\gamma^u = \gamma^l$ and $K^u = K^l$, so that $C_o = 0$. The Gibbs adsorption equation[96] shows that anything which binds to or dissolves in the membrane can change γ and K. If it does so preferentially in one monolayer, it can produce curvature. This has been suggested to be the mechanism by which some drugs affect erythrocyte shape,[97] and transmembrane gradients of calcium ions break black lipid membranes.[98]

Since γ is a function of lipid composition, C_o can also be made nonzero by asymmetry in lipid distribution between the two monolayers. Experimental measurements show that curvature affects the equilibrium lipid distribution.[99-101] However, this is equivalent because of the Maxwell relation $\partial \mu_i / \partial A = \partial \gamma / \partial N_i$, where A is the membrane area, and μ_i and N_i are the chemical potential and number of species "i" molecules in the membrane. Natural membranes are known to have asymmetric lipid distributions,[102,103] so that this effect may be important in them too. This has not yet been studied though. The binding of polyvalent ligands to one monolayer can also change its interfacial tension. This has been suggested to be the mechanism of endocytosis and virus budding.[104]

When the constituent molecules can migrate between the monolayers, the curvature-dependence of their equilibrium distribution makes C_o change with time. In a membrane constrained to have some particular curvature, C_o approaches $n_{xx}+n_{yy}$. This relieves the curvature stress.[105] However, the relaxation occurs much more slowly than does bending, and can thus usually be ignored.

So far, we have assumed that the monolayers are uniform throughout their thickness. This neglects differences between the hydrocarbon and polar regions, which give each monolayer an intrinsic curvature.[106,107]

This effect cancels out in symmetric membranes, however. More generally, it makes γ^q and K^q (q="u","l") depend explicitly on $n_{xx}+n_{yy}$. This makes the theory more complicated, but adds no new physical content at the present stage of analysis.

iii. Field Equation

The preceding discussion considered mainly the energy density. One needs the membrane shape to calculate the total energy. For simplicity, we arbitrarily chose a simple family of shapes, and compared their energies. Though convenient for illustration, this has no real justification. We now discuss the systematic computation of shape. The procedure is to derive a differential equation whose solution is the desired shape. One can then study actual membranes. We will see that the model correctly predicts the shape of red blood cells.

Discussion of how the differential equation is derived will be deferred until section I.E. Here we consider only its solutions.

So far, we have cared only about small portions of the membrane, so that it was convenient to use a local coordinate system around each point. However, it is expedient to use the same coordinates everywhere when studying the overall shape. Two coordinates suffice if we consider only axially symmetric shapes. Let z refer to distance along the symmetry axis, and x, in a perpendicular direction. Then call $z(x)$ the distance from the x axis to the membrane at x. Also let $\Psi(x)$ denote the angle between the symmetry axis and $\vec{n}$. These definitions are shown in

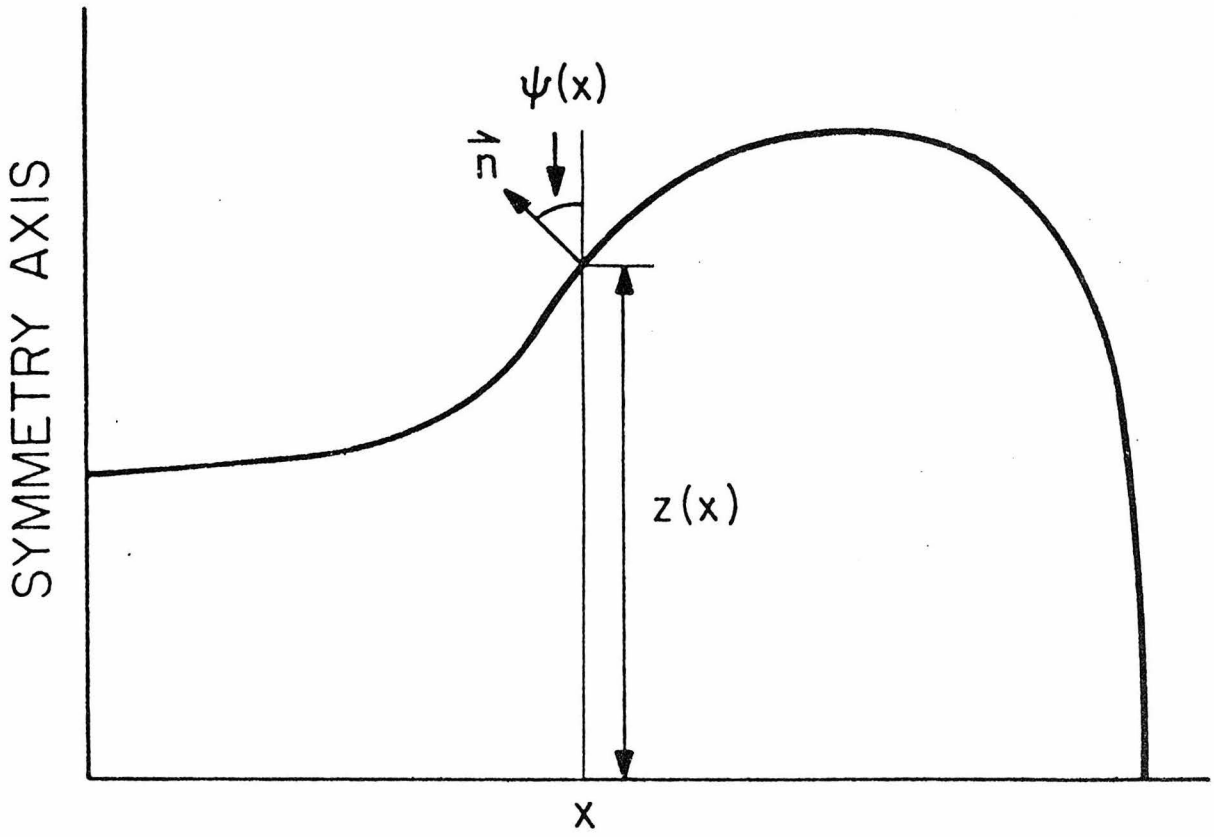

1. Definitions of ψ and z.

figure 1. It can be proved that $n_{xx}+n_{yy} = c_p+c_m$, where:[88]

$$c_p = \sin(\Psi)/x \qquad \text{and} \qquad c_m = \cos(\Psi)\,\frac{d\Psi}{dx} \tag{16}$$

c_m and c_p are the curvatures in the directions of meridians and parallels respectively. It immediately follows that:

$$\frac{dc_p}{dx} = \frac{c_m - c_p}{x} \tag{17}$$

By minimizing the energy, we obtain:[108]

$$\frac{dc_m}{dx} = \frac{x}{1-x^2c_p^2}\left(\tfrac{1}{2}c_p\left[(c_p-C_o)^2 - c_m^2\right] + \frac{\lambda c_p}{K_c} + \frac{\Delta P}{2K_c}\right) \tag{18}$$

where λ is the membrane tension. We can solve these equations to obtain c_p. Then, since $\frac{dz}{dx} = -\tan\Psi$, we have:

$$z(x) - z(0) = -\int_0^x x\, c_p\, (1-x^2c_p^2)^{-\frac{1}{2}}\, dx \tag{19}$$

Though these equations may seem frightfully complicated, they have been solved previously.[108] We consider only their qualitative significance.

We are trying to find why membranes have particular shapes; pictures of cells reveal a diversity of shapes. The best studied system is the mammalian red blood cell. It has no rigid cytoplasmic structures, so that its shape is an intrinsic property of the membrane.

The basic observation is that its normal shape is a biconcave disk. An immediate question is where the dimples come from. Until recently,[109] it was believed that they

were caused by membrane heterogeneity or cytoplasmic structures. Typical ideas were attractive forces between the dimples,[90] possibly caused by fibers connecting their membranes;[89] or interfacial tension differences between them and the equator.[110] However, more recent work forces the rejection of these ideas. Extensive studies on the mechanics[111,112] and morphology[113] of this membrane have not confirmed any ideas of fibers or heterogeneity. Micromanipulation studies show that the dimples can be pushed around in the membrane.[112] Furthermore, these explanations for the biconcave shape ignore the observations that drugs or changes in the medium can reversibly cause the cells to acquire many other shapes.[114]

The pioneering attempt to explain red cell shape on the basis of curvature energy[109] was not very convincing, because of its poor agreement with experiment. The difficulty was that it ignored the intrinsic curvature, C_o. However, the solution of Helfrich's equations[108] does accurately predict the shape, using only one adjustable constant, C_o. Though the equations may seem to contain others, they do not matter. λ is merely a Lagrange multiplier used to keep the area constant, while ΔP is one for the volume. K_c does not matter either: it occurs only in the combinations $\Delta P/K_c$ and λ/K_c. When λ and ΔP are calculated, it is these ratios which are found.

The significant conclusion is that the normal shape arises when C_o is negative. The lowest bending energy of any membrane region occurs when it is concave. Since the membrane is a closed shell, it must be convex somewhere. The dimples arise when the membrane tries to minimize its energy.

The normal shape occurs when $C_o r_o = -3$, where r_o is the radius of a sphere whose surface area is the same as the cell's. When C_o varies, there is a variety of other predicted shapes,[108] which have been observed in drug-treated cells. This agrees with the experimental observation that drugs which might be expected to change C_o also produce shape changes.[97]

iv. Overview of the Equilibrium Theory

Let us now consider the fundamental lessons provided by the equilibrium theory. We will extract those parts of the analysis which are applicable to any physical system, especially membrane OP's.

The first step in our analysis was finding the relevant symmetries. We pictured the membrane as a two dimensional isotropic continuum, surrounded by isotropic media. This implies that the energy of a bend is independent of its orientation in the membrane or in space, ruling out any dependence of the energy on $\vec{n}$ itself. Regarding the n_{ij}'s (i,j=x,y) as a matrix, N, the simplest possible contributions to the energy density are the trace and determinant of N. However, the latter's integral over the membrane is shape-independent, and thus has no physical significance. We then showed that the existence of an equilibrium state requires the energy to depend at least quadratically on trace N. We were thus led to the simplest plausible formula: $w_c=\frac{1}{2}K_c(\text{trace } N - C_o)^2$. Though there is no guarantee that this is correct, it is the easiest guess. Only if it leads to predictions inconsistent with experiment are more complicated models worthwhile. We saw that the theory is consistent with the observed red cell shape. In the next section it will be seen to pass an even more

stringent test.

Similar considerations also lead to our model. There, attention is focussed on a scalar order parameter. Exactly as before, we find the simplest plausible dependence of the energy density on it. We then calculate its experimental consequences and test them.

Helfrich's model also allows us to rationalize the effects of various drugs on red cell shape, and to propose mechanisms for membrane shape changes. While these ideas have not yet been definitively tested, they provide a basis for future work. Our model of protein precipitation presently has similar status, suggesting how protein cohesion is modulated. We will see, however, that it also leads to correct predictions about other phenomena.

Another basic concept is that of stability. Among physical systems in general, one often finds sudden changes when some parameter is varied. This happens when some previously stable state becomes unstable. Examples are phase transitions as the temperature changes, or the collapse of columns with increases in their loads. In Helfrich's model, ellipsoidal membranes become unstable for certain values of C_o or ΔP. Similarly, proteins are sometimes unstable against aggregation in our model.

A slight generalization of the preceding theory allows us to study fluctuations around the equilibrium shape. This we turn to next.

2. BENDING FLUCTUATIONS

i. Introduction

In the preceding sections, we found the equilibrium shape by minimizing the energy. Since forces are derivatives of the energy, this is equivalent to requiring that the forces everywhere sum to zero. After calculating the forces in an arbitrarily shaped membrane, we can use Newton's laws to calculate the time dependence of its shape. This yields a description of its relaxation back to equilibrium. However, it does not matter whether the original distortion is produced by experimental manipulation or thermal fluctuation. Thus, the same calculation also reveals the characteristics of these fluctuations. The theoretical apparatus we need is based on the equipartition and fluctuation-dissipation theorems. One goal of this section is to introduce them.

Rather than presenting an abstract mathematical analysis, we illustrate the theory with concrete problems. We concentrate mainly on the bending fluctuations of red blood cells. We will see that their behavior is consistent with the Helfrich model.

When red cells are observed with phase contrast optics, they are seen to shimmer. This is attributed to thickness fluctuations, caused by membrane bending.[115] Though a variety of evidence suggests that the cause is not

fluctuations in the oxidation state or concentration of hemoglobin, the best evidence for this is the success of the bending theory. Since the phase retardation is proportional to cell thickness, the flicker can be used to measure bending fluctuations.

ii. Experimental Results

We first discuss what can be measured.[115] Consider a cell with its symmetry axis parallel to the optical axis of the microscope, and call $d(\vec{r},t)$ its thickness at position $\vec{r}$ and time t. Also let $\delta d(\vec{r},t)$ be the deviation of $d(\vec{r},t)$ from its equilibrium value. Finally, denote the temporal Fourier transform of $\delta d(\vec{r},t)$ by $\delta d_\omega(\vec{r})$. If one measures the image intensity at the point corresponding to $\vec{r}$, and applies it to a band pass filter centered on frequency ω, the output is proportional to $\delta d_\omega(\vec{r})$. It is more useful to measure the correlation function, $G(\vec{r},\omega) = \langle \delta d_\omega(0)\ \delta d_\omega(\vec{r}) \rangle$, where the brackets denote time averaging. This is directly measurable by filtering and multiplying the outputs of two photomultipliers, focussed on the points 0 and $\vec{r}$. It will later be seen that we really want $G'(r,\omega)$, the temporal Fourier transform of $\langle \delta d(0,0)\ \delta d(r,t) \rangle$. However, different frequency components of δd are independent in the present harmonic model. Thus $\langle \delta d_\omega(0)\ \delta d_{\omega'}(\vec{r}) \rangle = \langle \delta d_\omega(0) \delta d_\omega(\vec{r}) \rangle \delta(\omega - \omega')$, where $\delta(\omega - \omega')$ is a Dirac δ. The convolution theorem then shows that $G(\vec{r},\omega) = G'(\vec{r},\omega)$.

We next consider the experimental measurements of $G(\vec{r},\omega)$.[115] We discuss only the qualitative features, and compare them to the predictions of Helfrich's model. $G(0,\omega)$ describes the fluctuations at a single point. At frequencies

between 1 and 30 Hertz, $G(0,\omega)$ is proportional to ω^{-m}, where $1.3 < m < 1.45$. It is buried under noise at higher frequencies, and levels off at lower ones. When measuring the r-dependence of G, one finds a peak at $r=0$, whose wings dip below zero near $r=6\mu$. G rises through zero near $r=8\mu$, and soon thereafter is obscured by noise. Repeating the measurement at various frequencies, the shape is found to be independent of ω. Though there are slight differences, the curves can be superimposed by a frequency-dependent rescaling. Thus, $G(\vec{r},\omega)=G(0,\omega)f(\frac{r}{\lambda_\omega})$, where f and λ_ω are defined by this equation. λ_ω is proportional to ω^{-n}, $.12 < n < .19$. The crucial features we seek to explain are the factoring of $G(\vec{r},\omega)$ and the values of n and m.

iii. Mean Square Fluctuation Amplitudes

As background to the calculation of fluctuation dynamics, we will study their statics. We do this by reformulating Helfrich's model so that our task reduces to a trivial application of the equipartition theorem.

Consider a roughly planar membrane, parallel to the x-y plane. As before, we call the membrane normal $\vec{n}$. If the ripples are small, then simple geometry shows that $n_i = \partial u/\partial i$ $(i=x,y)$ where u is the deviation from the mean of the membrane elevation. The curvature energy density thus becomes $w_c = \frac{1}{2}K_c(\partial^2 u/\partial x^2 + \partial^2 u/\partial y^2)^2$. We have set $C_o = 0$ because it is irrelevant to our purposes here.

We next expand u in Fourier components: $u_{\vec{q}} = \int u(\vec{r})\ e^{i\vec{q}\cdot\vec{r}} d^2r$. Expressing the total energy in terms of the $u_{\vec{q}}$'s, one obtains:

$$E_c \equiv \int d^2r\ w_c = \frac{K_c}{2A} \sum_{\vec{q}} q^4\ u_{\vec{q}}^2 \qquad (20$$

where A is the membrane area.

We note that E_c is quadratic in the $u_{\vec{q}}$'s. The equipartition theorem asserts that the mean energy of each is $\frac{1}{2}k_BT$. We thus find the mean square amplitude of component $\vec{q}$:

$$\langle |u_{\vec{q}}|^2 \rangle = \frac{Ak_BT}{K_c q^4} \qquad (21$$

Each of the bending modes, $u_{\vec{q}}\ e^{i\vec{q}\cdot\vec{r}}$, acts as a

diffraction grating of spacing $2\pi/q$. By calculating the light scattered from each, and summing over $\vec{q}$, one can calculate the intensity of the scattered light. It is proportional to $\sum_{\vec{q}} <|u_{\vec{q}}|^2> c_{\vec{q}}^2$, where $c_{\vec{q}}$ is the scattering amplitude of mode $\vec{q}$. This approach has been used to study bending fluctuations of the monolayers at surfaces of soap films.[116] There K_c is controlled by the electrostatic and van der Walls interactions between the monolayers, so that light scattering can be used to measure these forces.

In a less trivial model than we are considering here, the q^4 factor would be replaced with a polynomial in q. If it has a zero, say q_z, then $<|u_{q_z}|^2>$ would naively seem infinite. However, the model breaks down for sufficiently large deformations. Effects that we have neglected would provide an additional restoring force for mode q_z, so that it would remain finite, though large. The equilibrium structure would then contain ripples of wavevector q_z. This has been suggested as the source of the corrugations seen in certain lipid phases.[117,118]

We can use equation 21 to find the mean square amplitude of red cell thickness fluctuations. If we picture the cell as two parallel membranes, at elevations z_1 and z_2, then its thickness is $d=z_1-z_2$. If the fluctuations in each membrane are uncorrelated with those in the other, then:

$$\langle |\delta d(\vec{q})|^2 \rangle = 2\langle |u_{1\vec{q}}|^2 \rangle = \frac{2Ak_BT}{K_c q^4} \qquad (22$$

where $\delta d(\vec{q})$ is the Fourier transform of $\delta d(\vec{r})$. $u_{1\vec{q}}$ is the amplitude of the $\vec{q}$'th mode in the membrane at z_1: since the membranes are identical, we could just as well have picked the other one.

We next calculate the amplitudes of fluctuations with particular wavevector and frequency. Summing over frequency should yield equation 22 again. This provides a check of the calculation.

iv. Fluctuation Dynamics

We first seek equations relating the forces and velocities in the membrane and its surroundings. Once we have them, we can calculate the spectrum of red cell shape fluctuations. We begin by formalizing the requirements that the membrane and its environment exert equal forces on one another, and that their velocities be equal.

The curvature force (i.e., the zz component of the membrane stress) is given by the functional derivative of the curvature energy:

$$f_c = -\frac{\delta E_c}{\delta u} = -\left[\frac{\partial^2}{\partial x^2}\frac{\partial w_c}{\partial u_{xx}} + \frac{\partial^2}{\partial y^2}\frac{\partial w_c}{\partial u_{yy}}\right] = -K_c\left[\frac{\partial^4 u}{\partial x^4} + \frac{\partial^4 u}{\partial y^4}\right] \quad (23$$

where $u_{ii} = \partial^2 u / \partial i^2$ (i=x,y). This equation is derived in section I.E where we explain functional derivatives. f_c is also the force exerted by the membrane on the surrounding fluid. This must equal the difference across the membrane of the fluid forces arising from pressure and viscous dissipation. The viscous stresses at each side of the membrane are $\pm 2\eta \frac{\partial v_z}{\partial z}$, where η is the shear viscosity, v_z is the z component of fluid velocity, and the derivative is evaluated at the membrane surface. The plus sign refers to the upper surface of the membrane, and minus, the lower one. Finally, we call the pressure difference across the membrane ΔP.

To a fair approximation, we can ignore viscous

dissipation outside the cell. The viscosity is smaller there, so that equal velocity gradients produce less force there than inside. Furthermore, the velocity field produced by membrane bending decays over a larger distance outside, so that the gradients too are smaller there. We can also ignore viscous dissipation within the membrane, since its volume is negligible compared to that of its surroundings.

Combining these equations, we obtain the force balance equation for each membrane:

$$(-1)^i \left[2\eta \frac{\partial v_z}{\partial z}\bigg|_{z_i} + \Delta P \right] + K_c \left[\frac{\partial^4 u_i}{\partial x^4} + \frac{\partial^4 u_i}{\partial y^4} \right] = 0 \qquad (i=1,2) \quad (24$$

We supplement this with the velocity continuity requirements:

$$v_z(z_i) = \frac{\partial u_i}{\partial t} \qquad \vec{v}_{||}(z_i) = 0 \qquad (i=1,2) \qquad (25$$

where t is time and $\vec{v}_{||}$ is the component of fluid velocity parallel to the membrane. The second of these equations follows because we are neglecting motion within the plane of the membrane. Finally, we need equations for the fluid velocity. We take the linearized Navier-Stokes equations for an incompressible fluid:

$$\text{div } \vec{v} = 0 \qquad \rho \frac{\partial v}{\partial t} = \eta \text{ div grad } \vec{v} - \text{grad } P \qquad (26$$

where ρ is the mass density of the fluid. The solution of these equations is a tedious matter. We will discuss only the results.[115]

What we really seek are the fluctuations in d; but

these equations yield the deterministic behavior of d starting from some arbitrary shape. However, we will see that these two descriptions are equivalent. Suppose that we apply an arbitrary force, $(-1)^i F(\vec{r},t)$ $(i=1,2)$ to the membranes. This makes the thickness change by some amount, Δd. Since equations 24 to 26 are linear, there exists some function, χ , the susceptibility or response function, such that:

$$\Delta d(\vec{r},t) = \int d^2\vec{r}'\, dt'\, \chi(\vec{r}-\vec{r}',t-t')F(\vec{r}',t') \qquad (27$$

If we set $F(r,t)=f\ e^{i(\vec{q}\cdot\vec{r}+\omega t)}$, then:

$$\Delta\tilde{d}(q,\omega) = fA\,\tilde{\chi}(q,\omega) \qquad (28$$

where $\Delta\tilde{d}$ and $\tilde{\chi}$ are the Fourier transforms of Δd and χ respectively. The fluctuation-dissipation theorem[119] asserts that:

$$\langle |\delta d(\vec{q},\omega)|^2 \rangle = -\frac{k_B T}{\pi\omega}\ \mathrm{Im}\,\tilde{\chi}(\vec{q},\omega) \qquad (29$$

where Im denotes the imaginary part. This solves our problem, since χ can be obtained by adding $(-1)^i F(\vec{r},t)$ to the left side of equation 24, and solving it. The spatial Fourier transform of equation 29 then yields $G(\vec{r},\omega)$.

After a long calculation, one finds:[115]

$$\tilde{\chi}(\vec{q},\omega) = \frac{Aq^2d^3/24\eta}{i\omega + K_c q^6 d^3/24\eta} \qquad (30$$

Fourier transforming and substituting into equation 29 yields:

$$G(\vec{r},\omega) = G(0,\omega)\ f(\frac{r}{\lambda\omega}) \qquad (31$$

with: $$G(0,\omega) = \frac{2k_BTd}{3^{1/3}(2\pi)^3 \eta^{1/3} K_c^{2/3} \omega^{4/3}} \quad (32$$

$$\lambda_\omega = \left(\frac{K_c d^3}{24\eta\omega} \right)^{1/6} \quad (33$$

and: $$f(x) = \int_0^{2\pi} d\theta \int_0^{\infty} dq \; \frac{e^{iqx\cos\theta} q^3}{1 + q^{12}} \quad (34$$

We immediately note several features of these equations. Most obviously, we see that $G(r,\omega)$ factors in the same way as that found experimentally. λ_ω is predicted to be proportional to ω^{-n}, with $n=1/6$. This is consistent with the experimental result, $.12 < n < .19$. It is also predicted that $G(0,\omega)$ is proportional to ω^{-m}, with $m=4/3$. Here, experiment shows $1.3 < m < 1.45$, also consistent with the theory. Numerical evaluation of $f(\frac{r}{\lambda_\omega})$ shows that it too is quantitatively accurate.[115] We thus see that the model successfully reproduces the main features of the experimental data.

A crucial feature of the red cell is that it is nonspherical, so that it is possible for the membrane to bend, while remaining constant in area. However, this is no longer possible when the cell is made spherical. Then, the shape fluctuations are controlled by stretching, rather than bending, energy. Unless the tension is near zero, stretching fluctuations have a smaller amplitude and higher frequency than bending ones. This accounts for the absence of flicker in osmotically sphered red

cells.[115,120]

The higher energy of stretching can be understood by reconsidering the thermodynamics of bending. We assumed that the membrane contains a surface whose area is unaffected by bending. The energy change arises from the slight compression or expansion of each monolayer. There is a partial cancellation between the energy changes of each, exact when they are identical and $K^u=K^l=0$. This cannot occur when the original shape is spherical: both monolayers undergo essentially identical deformations.

Bending must also be accompanied by stretching in planar membranes. The bending modes here have been observed with optical heterodyne spectroscopy. As one would expect, their frequency is higher than in the red cell: in the kilohertz range.[121,122]

v. Overview of Fluctuation Dynamics

We have seen that a slight generalization of the static theory allowed us to study bending dynamics. The key steps were the coupling of the membrane to its surroundings, and the calculation of the response function. The first damped the bending oscillations, while the second created them. However, they can arise from either experimental manipulation or thermal fluctuation. These two situations are equivalent because of the fluctuation-dissipation theorem. It leads to the fluctuation spectrum.

As we saw, Helfrich's model does correctly predict that spectrum. One might guess by analogy that similar considerations will lead to definitive tests of our model. A crucial difference is that the OP is not necessarily coupled to the external media, while the curvature is. The hydrodynamic equations relevant to the OP are an intrinsic property of the membrane. It is a task for future workers to find them.

Another important idea was the equipartition theorem: it allowed us to calculate the fluctuation amplitudes without invoking their dynamics. We also saw that fluctuations are large when there is no force opposing them. Indeed, it is misleading to view them as fluctuations: they are a part of the static structure. We encounter this

phenomenon again in our model. Diffusion does not oppose aggregation when the protein chemical potential is a decreasing function of concentration. A precipitate is present at equilibrium.

Our review of membrane elasticity has been very limited, serving mainly to show that field theory is relevant to membranes. The elastic modes generally have several branches, of which we have considered only one.[123] We have examined only small deformations, neglecting the nonlinear viscoelasticity of membranes.[29-33] We have also ignored thickness changes, important in such phenomena as dielectric breakdown[124-126] and nonlinear capacitance.[127-129] We will later return to these effects, and find that our OP is probably membrane thickness.

E. MATHEMATICAL INTERLUDE

Consider a system whose state is specified by some function of position, say $s(\vec{r})$. In this section we will relate the behavior of s to its influence on the energy, E_s. It often occurs that $E_s = \int d^2\vec{r}\ e_s(\vec{r})$, where $e_s(\vec{r})$ is an energy density dependent on $s(\vec{r})$ and $\nabla s(\vec{r})$: $e_s(\vec{r}) = e_s(s(\vec{r}), \nabla s(\vec{r}))$. In bending theory, $\vec{n}$ and w_c play the roles of s and e_s respectively; the OP and its energy density do in our model. For concreteness, we assume the system to be two dimensional, though nothing we do here depends on this. Also, it does not matter whether s is a scalar or vector, except that "∇" denotes gradient in one case, and divergence in the other.

The equilibrium state is that which minimizes the energy. In many cases, e_s would be minimal if s everywhere equalled some constant. That would then be the unconstrained equilibrium. There may, however, be externally imposed boundary conditions which prevent attainment of that state. For instance, the red cell bending energy would be minimal if its membrane were everywhere concave: an impossible situation in a closed shell. Analogously, in our model, proteins perturb the nearby OP. Our task is to find the $s(\vec{r})$ which minimizes E_s, subject to these constraints. We can do this by deriving a differential equation whose solution is the desired $s(\vec{r})$. Our procedure

is discussed in many textbooks which can be consulted for further details; the one by de Gennes[130] is especially relevant.

When $s(\vec{r})$ is changed by a small amount, $\delta s(\vec{r})$, the linear variation is E_s is:

$$\delta E_s = \int d^2\vec{r}\, \delta e_s = \int d^2\vec{r} \left[\delta s \frac{\partial e_s}{\partial s} + \delta(\nabla s) \frac{\partial e_s}{\partial(\nabla s)} \right] \quad (1$$

This must be zero when E_s is minimal: we have expanded e_s as a Taylor series in s and ∇s, and dropped all terms beyond the linear ones. As in elementary calculus, the linear terms vanish in a series expansion around a minimum. We seek constraints on s which insure this.

The $\delta(\nabla s)$ term can be integrated by parts to yield:

$$\delta E_s = \int d^2\vec{r}\ \ \delta s \left[\frac{\partial e_s}{\partial s} - \nabla \cdot \frac{\partial e_s}{\partial(\nabla s)} \right] \quad (2$$

For general δs, there would also be a surface term, the integral over the membrane boundary of $\delta s(\partial e_s/\partial(\nabla s))$. However, we require $s(\vec{r})$ to satisfy the boundary conditions, so that δs, and thus δe_s, vanish on the boundary.

We now set $\delta E_s = 0$. Since δs is arbitrary except on the boundary, the bracketed factor in equation 2 must vanish. We thus get the Euler-Lagrange equation:

$$\frac{\partial e_s}{\partial s} - \nabla \cdot \frac{\partial e_s}{\partial(\nabla s)} = 0 \quad (3$$

This solves our problem, since any $s(\vec{r})$ which satisfies this equation also minimizes E_s.

In the bending theory, this is how the field equation was derived. Similarly, this is how we obtain the field equation for the OP in our model. It should be noted that we have assumed the differential area element, $d^2\vec{r}$, to be independent of s. Bending produces local area changes, so that this assumption is violated in Helfrich's model. We can avoid this by projecting the membrane into some plane, say the x-y plane. The Jacobian for this transformation is $(1-n_x^2-n_y^2)^{-\frac{1}{2}}$. e_s is actually that times w_c: this is why the field equation is so complicated. In our model, OP variations are assumed not to affect membrane shape. Our field equation is thus much simpler.

We found equation 3 by minimizing the energy. However, it can also be obtained by requiring the net force to vanish everywhere. A force is generally minus some derivative of the energy. We seek the derivative of E_s with respect to $s(\vec{r})$ at a certain point. We begin by defining the functional derivative. Consider the case $\delta s = \varepsilon \delta(\vec{r}-\vec{r}')$, where $\delta(\vec{r}-\vec{r}')$ is a Dirac δ, $\vec{r}'$ is some point in the membrane, and ε some constant. Then the functional derivative is: $\frac{\delta E_s}{\delta s} = \frac{\partial E_s}{\partial \varepsilon}\Big|_{\varepsilon=0}$. Imitating the previous derivation, we find the membrane stress:

$$f_s = -\frac{\delta E_s}{\delta s} = -\frac{\partial e_s}{\partial s} + \nabla \cdot \frac{\partial e_s}{\partial(\nabla s)} \qquad (4$$

The force on any region is found by integrating the stress

over it. We thus see that the forces on s vanish when it satisfies the field equation.

So far, we have assumed e_s to depend only on s and ∇s. However, it is trivial to generalize to cases where it depends on higher derivatives too. In the coordinates we used to study bending fluctuations, w_c depended on $\nabla^2 u$, for instance. Repeating the derivation of equation 3, we find that it is supplemented by $(-1)^n \nabla^n \frac{\partial e_s}{\partial(\nabla^n s)}$ whenever e_s also depends on $\nabla^n s$. This leads to equation I.D.23.

F. OBSERVATION OF MEMBRANE PROTEIN PARTICLES

Much of the present theory is based on the analysis of protein clustering and its modulation. Crucial to our work is the existence of an experimental procedure for visualizing protein particles. This method is freeze-fracture electron microscopy, which we now describe. Our review is very limited; many others are available for the reader interested in more details.[5,131-134]

The first step is freezing the specimen by plunging it into a coolant. The growth of ice crystals must somehow be prevented, because it damages membranes.[135,136] One way is to make the specimen into a mist by forcing it through a narrow nozzle.[137] When the droplets contact the coolant, their small size lets them freeze too rapidly for much crystal growth to occur. The other way, used more often, is to include a cryoprotectant in the solution.[135] The most common ones, such as glycerol and dimethyl sulphoxide, form eutectics with water. Because the rate of crystal growth is less at low temperatures, the freezing point depression decreases the grain size.[138] Much of the damage to membranes is mediated by osmotic effects, caused by the expulsion of solutes from water as it crystallizes.[139] This too is lessened by cryoprotectants.

Once the sample is embedded in amorphous or microcrystalline ice, the next step is to fracture it. A

cleavage plane roughly parallel to a membrane is more likely to travel along its center than through the nearby water or the membrane-water interface.[140] This happens because the latter are bound together by hydrogen bonding, while much weaker dispersion forces hold the two faces of the membrane together.

The fracturing process yields ice chips, portions of whose surfaces were formerly the middle planes of membranes. In one variant, known as freeze-etching, the ice is allowed to sublime. Its surface recedes until a membrane is reached, thus revealing its outer surface.[141]

The ice is then exposed to a point source of metal atoms, which then encrust its surface except in shadows. The specimen is next melted or dissolved. This frees the metal replica, which can then be visualized by electron microscopy. Surface features, such as bumps and holes in the membrane, are disclosed by their shadows.

This procedure reveals that membranes contain particles, typically about 10 nm in diameter.[142] Their size, shape, and abundance vary between different membranes, and even between different regions of a single membrane. Often, two or more particle types are interspersed among one another.

Studies with synthetic membranes show that these particles are formed only in the presence of proteins,

though little is known about how the proteins are arranged within them. Comparisons of the number and size of particles to that of their constituent proteins show that there are several protein molecules per particle.[143,144] Protein assembly into particles is analogous to micelle formation:[145] no particles are visible below a certain protein concentration, while above it they are. Then their size is independent of the amount of protein. It is presently unknown if the particles contain lipid, or if their shape is altered during the freeze-fracture process. Neither is it known what proportion of the membrane proteins they contain. However, we are concerned here only with the interactions between pre-existing particles; their formation and internal structure need not concern us.

We use the freeze-fracture technique only to find the positions of protein particles, thus allowing analysis of their distribution. One can also perform statistical tests to see if there is any tendency towards clustering or other heterogeneity in their arrangement. Because different lipid phases have different textures,[146] one can study the partition of proteins between coexisting lipid phases. Specialized membrane regions, such as intercellular junctions, can be examined to see what efffect they have on the arrangement of nearby particles.

REFERENCES FOR CHAPTER I

1. T.L. Steck J. Mol. Biol. 66: 295-305 (1974)
2. G.M. Edelman Science 192: 218-226 (1976)
3. K. Wang & F.M. Richards J. Biol. Chem. 249: 8005-8018 (1974)
4. G.L. Nicholson Biochim. Biophys. Acta 457: 57-108 (1976)
5. A.J. Verkleij & P.H.J. Th. Ververgaert Ann. Rev. Phys. Chem. 26: 101-122 (1975)
6. R.L. Juliano Biochim. Biophys. Acta 300: 341-378 (1973)
7. T.L. Steck J. Cell. Bio. 62: 1-19 (1974)
8. E. Schechter, L. Letellier, & T. Gulik-Krzywiki Eur. J. Biochem. 49: 61-76 (1974)
9. W. Kleemann & H.M. McConnell Biochim. Biophys. Acta 419: 206-222 (1976)
10. J. Melhorn & L. Packer Biophys. J. 16: 613-625 (1976)
11. L. Finegold Biochim. Biophys. Acta 448: 393-398 (1976)
12. T.P. Copps, W.S. Chelack, & A. Petkau J. Ultrastruct. Res. 55: 1-3 (1976)
13. L. Jarett & R.M. Smith J. Supramol. Struct. 6: 45-59 (1977)
14. H.K. Kimelberg Mol. Cell. Biochem. 10: 171-190 (1976)

15. C. Tanford "The Hydrophobic Effect" John Wiley & Sons New York 1973

16. D.F.H. Wallach & R.J. Winzler "Evolving Strategies and Tactics in Membrane Research" Springer-Verlag New York 1974

17. C.G. Duck-Chong Enzyme 21: 174-192 (1976)

18. R.S. Decker & D.S. Friend J. Cell Bio. 62: 32-47 (1974)

19. L.A. Staehlin J. Cell Bio. 71: 136-158 (1976)

20. D.S. Friend & I. Rudolf J. Cell Bio. 63: 466-479 (1974)

21. P. Satir & B. Satir pp.233-249 in: "Control of Proliferation in Animal Cells" B. Clarkson & R. Baserga, eds. Cold Spring Harbor Laboratory 1974

22. J. Chevalier J. Microscopie 20: 247-258 (1974)

23. K.H. Pfenninger & R.P. Bunge J. Cell Bio. 63: 180-196 (1974)

24. C.R. Kahn J. Cell Bio. 70: 261-286 (1976)

25. S. Jacobs & P. Cuatrecasas Biochim. Biophys. Acta 433: 482-495 (1976)

26. J.A. Peterson, R.E. Ebel, D.H. O'Keeffe, T. Matsubara, &. R.W. Estabrook J. Biol. Chem. 251: 4010-4016 (1976)

27. C.S. Yang Life Sci. 21: 1047-1058 (1977)

28. A.S. Kaprel'yants & D.N. Ostrovskii Biokhimya 40: 1210-1215 (1975)

29. E.A. Evans & R.M. Hochmuth Biophys. J. 16: 1-11, 13-26 (1976)

30. E.A. Evans, R. Waugh, & L. Melnik Biophys. J. 16: 585-600 (1976)

31. E.A. Evans & P.L. LaCelle Blood 45: 29-43 (1975)

32. R.M. Hochmuth, E.A. Evans, & D.F. Colvard Microvasc. Res. 11:155-159 (1976)

33. R. Waugh & E.A. Evans Microvasc. Res. 12: 291-304 (1976)

34. S.J. Singer & G.L. Nicholson Science 175: 720-731 (1972)

35. M.S. Bretscher Science 181: 622-629 (1973)

36. R. Glaser & A. Leitmanová Studia Biophys. 48: 219-229 (1975)

37. B.S. Bull & J.D. Brailsford Blood 41: 833-844 (1973)

38. E.A. Evans & R.M. Hochmuth J. Membrane Bio. 30: 351-362 (1977)

39. F.H. Kirkpatrick Life Sci. 19: 1-18 (1976)

40. A. Elgsaeter & D. Branton J. Cell Bio. 63: 1018-1030 (1974)

41. A. Elgsaeter, D.M. Shottun, & D. Branton Biochim. Biophys. Acta 426: 101-122 (1976)

42. H.U. Luts, S.-C. Liu, & J. Palek J. Cell Bio. 73: 548-560 (1977)

43. M.P. Sheetz & S.J. Singer J. Cell Bio. 73: 638-646 (1977)

44. G.B. Ralston Biochim. Biophys. Acta 455: 163-172 (1976)

45. L.G. Tilney & P. Detmers J. Cell Bio. 66: 508-520 (1975)

46. C.F. Fox pp.279-306 in: "Biochemistry of Cell Walls and Membranes" C.F. Fox, ed. Butterworths London 1975

47. D. Papahadjopoulos, W.J. Vail, & M. Moscarello J. Membrane Bio. 22: 143-164 (1975)

48. W. Curalto, J.D. Sakura, D.M. Small, & G.G. Shipley Biochemistry 16: 2313-2319 (1977)

49. D. Chapman, B.A. Cornell, A.W. Eliasz, & A. Perry J. Mol. Bio. 113: 517-538 (1977)

50. H. Trauble & P. Overath Biochim. Biophys. Acta 307: 491-512 (1973)

51. J.M. Boggs, D.D. Wood, M.A. Moscarello, & D. Papahadjopoulos Biochemistry 16: 2325-2329 (1977)

52. H.K. Kimelberg & D. Papahadjopoulos J. Biol. Chem. 249: 1071-1080 (1974)

53. C. Hidalgo, N. Ikemoto, & J. Gergely J. Biol. Chem. 251: 4224-4232 (1976)

54. T.R. Hesketh, G.A. Smith, M.D. Houslay, K.A. McGill, N.J.M. Birdsall, J.C. Metcalfe, & G.B. Warren Biochemistry 15: 4145-4151 (1976)

55. A. Stier & E. Sackmann Biochim. Biophys. Acta 311: 400-408 (1973)

56. L. Thilo, H. Trauble, & P. Overath Biochemistry 16: 1283-1290 (1977)

57. J.M. Boggs, W.J. Vail, & M.A. Moscarello Biochim. Biophys. Acta 448: 517-530 (1976)

58. M.A. Hemminga & J.F.M. Post Biochim. Biophys. Acta 436: 222-234 (1976)

59. Y.S. Chen & W.L. Hubbell Exp. Eye Res. 17: 517-531 (1973)

60. C.R. Hackenbrock, M. Hochli, & R.M. Chau Biochim. Biophys. Acta 455: 466-484 (1976)

61. V. Speth & F. Wunderlich Biochim. Biophys. Acta 291: 621-628 (1973)

62. W. Kleemann & H.M. McConnell Biochim. Biophys. Acta 345: 220-230 (1974)

63. R. James & D. Branton Biochim. Biophys. Acta 323: 378-390 (1973)

64. F. Wunderlich, D.F.H. Wallach, V. Speth, & H. Fischer Biochim. Biophys. Acta 373: 34-43 (1974)

65. D. Marsh, A. Watts, & P.F. Knowles Biochim. Biophys. Acta 465: 500-514 (1977)

66. J.E. Rothman J. Theor. Bio. 38: 1-16 (1973)

67. S.G. Whittington & D. Chapman Trans. Faraday Soc. 62: 3319-3324 (1966)

68. K. Nagai J. Chem. Phys. 47: 4690-4696 (1967)

69. F.A. Vandenheuvel Chem. Phys. Lipids 2: 372-395 (1968)

70. G. Lagaly Angew. Chem. Int. Ed. Engl. 15: 575-586 (1976)

71. J.T. Bender Macromol. 10: 162-168 (1977)

72. M.B. Jackson Biochemistry 15: 2555-2561 (1976)

73. D. Marsh J. Membrane Bio. 18: 145-162 (1974)

74. P. Bothorel, J. Belle, & B. Lamaire Chem. Phys. Lipids 12: 96-116 (1971)

75. H. Schindler & J. Seelig Biochemistry 14: 2283-2287 (1975)

76. J.A. McCammon & J.M. Deutch J. Amer. Chem. Soc. 97: 6675-6681 (1975)

77. S. Ohki J. Theor. Bio. 15: 346-361 (1967)

78. J.F. Nagle J. Chem. Phys. 58: 252-264 (1973); 63: 1255-1261 (1975)

79. J.F. Nagle Proc. Roy. Soc. London A337: 569-589 (1974)

80. J.F. Nagle J. Membrane Bio. 27: 233-250 (1976)

81. H.L. Scott Biochim. Biophys. Acta 406: 329-346 (1975)

82. F.W. Wiegel J. Statistical Phys. 13: 515-530 (1975)

83. S. Marčelja Biochim. Biophys. Acta 367: 165-176 (1974)

84. S. Marčelja Biochim. Biophys. Acta 455: 1-7 (1976)

85. L.D. Landau & E.M. Lifshitz "Statistical Physics" chapter 14 Pergamon Press London 1958

86. G. Toulouse & P. Pfeuty "Introduction au Groupe de Renormalisation" chapter 2 Presses Universitaires de Grenoble Grenoble 1975

87. deleted

88. W. Helfrich Z. Naturforsch. 28c: 693-703 (1973)

89. B.B. Shrivastav & A.C. Burton J. Cell. Physiol. 74: 101-114 (1968)

90. B.B. Shrivastav & A.C. Burton Can. J. Physiol. Pharmacol. 48: 359-368 (1970)

91. R. Goldman, T. Pollard, & J. Rosenbaum, eds. "Cell Motility, Book A" section 3 Cold Spring Harbor Laboratory 1976

92. W. Helfrich Phys. Lett. 43A: 409-410 (1973)

93. W. Helfrich Z. Naturforsch. 29c: 182-183 (1974)

94. E.A. Evans Biophys. J. 14:923-931 (1974)

95. E.A. Evans & R. Waugh J. Colloid Interface Sci. 60: 286-298 (1977)

96. R. Defay, I. Prigogine, A. Bellmans, & D.H. Everett "Surface Tension and Adsorption" Longmans, Green London 1966

97. M.P. Sheetz, R.G. Painter, & S.J. Singer J. Cell Bio. 70:193-203 (1976)

98. S. Ohki Biochim. Biophys. Acta 255: 57-65 (1972)

99. P.L. Yeagle, W.C. Hutton, R.B. Martin, B. Sears, & C.-H. Huang J. Biol. Chem. 251: 2110-2112 (1976)

100. J.N. Israelachvilli Biochim. Biophys. Acta 323: 659-663 (1973)

101. D.M. Michaelson, A.F. Horowitz, & M.P. Klein Biochemistry 12: 2637-2645 (1973)

102. L.D. Bergelson & L.I. Barsukov Science 197: 224-230 (1977)

103. J.E. Rothman & J. Lenard Science 195: 743-753 (1977)

104. J.A. Hewett J. Theor. Bio. 64: 455-472 (1977)

105. W. Helfrich Z. Naturforsch. 29c: 510-515 (1974)

106. H. Gruler Z. Naturforsch. 30c: 608-614 (1975)

107. A.G. Petrov & A. Derzhanski J. de Phys. 33(coll. 3): 155-160 (1976)

108. H.J. Deuling & W. Helfrich Biophys. J. 16: 861-868 (1976)

109. P.B. Canham J. Theor. Bio. 26: 61-81 (1970)

110. Y.C.B. Fung & P. Tong Biophys. J. 8: 175-198 (1968)

111. R.P. Rand & A.C. Burton Biophys. J. 4: 115-135 (1964)

112. B.S. Bull & J.D. Brailsford Blood 41: 833-844 (1973)

113. R.F. Baker Fed. Proc., Fed. Amer. Soc. Exp. Biol. 26: 1785-1801 (1967)

114. M. Bessis, R.I. Weed, & P. Leblond "Red Cell Shape" Springer-Verlag New York 1973

115. F. Brochard & J.F. Lennon J. de Phys. 36: 1035-1047 (1975)

116. A. Vrij J. Colloid Sci. 19: 1-27 (1964)

117. W. Helfrich Z. Naturforsch. 29c: 692-693 (1974)

118. C. Gebhart, H. Gruler, & E. Sackmann Z. Naturforsch. 32c: 581-596 (1977)

119. R. Kubo Rept. Prog. Phys. 29: 255-284 (1966)

120. F. Brochard, P.G. DeGennes, & P. Pfeuty J. de Phys. 37: 1099-1104 (1976)

121. E.F. Grabowski & J.A. Cowen Biophys. J. 18: 23-28 (1977)

122. J.D. Hestenes & D.B. Chang J. Colloid Interface Sci. 42: 120-130 (1973)

123. L. Kramer J. Chem. Phys. 55: 2097-2105 (1971)

124. D.H. Michael, M.E. O'Neill, & J.C. Zuercher J. Fluid Mech. 47: 609-623 (1971)

125. J.A. Crowley Biophys. J. 13: 711-724 (1973)

126. H.G.L. Coster & J. Zimmerman J. Membrane Bio. 22: 73-90 (1975)

127. S.H. White & T.E. Thompson Biochim. Biophys. Acta 323: 7-22 (1973)

128. R. Benz & K. Janko Biochim. Biophys. Acta 455: 721-738 (1976)

129. E.A. Evans Biophys. J. 15: 850-852 (1975)

130. P.G. de Gennes "The Physics of Liquid Crystals" chapter 3 Clarendon Press Oxford 1974

131. S. Bullivant pp. 67-112 in: "Advanced Techniques in Biological Electron Microscopy" J.K. Koehler, ed. Springer-Verlag New York 1975

132. C. Stolinski & A.S. Breathnacii "Freeze-Fracture Replication of Biological Tissues" Academic Press London 1975

133. J.K. Koehler Adv. Biol. Med. Phys. 12: 1-84 (1968)

134. D. Branton Phil. Trans. Roy. Soc. London B261: 133-138 (1971)

135. P. Mazur Science 168: 939-949 (1970)

136. C. Sandri, J.M. Van Buren, & K. Akert "Membrane Morphology of the Vertebrate Nervous System" vol. 46 of: "Progress in Brain Research" Elsevier Scientific Publishing Co. Amsterdam 1977

137. P.H.J. Th. Ververgaert, A.J. Verkleij, J.J. Verhoeven, & P.F. Elbers Biochim. Biophys. Acta 311: 651-654 (1973)

138. B.J. Luyet pp. 27-43 in: "The Frozen Cell" G.E.W. Wolstenholme & M. O'Connor, eds. J.A. Churchill London 1970

139. J. Farrant & A.E. Woolgar pp.97-114 in ref. 138

140. D. Branton & D.W. Deamer "Membrane Structure" section III.B vol. II.E.1 of "Protoplasmatologia" Springer-Verlag New York 1972

141. K. Muhlenthaler Int. Rev. Cytol. 31: 1-19 (1970)

142. chapter 5 of ref. 132

143. D.A. Goodenough Cold Spring Harbor Symp. Quant. Biol. 40: 37-43 (1975)

144. J.P. Changeux et al. Cold Spring Harbor Symp. Quant. Biol. 40: 211-230 (1975)

145. J.P. Segrest, T. Gulik-Krzywicki, & C. Sardet Proc. Nat. Acad. Sci. USA 71: 3294-3298 (1974)

146. P. Pinto da Silva J. Microscopie 12: 185-192 (1971)

II. PROTEIN INTERACTION THEORY

A. FEW PARTICLE CASE

1. ORDER PARAMETER

We are interested in membranes whose state is specified by a single order parameter, φ, which we assume to be a scalar function of position. Our task is to describe φ in thermodynamic terms. This is feasable when $\vec{\nabla}\varphi$ is small enough that there exists some length, l, over which φ is roughly constant, while macroscopic thermodynamics is valid in regions of area l^2. We can then replace extensive variables with their densities. At each point, the latter obey the same laws as the former would in a uniform system.

We are concerned with the φ-dependence of the Gibbs free energy density, g. Unless there is some constraint on φ, $\partial g/\partial\varphi = 0$ at equilibrium. We will soon see that g must depend on $\vec{\nabla}\varphi$ in addition to φ. It is convenient to set $g = g^o + \varepsilon[\varphi, \vec{\nabla}\varphi]$, where $\varepsilon = 0$ when φ is everywhere at unconstrained equilibrium. We next expand ε as a Taylor series around the equilibrium state, $\varphi = \varphi_o$:

$$\varepsilon[\varphi, \vec{\nabla}\varphi] = \varepsilon[\varphi] = \varepsilon = K_1(\vec{\nabla}\varphi)^2 + K_2(\varphi - \varphi_o)^2 + \ldots \quad (1$$

Inclusion of linear terms would destroy the stability of the equilibrium state, while higher order terms would preclude nearly exact solutions. Since we are concerned

only with the OP-dependence of the free energy, we can usually ignore its remaining, OP independent, parts. Sometimes we also need to consider the entropy of mixing proteins and lipids.

The physical significance of equation 1 is easy to see. The first term produces the cooperativity, an energetic cost for spatial variation of the OP. Without it, protein perturbations would be limited to the directly affected lipids, rather than extending farther away. The second term provides a restoring force tending to keep the OP at its equilibrium value.

Many simple membrane models are based on expressions similar to equation 1. Consider the thickness, h, for instance. If the membrane is pictured as a thin slab of liquid, h is governed by the interfacial tension, γ. Small deformations locally change the area by $\frac{1}{2}(\vec{\nabla} h)^2$. On the other hand, γ is minimal at the equilibrium thickness, h_o, so that its dependence on h is at least quadratic.[1] We find that the energetic cost of sufficietly small thickness changes is $\frac{1}{2}\gamma_o(\vec{\nabla} h)^2 + \frac{1}{2}(\partial^2\gamma/\partial h^2)(h-h_o)^2$, where γ_o is the minimum value of γ. This is the same as equation 1. Similar expressions describe various liquid crystal order parameters,[2] composition in some models of phase separations,[3] and perhaps hydrophobic interactions.[4] This shows that equation 1 places little restriction on

the identity of the OP.

An expression formally equivalent to equation 1 has recently been presented by Kleemann and McConnell.[5] However, they were interested only in using it to describe protein effects on spin label partitioning, and did not mention its deeper significance.

Models based on the same idea as ours, but using very different descriptions of the OP, have recently been presented by Marčelja[6] and Schröder.[7] Comparison to these models is deferred until section IV.B.

Φ is a thermodynamic quantity which we use to describe protein interactions. Equation 1 describes the lipids, however, so that confirming it requires studies of the lipids themselves. By analogy to the work which led to acceptance of the continuum model of liquid crystals,[8,9] the definitive test is likely to be a comparison of experimental and theoretical spectra of OP fluctuations. This requires a molecular definition of Φ, for instance in terms of orientation or conformation. We return to this in chapter V.

We have so far ignored thermodynamic variables other than Φ. However, their boundary conditions (i.e., isothermal versus adiabatic) may affect K_1 and K_2. We now examine this explicitly.

Consider some extensive variable, q, and the

thermodynamic potential, G^q, which controls the system when q is held constant. The force conjugate to q is $Q = \left(\frac{\partial G^q}{\partial q} \right)_\varphi$. If we replace the constraint on q with one on Q, the potential becomes $G^Q = G^q - Qq$. For example, q and G^q are entropy and energy when Q and G^Q are temperature and Helmholtz free energy respectively.

In a fixed-x ensemble (x="q","Q") the effective value of K_2 is $K_2^x = \frac{1}{2} \left(\frac{\partial^2 g^x}{\partial^2 \varphi} \right)_x$, where g^x is the G^x density and the derivative is evaluated at $\varphi = \varphi_o$. A simple calculation then shows $K_2^Q = K_2^q + \frac{1}{2} \left(\frac{\partial Q}{\partial \varphi} \right)_{q^*} \left(\frac{\partial q^*}{\partial \varphi} \right)_Q$, where q^* is the q density. The analogous formula for K_1 is obtained by replacing "φ" with "$\vec{\nabla}\varphi$". The obvious generalization to the several variable case allows us to relate the elastic constants of one ensemble to those of any other. Since membranes have generally been studied under isothermal isobaric conditions, we derived K_1 and K_2 from the Gibbs free energy. In other ensembles, K_1 and K_2 have different values, but the theory is otherwise unchanged. We can thus ignore thermodynamic variables other than φ, though they do have some effect.

In the absence of constraints on φ, the equilibrium state of the lipids is $\varphi = \varphi_o$. However, proteins force the adjacent OP to some other value. Our goal is find the equilibrium OP then. Minimizing the energy yields the field equation:

$$\left(\frac{\nabla^2}{\eta^2} - 1\right)\varphi + \varphi_o = 0 \qquad (2$$

where $\eta^2 = K_2/K_1$. The solution to this equation is the desired OP.

η^{-1} is a correlation length which frequently appears in this theory. Whenever a spatial variable, r, occurs in final results, it is always in the combination ηr. For instance, a perturbation at the origin yields an effect of the form $\exp(-\eta r)$, so that its range is roughly η^{-1}. Lipid-mediated protein interactions will be seen to have a similar range.

Equation 2 is the foundation of the theory. Solving it is the first step in finding the energy of any protein arrangement. Substituting the solution back into equation 1 gives the energy density. Finally, the total energy is obtained by integrating this density over the entire membrane. Repeating this process for various configurations yields their relative energies.

In the next several sections, this is done for membranes containing one or two protein particles. We start by describing the boundary conditions for the field equation.

2. PROTEIN-LIPID INTERACTIONS

Our next task is to specify how proteins affect the OP. Microscopic models start by considering how the interaction of lipids with a protein particle changes their configurational potential. Thermodynamics lets us avoid this complexity. We assume that the OP is forced to to some value, $\bar{\varphi}$, adjacent to proteins. In a more detailed theory, $\bar{\varphi}$ would represent the lowest energy state of the lipids there. We later examine this point in greater detail.

We also need to specify the shape of protein particles. We assume them to be circles of radius r_o. Freeze-fracture pictures show this to be a crude simplification. It does not matter, though. The OP is roughly constant over distances comparable to κ^{-1}, so that we can ignore details of protein shape when $r_o \ll \kappa^{-1}$. We will later find this to be the case.

We can now solve the field equation. The boundary conditions are $\varphi = \bar{\varphi}$ on the protein perimeter, and $\varphi \to \varphi_o$ far from it. For simplicity, we take the protein to be centered on the origin. We can then find φ_1, the OP when there is only one protein particle:

$$\varphi_1(\vec{r}) = \varphi_o + (\bar{\varphi} - \varphi_o)\, e^{-\kappa(r-r_o)} = \varphi_o + \Delta\, e^{-\kappa r} \qquad (3$$

where $\Delta = (\bar{\varphi} - \varphi_o)\, e^{\kappa r_o}$, and $\vec{r}$ is some point in the membrane. The system is rotationally symmetric, so that φ_1 depends

only on the magnitude of $\vec{r}$. Δ is a measure of how much the lipids are perturbed by proteins. In the absence of a molecular interpretation for the OP, $\bar{\varphi}$, φ_o, and r_o are significant only via their combination in Δ.

We next compute the self energy, the difference in OP energy between a membrane with one particle, and one with none. The OP energy is zero in the absence of protein, so that we can find the self energy, E_1, by substituting φ_1 into equation 1 and integrating over the membrane:

$$E_1 = \int d^2\vec{r}\, \epsilon[\varphi_1(\vec{r})] = 2\pi K_1 \Delta^2 (\eta r_o + \tfrac{1}{2}) \qquad (4$$

Since lipids are excluded from the interior of the protein, the integral has been limited to the region $r > r_o$. It often occurs that $\eta r_o \ll 1$, in which case $\Delta \sim \bar{\varphi} - \varphi_o$ and:

$$E_1 \sim \pi K_1 (\bar{\varphi} - \varphi_o)^2 \qquad (5$$

E_1 is an important quantity, which repeatedly turns up in our results. The most obvious role of E_1 immediately follows from its definition. The change in OP energy when a particle moves from one lipid phase to another is the difference of E_1 between them. This equals the free energy of transfer when the OP-independent interactions are the same in both phases. Thus E_1 can control the partition of proteins between coexisting lipid phases.

E_1 also scales the lipid-mediated interactions between proteins. Our potentials always contain a factor of E_1, so

that comparisons with other interactions, of magnitude E*, depend on the ratio E_1/E^*. For instance, it will be seen that the lipid-mediated interactions sometimes cause protein aggregation. This is opposed by thermal motions, with typical energy k_BT. The aggregation tendency is thus controlled by the ratio E_1/k_BT. Large values of it are conducive to aggregation.

Let us now examine some approximations implicit in the preceding discussion. So far, we have represented protein-lipid interactions by setting the OP equal to $\bar{\varphi}$ adjacent to the protein. In reality, these interactions extend away from it, and $\bar{\varphi}$ may be lipid-dependent. We can estimate the error as follows.

We start by studying the lipids adjacent to a protein. The non-gradient part of their energy was previously $\mathcal{E}_n = K_2(\varphi - \varphi_o)^2$. They were coupled to the protein only via the boundary conditions. In more detailed models, it adds another term to their energy density. $\mathcal{E}_n$ then becomes $\mathcal{E}^* = \mathcal{E}_n + K_3(\varphi - \varphi^*)^2$. K_3 and φ^* describe the protein-lipid interaction. By the same reasoning as before, the K_3 term is the simplest plausable coupling.

$\mathcal{E}^*$ is minimal when $\varphi = \dfrac{K_2\varphi_o + K_3\varphi^*}{K_2 + K_3} \equiv \bar{\varphi}$. Earlier, we assumed that $\bar{\varphi}$ was independent of the lipid. We see here that this is equivalent to $K_3 \gg K_2$: then $\bar{\varphi} = \varphi^*$.

Otherwise, $\bar{\varphi}$ is influenced by the lipids, moving from φ^* towards φ_o as K_3/K_2 falls. Detecting this would require systematic comparisons of E_1 between various lipids: this remains for the future. In any particular phase, the only consequence is a reduction in the effective value of E_1.

When calculating the total energy, we integrated ε_n over the entire membrane. We should have instead used ε^* near the protein. We now estimate the error. If the protein-lipid interaction extends a distance L, it affects an area of roughly $2\pi r_o L$. In that region, $\varphi \sim \bar{\varphi}$, so that:

$$\varepsilon^* - \varepsilon_n = K_2 R(\varphi^* - \varphi_o)^2 \sim \eta^2 R E_1/\pi \qquad (6$$

where $R=K_2K_3/(K_2+K_3)^2$. The error is thus $2r_oL\eta^2RE_1$, which is small when $2r_oL\eta^2R \ll 1$. We are interested in the case $K_3 > K_2$, so that $R < 1$. It will later be seen that $\eta r_o \sim 1/5$ to $1/2$. L is harder to estimate, but is probably comparable to the range of the direct interactions between proteins, roughly 1 to 5 nm. We will also find that η^{-1} is roughly 10 nm, so that $\eta L \sim 1/10$ to $1/2$. We finally obtain $2r_oL\eta^2 \sim 1/25$ to $1/2$. The error is thus small, especially when $K_3 \gg K_2$.

We have also assumed that the internal state of the protein does not depend on the adjacent lipids. If, for instance, binding a specific lipid caused a conformational

change in the protein, then that lipid could affect r_o or $\overline{\varphi}$. As with the other approximations, this would matter only in comparisons between different membranes. We can ignore it here.

3. PROTEIN-PROTEIN INTERACTIONS

Our next task is to calculate the protein-protein interaction potential, V(r'), where r' is the separation. We start by specifying the boundary conditions and solving the field equation. We can then calculate E_2, the OP energy of a membrane containing two protein particles. Then $V = E_2 - E_1^{(1)} - E_1^{(2)}$, where $E_1^{(1)}$ and $E_1^{(2)}$ are the self energies of the two particles, not necessarily the same.

The potential is experimentally detectable only in large populations of particles. Though the two particle analysis is useful for getting a crude picture of the many particle case, a more complicated theory is needed to focus it. This section serves as background to that theory.

If one attempts to calculate E_2 by imitating the method used for E_1, the field equation is intractable. The difficulty arises because the boundary consists of two circles, which require the use of bipolar coordinates.[10] They separate the Laplacian, but unfortunately, not our field equation. We avoid this by setting $\varphi = \varphi_0 + (\bar{\varphi} - \varphi_0)e^{\eta r_0}$ at the particle center. This is equivalent to the previous boundary condition in the one particle case. However, it introduces an error in the two particle case because φ is then not held constant on the protein perimeters. But $\eta r_0 \ll 1$, so that φ is

nearly constant in regions the size of a protein, and the error is small.

Consider a protein particle centered at the origin, and one at $\vec{r}'$. Call the former "1" and the latter "2", appending these subscripts to Δ and $\bar{\varphi}$. For simplicity, we assume that their radii are equal. These definitions are shown in figure 2.

We can now solve the field equation, and find φ_2, the OP when there are two particles:

$$\varphi_2(\vec{r}) = \varphi_o + C_1\, e^{-\eta|\vec{r}|} + C_2\, e^{-\eta|\vec{r}-\vec{r}'|} \qquad (7$$

with: $$C_{\substack{1\\2}} = \tfrac{1}{2}\,\mathrm{csch}(\eta|\vec{r}'|)\,(\Delta_{\substack{1\\2}}\, e^{\eta|\vec{r}'|} - \Delta_{\substack{2\\1}}) \qquad (8$$

Substituting φ_2 into equations 1 and 4 we get:

$$E_2(r') = E_1^{(1)} + E_1^{(2)} + 2\,K_2(C_1^2 - \Delta_1^2 + C_2^2 - \Delta_2^2)\,N(0) + 4\,K_2\,C_1\,C_2\,N(r') \qquad (9$$

with: $$N(r') = \int d^2\vec{r}\;\exp(-\eta|\vec{r}|)\,\exp(-\eta|\vec{r}-\vec{r}'|) \qquad (10$$

We have made the approximation of integrating ε over the entire membrane, including the protein interiors. This introduces negligible error: each factor in $N(r')$ is significant over a region of radius roughly η^{-1} whose area is $\pi\eta^{-2}$, while the area of each particle is πr_o^2. The error is thus of order $\eta^2 r_o^2$, which is small since $\eta r_o \ll 1$ in cases of interest.

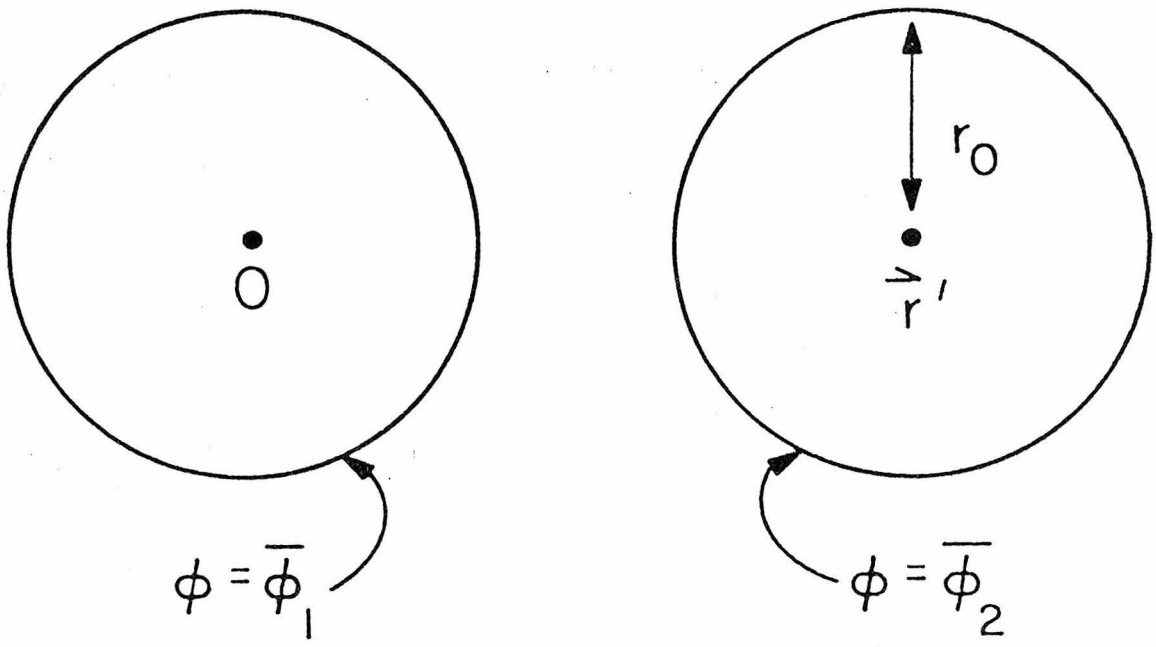

2. Two particle boundary conditions. The circles represent protein particles.

Introducing the notation:

$$u = e^{\eta r'} \qquad F = \Delta_1/\Delta_2 \qquad S = \sinh \eta r' \tag{11}$$

we get:

$$V(r') = \frac{E_1^{(2)}}{4S^2}\left[-4Fu + (F^2+1)(3-u^{-2}) + 2Q(r')(Fu^2 - (F^2+1)u + F)\right] \tag{12}$$

where $Q(r') = N(r')/N(0)$.

Although this expression is cumbersome, it simplifies in several useful cases. We first consider its numerical value, shown in figure 3. It can be seen that the potential has an attractive core, which is surrounded by a repulsive barrier when $F > 0$. The height and radius of the barrier both increase with F, as shown in figure 4. At large distances, V becomes a decreasing exponential, which is repulsive or attractive for $F \leq 0$ or $F > 0$ respectively.

The most important case is F=1, corresponding to identical proteins. Here, the attractive core has a depth of E_1 and is surrounded by a barrier, roughly of height $E_1/3$. Before we study these results in detail, we consider their significance.

We have now seen the most important prediction of the theory: proteins which perturb the OP also bind to one another. Under some circumstances this leads to a slight clustering tendency; but under others, precipitation

captions

3. Numerical evaluation of the two particle potential, equation II.A.12. Results for various values of $F < 0$ are shown in A; and for $F > 0$ in B. The case $F=1$ is shown on an expanded scale in C.

4. Height and location of the barrier in the two particle potential. The upper curve shows the barrier energy, V_m; the lower shows its location, d.

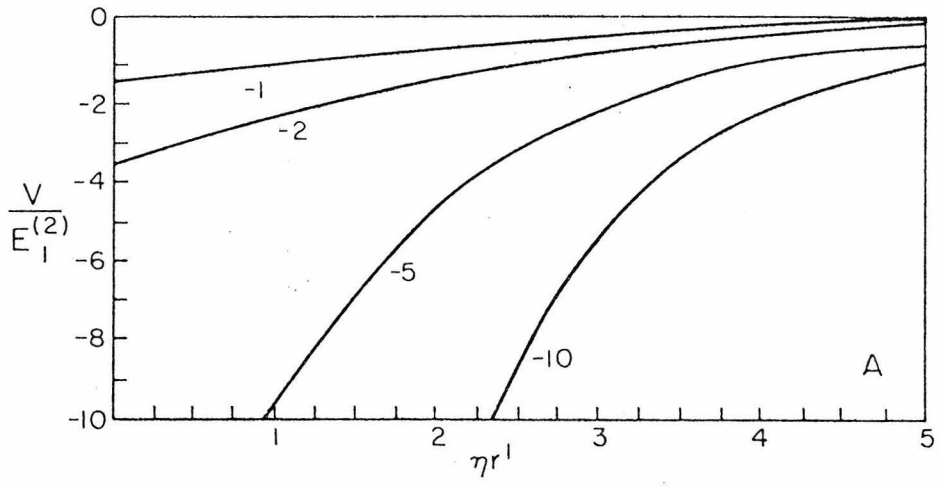
0
-2
-4
-6
-8
-10
V / E(2)1
-1
-2
-5
-10
A
1
2
3
4
5
ηr1

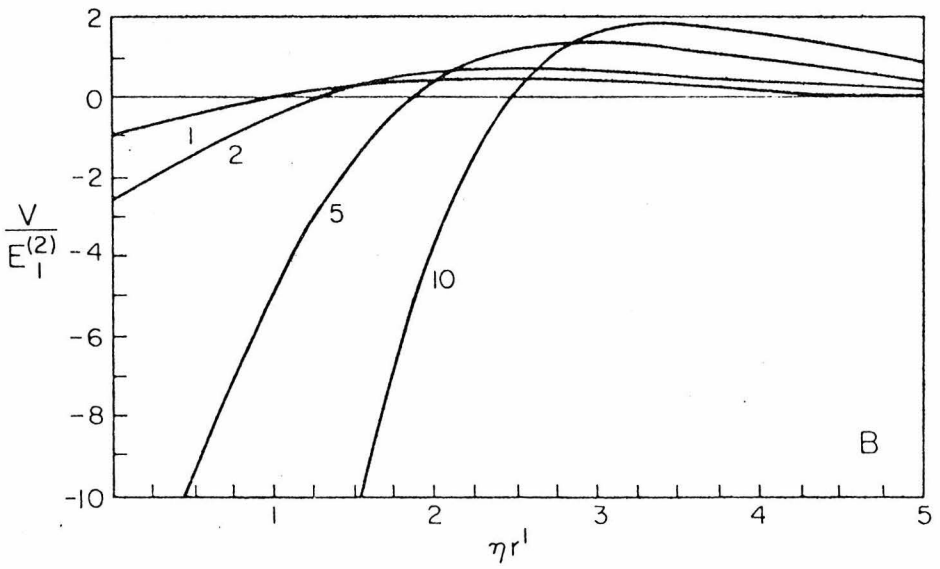
2
0
-2
-4
-6
-8
-10
V / E(2)1
1
2
5
10
B
1
2
3
4
5
ηr1

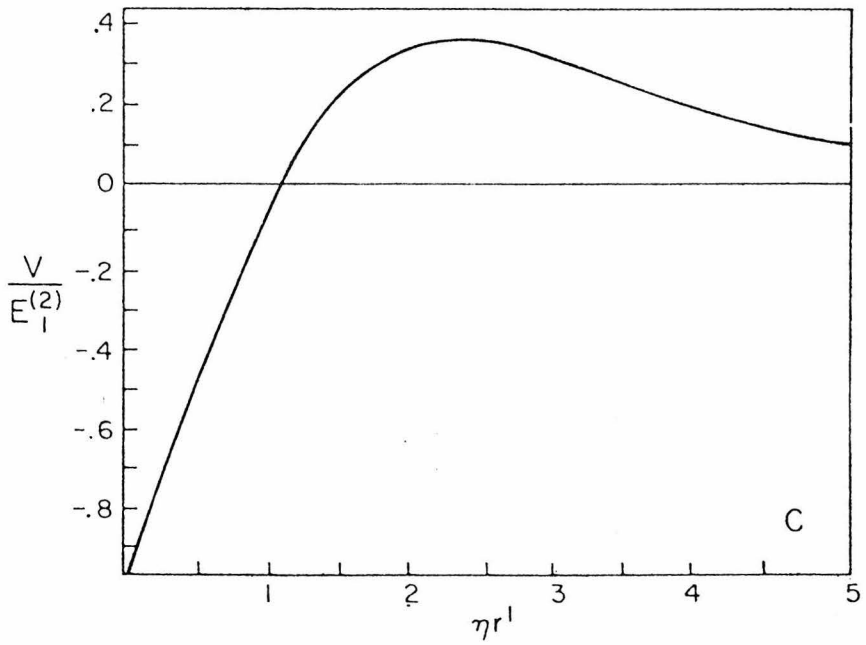
.4
.2
0
-.2
-.4
-.6
-.8
V / E(2)1
C
1
2
3
4
5
ηr1

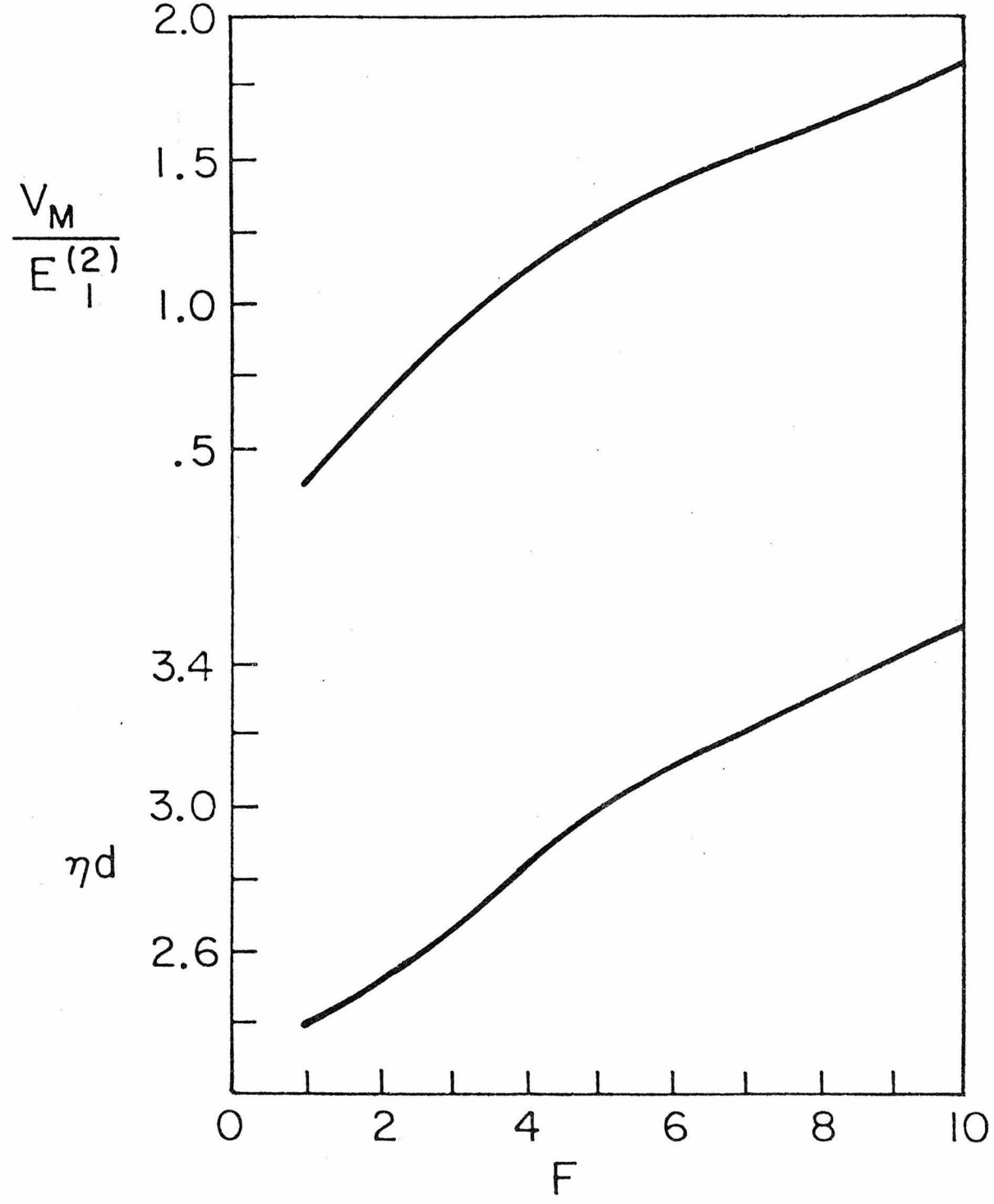
2.0
1.5
$\frac{V_M}{E_1^{(2)}}$
1.0
.5
3.4
3.0
ηd
2.6
0
2
4
6
8
10
F

of large aggregates. We can estimate when each occurs by noting that the barrier is near $\pi r' = 2.5$. The mean nearest neighbor separation is thus less than the distance of maximal repulsion when the number density of particles exceeds $\frac{1}{\pi}\left(\frac{\pi}{2.5/2}\right)^2 \sim \pi^2/5$. Aggregation is then opposed only by thermal motions, and happens at sufficiently low temperature. We will later see that it can occur at even lower densities, though it is then retarded by the barrier.

Detailed analysis of the theory's experimental significance will be deferred until it is generalized to the many particle situation. We first study the two particle case in more detail, using approximations which let us understand its gross features.

We start with the short range behavior. When $\pi r' \ll 1$ $Q(r')$ becomes 1, so that $V(r')$ is:

$$E_1^{(2)} \quad \frac{2F(u^2+1) - 2(F+1)^2 u + (F^2+1)(3-u^{-2})}{(u - u^{-1})^2} \qquad (13$$

Setting $F=1$ and dropping the superscript from E_1, we find:

$$V = 2 E_1 \quad \frac{u^2 - 2u - 1}{(u+1)^2} \sim \tfrac{1}{2} E_1 (u^2 - 2u - 1) \qquad (14$$

since $u+1 \sim 2$.

We first calculate the binding energy, the change in energy when two particles move from infinite to zero separation. We find it by setting $r'=0$: V is then $-E_1$.

One might have guessed that even without mathematics. When the two particles are superimposed, the OP is that of a single particle. The total energy is then E_1, while it is $2E_1$ when they are far apart. The energy change when they bind is thus $-E_1$.

We find the binding energy in the case $F \neq 1$ by applying l'Hopital's rule twice to equation 13 at $r'=0$:

$$V_b = V(0) = -\tfrac{1}{4} E_1^{(2)} (3F^2 - 2F + 3) \qquad (15$$

This is shown in figure 5. One sees that V_b is always negative, and reaches its maximum value at $F=2/3$, where it is $-\frac{3}{4} E_1^{(2)}$. We can explain this behavior as follows. The two particle OP is the mean of the single particle OP's at distances much greater than r' away from the proteins. Since the energy depends quadratically on the OP, its difference between the interacting and non-interacting cases is proportional to:

$$\left(\frac{\Delta_1 + \Delta_2}{2} \right) - \Delta_1^2 - \Delta_2^2 = -\tfrac{1}{4} (3F^2 - 2F + 3)\Delta_2^2 \qquad (16$$

This estimate agrees with equation 15.

We next turn to the barrier, present for $F > 0$. Its location is $\eta r'=2.5$ when $F=1$. To understand why, consider the following estimate of its position. Note that the repulsive term in the numerator of equation 13 which most rapidly grows with increasing distance is $2Fu^2$. It was preceded by a factor of $Q(r')$ in the exact equation. Each

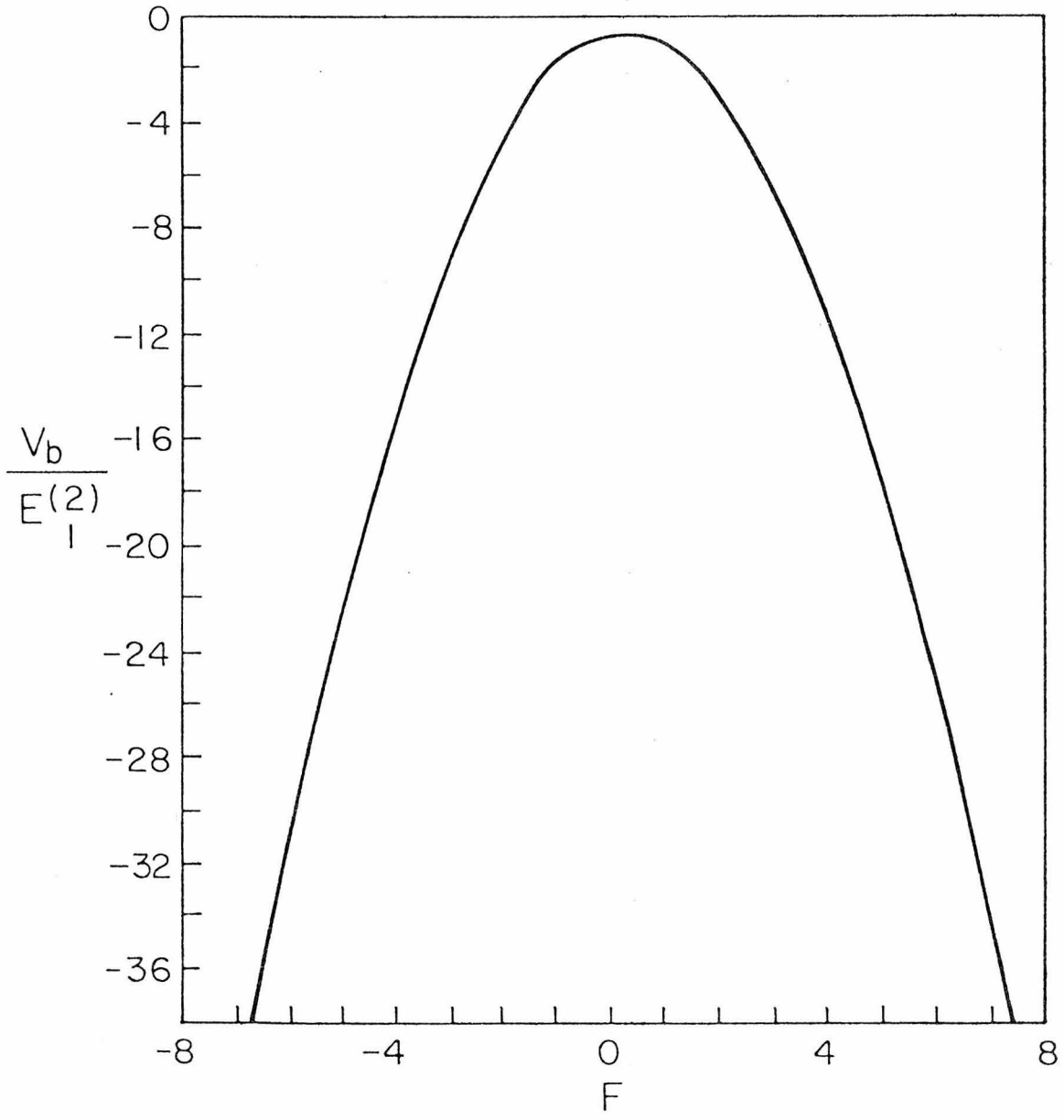

5. Two particle binding energy, equation II.A.15.

of the exponentials in Q(r') is significant in a circle of radius κ^{-1}. (Note equation 10.) When the separation of their centers increases to $2\kappa^{-1}$, their overlap becomes small, so that Q(r') does too. This is verified by looking at the numerical value of Q(r'), shown in figure 6. We thus guess that the barrier is near $\kappa r'=2$.

We finally consider an intuitive explanation for the qualitative behavior of V(r'). Its attractive component is caused by shrinkage of the region perturbed by the proteins as they approach one another. The barrier reflects an opposing process which also occurs then: growth of the perturbation in the region between the particles. This produces the barrier, while the former effect eliminates it at short distances. We can compare them as follows. The region "between" the proteins has width r' and length κ^{-1}, so that its area is $r'\kappa^{-1}$. The perturbation there is proportional to $2\ e^{-\frac{1}{2}\kappa r'}$ in the interacting case, while non-interacting particles would each produce one of $e^{-\frac{1}{2}\kappa r'}$. Thus the energy difference, per unit area there, is proportional to $(2\ e^{-\frac{1}{2}\kappa r'})^2 - 2(e^{-\frac{1}{2}\kappa r'})^2 = 2\ e^{-\kappa r'}$. Multiplying by the area, we find that the contribution to the potential arising from the perturbation increase is proportional to $r'\ e^{-\kappa r'}$. This achieves its maximum value when $\kappa r'=1$. Thus we again estimate a barrier near its actual location. In contrast, we have the case $F < 0$.

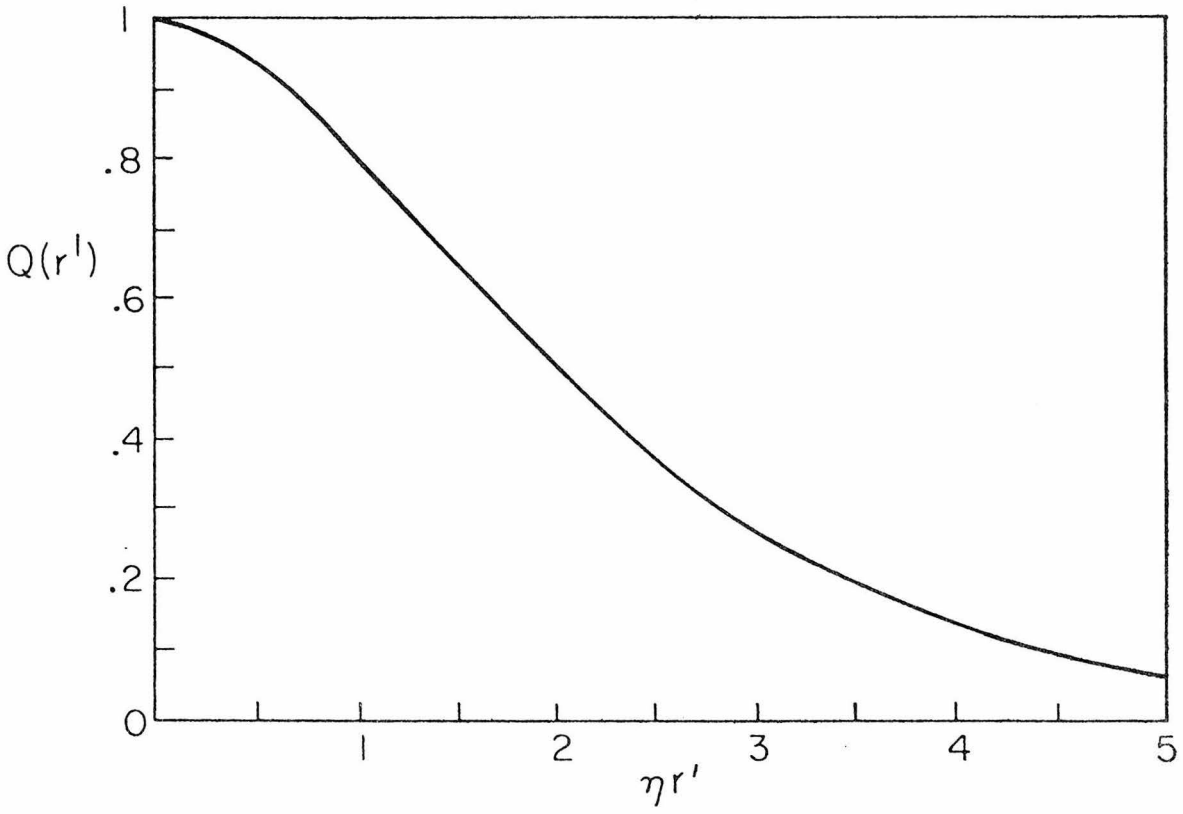

6. Numerical evaluation of Q(r'), equation II.A.12.

There the potential is mainly attractive. At all separations, the perturbation in the intermediate region is less than that produced by isolated proteins.

B. MANY PARTICLE CASE

1. INTRODUCTION

So far, we have considered membranes with only one or two protein particles. This is not experimentally realistic, however. Protein interactions are measurable only in large populations of particles. In this section we assemble the machinery needed to handle that situation.

The attractive core in the potential makes the proteins cluster. Because this is readily visible in freeze-fracture pictures, it provides an important way to test the theory. A tool needed for this is the pair correlation function: the mean density of particles at a given distance from any particular one. Actual measurements of it are described in section III. We are concerned here with its relation to the potential.

The basic goal of this section is to derive a formula specifying when aggregation occurs. It will also be seen that the strength of the interactions between particles falls as their concentration rises. When they form a precipitate, this weakening is limited to the particles within it.

We need to know the energy of membranes with many particles before studying these issues. The ensemble averaging needed for this is somewhat complicated. The

reader interested only in the biological significance of the theory can skip over the derivations without the final results losing their comprehensibility.

We start by briefly discussing the conventional theory of the relation between potentials and pair correlation functions.[11,12] It is generally assumed that the total potential energy, V, is pairwise additive. This means that it can be expressed as a sum of two particle potentials, v_{ij}: $V = \sum_{i,j;\ i<j} v_{ij}$. It is also assumed that v_{ij} depends only on d_{ij}, the distance between particles "i" and "j", so that $v_{ij}=v(d_{ij})$. The latter assumption is clearly true in the present model, the former requires more discussion. When these assumptions are valid, we have at low densities:

$$g(R) = \rho \exp(- v(R)/k_B T) \qquad (1$$

ρ is the mean particle density and g(R) is the pair correlation function.

It is a crucial assumption that the potential is pairwise additive. However, this is invalid in the present model. It is easy to see why. The interaction between two particles depends on the difference between the OP's with and without them. Proximity to other particles changes this difference, and thus the potential. One might conclude that it is hopeless to try extracting the potential from the correlation function. It will be

seen, though, that the only effect of the non-pairwise additivity is to change the potential by a constant factor. We can thus correct equation 1 by replacing v(R) with its effective value.

2. MEAN ENERGY DENSITY

Our first task is to derive a formula for the mean energy density when the number density of particles is not negligible compared with η^2. This is useful for solving several other problems.

The first is what effect the non-pairwise additivity has on the potential. A slight modification of the calculations in this section can answer it.

Another question is when the homogeneous state is stable against aggregation. One might expect it not to be: precipitation of the proteins restricts their influence to less of the membrane, thus lowering its energy. We want to know when it decreases enough to prevent thermal motion from redispersing the proteins, and how the subsequent clustering affects pair correlation functions.

Consider a collection of identical particles at positions $\{\vec{r}_i\}$. Much as in the two particle case, the order parameter is:

$$\Phi(\vec{r}) = \Phi_o + \sum_i c_i \lambda_i \qquad (2$$

where $\lambda_i = \exp(-\eta|\vec{r}-\vec{r}_i|)$. The c_i's are coefficients we seek to determine. The first step is to obtain a set

of simultaneous equations by setting $\vec{r}$ equal to each of the particle positions, and requiring that the boundary conditions be satisfied. We use the constraint $\varphi(\vec{r}_i)=\bar{\varphi}$, reasonable when $\kappa r_o \ll 1$. Taking $\vec{r}=\vec{r}_j$, we get:

$$\bar{\varphi} - \varphi_o = \Delta = c_j + \sum_{i \neq j} c_i \lambda_{ij} \qquad (3$$

where $\lambda_{ij} = \exp(-\kappa |\vec{r}_j - \vec{r}_i|)$ for $i \neq j$, and $\lambda_{ii}=0$. We next convert this to matrix notation. We define $\vec{c} = (c_1, c_2, \ldots, c_N)$, $\vec{\Delta} = (\Delta, \Delta, \ldots, \Delta)$, λ as the matrix of λ_{ij}'s, and $\underline{1}$ as the unit matrix. Substituting into equation 3, we can formally solve it and find:

$$\vec{c} = \vec{\Delta}(\underline{1} + \lambda)^{-1} \qquad (4$$

This is trivial to evaluate in the two particle case, but becomes intractable when there are many.

The following approximation allows us to determine $\vec{c}$. We assume that the membrane is homogeneous, so that each particle's neighbors have a similar arrangement. Because of this, all of the c_i's are roughly the same. We make the simplification that they are identical. This means that we ignore spatial variation in the concentration of proteins, as well as their particulate nature. Alternatively, this can be regarded as a kind of coarse graining in which each particle's position is averaged over a range comparable to the nearest neighbor separation. In this approximation $\vec{c}=q\vec{\Delta}$ for some scalar q. Then $\vec{\Delta}$

is an eigenvector of $(\underline{1} + \lambda)^{-1}$, and thus is also one of λ : $\vec{\Delta}\lambda = s\lambda$ for some scalar s. We have $q = \frac{1}{1+s}$, so that our problem reduces to finding s.

It is useful to define two new functions closely related to the pair correlation function, g(R). Consider an annulus bounded by circles of radius R and R+dR, centered on particle "i". We define $p_i(R)\,dR$ as the mean number of particles in the annulus, and $p_{ij}(R)\,dR$ as the probability that "j" is in it. Since the area of the annulus is $2\pi R\,dR$, the mean density in it is $p_i(R)/2\pi R = g(R)$. Calling the number of particles N, the probability that any particular one is "j" is 1/N. We conclude that $p_{ij}(R) = p_i(R)/N$ and that $g(R) = \frac{N}{2\pi R}\, p_{ij}(R)$.

We start by finding component j of $\vec{\Delta}\lambda$, by definition $\Delta \sum_{i\neq j} \lambda_{ij}$. Since $\vec{\Delta}$ is an eigenvector, this is independent of j, and $s = \sum_{i\neq j} \lambda_{ij}$. We next simplify the sum by replacing each term with its expectation value: $\langle \lambda_{ij} \rangle = \int p_{ij}(r)\, e^{-\eta r}\, dr$. This is independent of i and j because the particles are identical. We thus find:

$$s = \sum_{i\neq j} \int \frac{1}{N}\, p_j(r)\, e^{-\eta r}\, dr = \frac{N-1}{N} \int p_j(r)\, e^{-\eta r}\, dr \quad (5$$

However, $(N-1)/N \sim 1$ since there are many particles. Replacing $p_j(r)$ with the pair correlation function, we get: $s = 2\pi \int g(r)\, e^{-\eta r}\, r\, dr$. This yields the solution to

equation 4:

$$c = \frac{\Delta}{1 + 2\pi \int g(r) \exp(-\eta r)\, r\, dr} = \frac{\Delta}{1+G} \qquad (6$$

We now find φ by substituting this into equation 2:

$$\varphi = \varphi_o + \frac{\Delta}{1+G} \sum_i \lambda_i \qquad (7$$

The mean energy density of the proteins is thus:

$$\langle \mathcal{E} \rangle = K_1 \langle (\vec{\nabla} \varphi)^2 \rangle + K_2 \langle (\varphi - \varphi_o)^2 \rangle \qquad (8$$

$$= 2 K_2 \left(\frac{\Delta}{1+G} \right)^2 \left(\sum_i \lambda_i \right)^2 \qquad (9$$

All that remains is to evaluate the λ sum. As before, we do this by replacing the λ's with their expectation values. We have:

$$H^2 = \left\langle \left(\sum_i \lambda_i \right)^2 \right\rangle = \left\langle \sum_i \lambda_i \sum_{j \neq i} \lambda_j \right\rangle + \left\langle \sum_i \lambda_i^2 \right\rangle$$
$$\sim \left\langle \sum_i \lambda_i \right\rangle^2 + \left\langle \sum_i \lambda_i^2 \right\rangle = H_1^2 + H_2^2 \qquad (10$$

By the same arguments as were used for the λ_{ij}'s, we find:

$$H_1^2 = (2\pi\rho \int e^{-\eta r}\, r\, dr)^2 = \left(\frac{2\pi\rho}{\eta^2} \right)^2 \qquad (11$$

The only difference is that before we were concerned with the probability for finding particles at a given distance from some particular one, but here, from a given point. Thus the pair correlation function has been replaced with the mean number density, ρ. We similarly find:

$$H_2^2 = 2\pi\rho \int e^{-2\eta r}\, r\, dr = \frac{\pi\rho}{2\eta^2} \qquad (12$$

If we neglect the correlations between particle positions, $g(R)=\rho$ so that $G=H_1$.

Collecting these results, we finally obtain:

$$\langle \xi \rangle = 2 K_2 \left(\frac{\Delta}{1+G} \right)^2 (H_1^2 + H_2^2) = 2 K_2 \Delta^2 \frac{1 + \hbar^2/8\pi\rho}{(1 + \hbar^2/2\pi\rho)^2} \qquad (13$$

This is a very important formula, needed in most derivations of experimentally testable predictions. To gain an appreciation for it, let us now consider some cases where it simplifies.

When $\rho \ll \hbar^2/8\pi$, $\langle \xi \rangle$ becomes $E_1 \rho$. This would be expected. The mean energy density is just the self energy of the particles times their concentration in dilute systems. On the other hand, for $\rho \gg \hbar^2/8\pi$ it becomes $2 K_2 \Delta^2/(1 + \hbar^2/2\pi\rho)^2$. As ρ rises still further, this eventually becomes $2 K_2 \Delta^2 = \frac{2}{\pi} E_1 \hbar^2$. We thus see that the energy density has a "hyperbolic" dependence on the concentration, saturating at high ones.

The alert reader may have noticed that, strictly speaking, the λ_{ij}-averaging used to find G should have been done after it was substituted into equation 10. We are interested in $R= \langle (\frac{1}{1+s})^2 \rangle$, which we have approximated as $R' = (\frac{1}{1+\langle s \rangle})^2$. To see what this means, we expand R as:

$$\left\langle \sum_{n=0}^{\infty} (-1)^n (n+1) s^n \right\rangle = \sum_{n=0}^{\infty} (-1)^n (n+1) G_n^* \qquad (14$$

where $G_n^* = \langle s^n \rangle$. If we set $\langle s^n \rangle = \langle s \rangle^n$, we can sum the

series and find R=R'. Let us now determine when this is a valid approximation. Imitating the evaluation of H, we find $G_0^*=1$ and:

$$G_n^* = \sum^n t_n^{a_n} t_{n-1}^{a_{n-1}} t_{n-2}^{a_{n-2}} \cdots t_1^{a_1} \qquad (n \quad 0) \qquad (15$$

where: $$t_n = 2\pi \int_0^\infty e^{-n\eta r} g(r)\, r\, dr \sim \frac{2\pi\rho}{n^2\eta^2} \qquad (16$$

$\sum^n$ denotes the sum over all sets, $\{a_i\}$, of non-negative integers such that $\sum_{i=1}^{n} i\, a_i = n$.

G_n^* may be approximated by t_1^n except when $\frac{2\pi\rho}{\eta^2} \ll 1$. Then, however, the other terms do not matter because $G_n^* \sim 0$ for $n > 0$. For instance, note that the next largest term is $t_2 t_1^{n-2} = \frac{1}{4} t_1^{n-1}$. Whenever this is comparable to t_1^n, both are small. Thus, in either case $\langle s^n \rangle \sim \langle s \rangle^n$, so that $R \sim R'$.

Strictly speaking, this analysis is invalid when $\langle s \rangle > 1$ because the series diverge. However, the λ's are all less than one, so that we can expand R as a series in each of them. This method is much more complicated, but yields the same conclusion.

3. DEVIATIONS FROM PAIRWISE ADDITIVITY

We next consider the potential's deviation from pairwise additivity. Our procedure is practically identical to that used in the last section. We select two particles, "A" and "B". Their interactions with each other are calculated exactly, while those involving others are absorbed into ensemble averages.

We start from the obvious generalization of equation 2:

$$\varphi(\vec{r}) = \varphi_o + \sum_i c_i \lambda_i + c_A \lambda_A + c_B \lambda_B \qquad (17$$

If we now set $\vec{r}=\vec{r}_j$ this becomes:

$$\Delta = c_j + \sum_{i \neq j} c_i \lambda_{ij} + c_A \lambda_{Aj} + c_B \lambda_{Bj} \qquad (18$$

"A" and "B" are greatly outnumbered by the other particles, so that their effect on the OP is negligible except very close to them. We thus have $\sum_{i \neq j} c_i \lambda_{ij} \gg c_A \lambda_{Aj} + c_B \lambda_{Bj}$ unless j=A or j=B. We can thus approximate equation 18 as:

$$\Delta = c_j + \sum_{i \neq j} c_i \lambda_{ij} \qquad (19$$

Since we have ignored the effect of "A" and "B" on their neighbors, this is the same as equation 3. By setting $\vec{r}=\vec{r}_A$, and using the previously derived solution for the c's, we find:

$$\Delta_A = \frac{\Delta H}{1+G} + c_A + c_B \lambda_{AB} \qquad (20$$

Setting $\vec{r}=\vec{r}_B$, we get a similar equation with "A" and "B" interchanged.

If we now assume that "A" and "B" are identical to the other particles $\Delta_A = \Delta_B = \Delta$, and we find:

$$c_A = c_B = \frac{\Delta}{1 + \lambda_{AB}} \left(1 - \frac{H}{1+G}\right) \qquad (21$$

In the two particle case, we found in equation II.A.8:

$$c_A = c_B = \frac{\Delta}{1 + \lambda_{AB}} \qquad (22$$

Comparison with the calculations of section II.A.3 thus shows that the background of other particles changes the two particle potential by a factor of $(1 - \frac{H}{1+G})^2$.

We can ignore H_2 because $H_2 \ll 1$ whenever $H_2 \gtrsim H_1$. If we set $H=H_1$ and use the other approximations of the previous section, the factor becomes $\left(\frac{\hbar^2}{\hbar^2 + 2\pi\rho}\right)^2$. At low densities, where $\rho \ll \hbar^2/2\pi$, it becomes unity. This means that the potential is pairwise additive, and identical to that in section II.A.3. On the other hand, it becomes $(\hbar^2/2\pi\rho)^2$ when $\rho \gg \hbar^2/2\pi$. In this case, the potential is weakened by its non-pairwise additivity.

This saturation has an important consequence when the proteins precipitate. The interactions between those within clusters are much weaker than of those outside. Both the binding strength and the barrier height are decreased. This increases the rate constants both for

binding and unbinding, the latter to a greater extent. Clustering may thus increase the initial rate of reactions in which the rate limiting step is the diffusion of enzyme and substrate proteins to or from each other. Proteins outside clusters still have to overcome the barrier to get in, so that this rate enhancement lasts only until the substrate originally in clusters is depleted.

It can be seen that the density dependence of the two particle potential is very similar to that of the mean energy density. We can understand this by noting that proteins shift the mean value of φ from φ_o to $\varphi_o + \Delta(\frac{H}{1+G})$. The effective value of Δ then becomes $\Delta(1 - \frac{H}{1+G})$, thus accounting for equation 21. On the other hand, the energetic cost of this shift is proportional to its square, as seen in equation 13.

4. STABILITY ANALYSIS

We have previously mentioned that the attractive core in the potential makes the proteins prone to aggregation. This is prevented by thermal motions at low densities, and by the weakening of the potential at high ones. Aggregation may occur at intermediate densities. We seek the boundaries between these behaviors.
We do this by determining whether protein diffusion amplifies or relaxes concentration gradients.

If we neglect changes in the number of particles, we have the conservation law:

$$\frac{\partial \rho}{\partial t} = -\vec{\nabla} \cdot \vec{J} \qquad (23$$

where $\vec{J}$ is the number flux of proteins. In linearized nonequilibrium thermodynamics[13-15] $\vec{J}$ is given by:

$$\vec{J} = -\rho M \vec{\nabla} \mu \qquad (24$$

where M is $D/k_B T$ and D is the protein diffusion coefficient. The protein chemical potential, μ, is:

$$\mu = \mu_o + \frac{\partial \langle \varepsilon \rangle}{\partial \rho} + k_B T \ln \rho \qquad (25$$

μ_o is its value in the reference state, taken here as proteins at unit density in a hypothetical membrane where $\Phi_o = \overline{\Phi}$: there the OP energy is zero. This energy gives rise to the second term. The last term is produced by the

ideal entropy. In a more exact theory, it would be the entropy of mixing proteins and lipids. We use its ideal value as a convenient approximation. For instance, the Flory-Huggins model[16] reduces to this form when the area fraction of the membrane occupied by proteins is small. The final answer is not very sensitive to the entropy, however. We could even ignore it without serious error at low concentrations.

Diffusion can inhibit aggregation only if $\vec{J}$ is antiparallel to $\vec{\nabla}\rho$. When they are parallel, proteins diffuse up concentration gradients. Equation 23 then predicts cluster growth. If we set $\rho\vec{\nabla}\mu = f(\rho)\vec{\nabla}\rho$, then stability against aggregation is equivalent to $f(\rho) > 0$. From equations 13 and 25 we find:

$$f(\rho) = \rho\frac{\partial\mu}{\partial\rho} = 8\,E_1\frac{\pi\rho}{\eta^2}\,\frac{1-7\pi\rho/\eta^2}{(1+2\pi\rho/\eta^2)^4} + k_BT \qquad (26$$

Our task is to find when f is negative. That happens when ρ is between the stability limits, values of ρ where f vanishes. For $\rho < \eta^2/7\pi$ both terms are positive, so f is too. When ρ increases beyond $\eta^2/7\pi$, the first term, and eventually f, become negative. Further growth of ρ augments the denominator more than the numerator, so that the magnitude of the first term eventually becomes less than k_BT. f becomes positive again.

Numerical evaluation of equation 26 yields the results shown in figure 7. It can be seen that the proteins are stable against aggregation at all densities when $E_1 < 1.5\ k_B T$. Then the attractive core in the potetial produces some clustering, though it is too weak to yield large aggregates. This is also the case in the low density stable region. Protein concentration fluctuations are amplified in unstable membranes, thus producing a precipitate. We later examine this in more detail. The lower stability limit is asymptotic to $\rho = \ell^2/7\pi$: aggregation never occurs when ρ is smaller than that, no matter how large E_1 is.

This discussion suggests several factors which may control the aggregation tendency of membrane proteins. The most obvious is the protein concentration, but there are also more subtle ones. Recalling the value of E_1 (equation II.A.5), one sees that it can be changed by varying Δ. One way to do this is via the protein, for instance by conformational or covalent modification. This could account for aggregation induced by proteolysis[17-19] or ligand binding.[20,21] The other way to change Δ is via the lipids. An example of this may be provided by drugs, such as primaricin, nystatin, and amphotericin B, which bind to the lipids and also cause protein aggregation.[22] Phospholipases[18,23] and lipid phase transitions can also

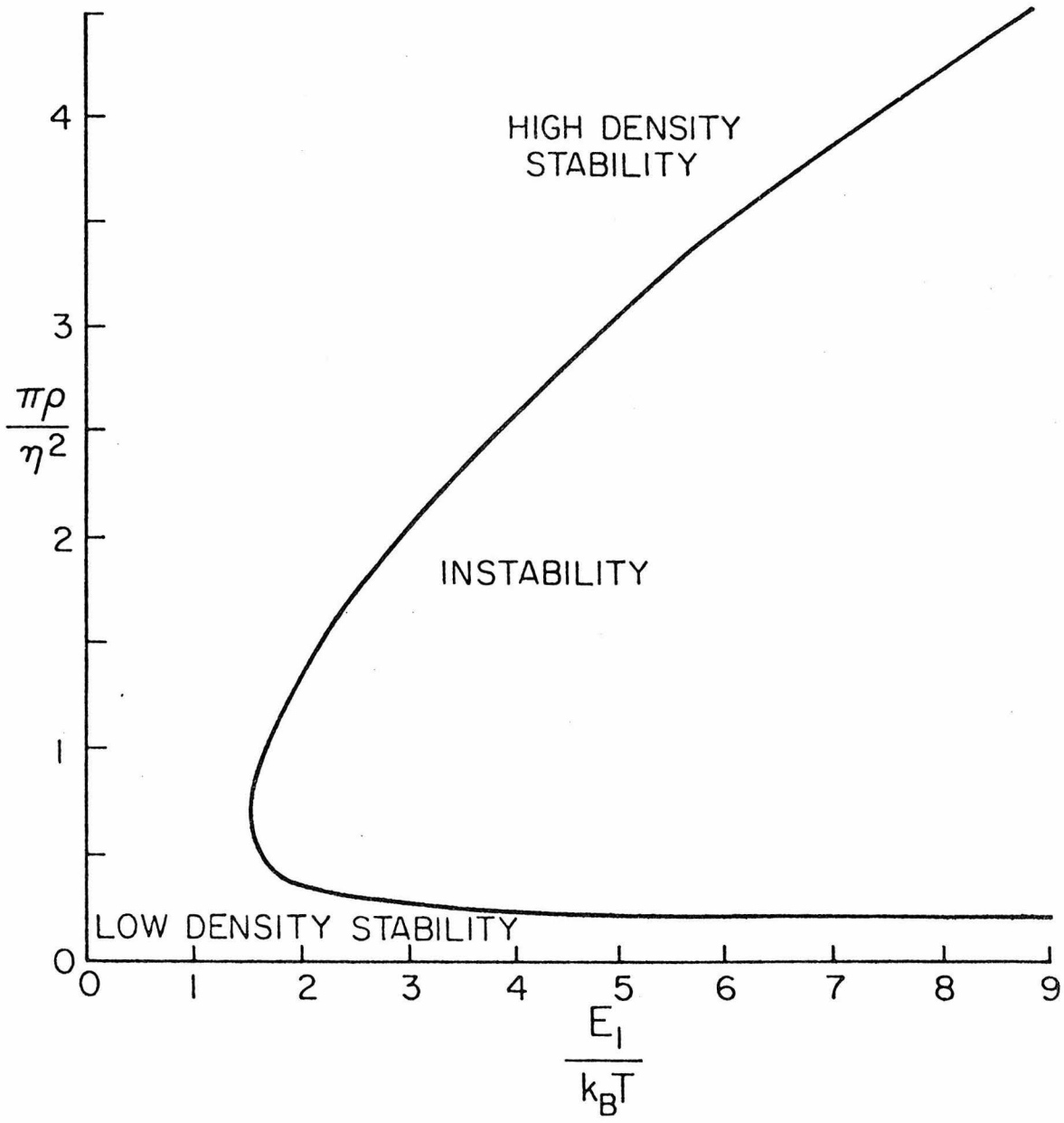

7. Results of the diffusional stability analysis.

make the proteins aggregate. The latter are more fully discussed later. Finally, the lower stability limit can be depressed by crosslinking agents, such as antibodies and lectins,[24-29] which produce additional attractions between the proteins.

We have so far considered only small deviations from uniformity. Once a region of increased density arises in an unstable membrane, it contracts until it becomes close-packed or reaches the upper stability limit. As this occurs, the particles must penetrate the repulsive barrier and bind one another. This barrier produces a corresponding one for cluster condensation, thus retarding it. When it is sufficiently slow, there may be hysteresis in membrane response to agents, such as temperature, which affect the aggregation tendency.

The following simplified picture of a cluster can be used to estimate the barrier height. Consider a collection of particles occupying a circular region of radius r. The mean particle density is $\rho = n/\pi r^2$ within the cluster. The mean energy density there is given by equation 13. Multiplying by πr^2, the area of the cluster, we find its internal energy:

$$E_{int} = \pi r^2 \langle \varepsilon \rangle = 2 K_2 \Delta^2 \pi r^2 \frac{1 + \kappa^2/8\pi\rho}{(1 + \kappa^2/2\pi\rho)^2} \quad (27$$

The cluster radius is controlled by the pressure, $P = -\frac{\partial E_{int}}{\partial a}$, where a is the cluster area. When P is negative, condensation is no longer retarded by the inter-particle potential. The barrier is thus the energy needed to compress the cluster from r_1, its initial radius, to r_c, where P vanishes: $E_{int}(r_c) - E_{int}(r_1) = -\int_{r_1}^{r_c} P\, dA$. This expression ignores the ideal contribution to the pressure. However, we are interested in the case $E_1 \gg k_B T$, so that the error is small.

We have also neglected the interfacial energy produced by the extension of the protein perturbation away from the cluster. This energy is several times E_1 per cluster, while the internal energy is rougly E_1 per particle, except in implausibly small clusters. We can thus ignore the interfacial energy unless there are only a few particles.

E_{int} is maximal for $\rho = n^2/2\pi$; it is then $\frac{5}{4}\, n\, E_1$. On the other hand, $\rho \sim n^2/7\pi$ near the lower stability limit, so that $E_{int} = \frac{105}{162}\, n\, E_1$ there. As the cluster contracts from some density near the stability limit to one near the barrier, the increase in its energy is $(\frac{5}{4} - \frac{105}{162})\, n\, E_1 \sim \frac{5}{8}\, n\, E_1$. The energy of each particle thus increases by $\frac{5}{8}\, E_1$. When this is sufficiently large compared to $k_B T$, cluster contraction beyond the barrier is retarded or prevented.

The initial energy rises when the initial concentration increases beyond the lower stability limit. This lowers the effective barrier. There is no barrier when the initial density is above $n^2/2\pi$. This might have been guessed: the nearest neighbor spacing is then less than the distance of maximal repulsion. There is no barrier to surmount.

5. EFFECTS OF PROTEIN REPULSION

We will later see that there is a short-range repulsion between proteins, in addition to the lipid-mediates attraction. We now study how this affects protein aggregation. Only minor changes in the earlier calculations are needed, so that the discussion can be brief.

We start by computing $\langle \varepsilon \rangle$, the mean energy density of a protein-containing membrane. $\langle \varepsilon \rangle$ is given by equation II.B.13 when there is no repulsion. If particle centers are unable to approach more closely than some distance, D, the calculation of G requires modification. We previously approximated g(R) as ρ, meaning that correlations between particle positions were neglected. If we picture the repulsion as hard core, then g(R)=0 for $r < D$. If we neglect all other correlations, $g(R)=\rho/(1-A_f)$ for $r \geq D$. A_f is the area fraction of the membrane occupied by the cores. In most membranes $A_f \ll 1$, so that $1-A_f \sim 1$. With these approximations, G still equals H_1, except that the integration domain now starts at D rather than zero. We find:

$$G = \frac{2\pi\rho}{\eta^2} \; e^{-\eta D} \; (\eta D+1) \equiv \frac{2\pi\rho}{\eta^2} \; b \qquad (28$$

Note that b=1 when D=0, so that G reverts to its former value. Combining this with the derivation of equation

II.B.13, we obtain:

$$\langle \varepsilon \rangle = 2 K_2 \Delta^2 \frac{1 + h^2/8\pi\rho}{(b + \eta^2/2\pi\rho)^2} \qquad (29$$

In section II.B.4. we showed that the proteins are stable against aggregation whenever $f(\rho) = \rho \frac{\partial^2 \langle \varepsilon \rangle}{\partial \rho^2} + k_B T > 0$. From equation 29, we find:

$$f(\rho) = 8 E_1 \frac{\pi\rho}{\eta^2} \frac{2 - b + (b^2 - 8b)\pi\rho/\eta^2}{(1 + 2b\pi\rho/\eta^2)^4} \qquad (30$$

As one would expect, this becomes identical to equation II.B.26 when D=0.

The results of a numerical evaluation of f are shown in figure 8.A. It can be seen that the main effect of repulsion is to raise the upper stability limit. As might be guessed, there is little effect on the lower one. Few of the particles are near one another at low densities, so that the repulsion has little effect on their arrangement or energy.

In section IV.A, we set E_1 equal to minus the value of the interparticle potential at closest approach. Because the potential is greater than $-E_1$ there, this is an underestimate. We can compensate for this by plotting the stability limits in terms of $E_{1,eff}=-V(D)$, the effective value of E_1. This is shown in figure 8.B. The error caused by approximating E_1 as $E_{1,eff}$ is partially cancelled by the

caption

8. Stability limits of particles with hard core repulsion.

A. Plotted in terms of E_1.

B. Plotted in terms of $E_{1,eff}$.

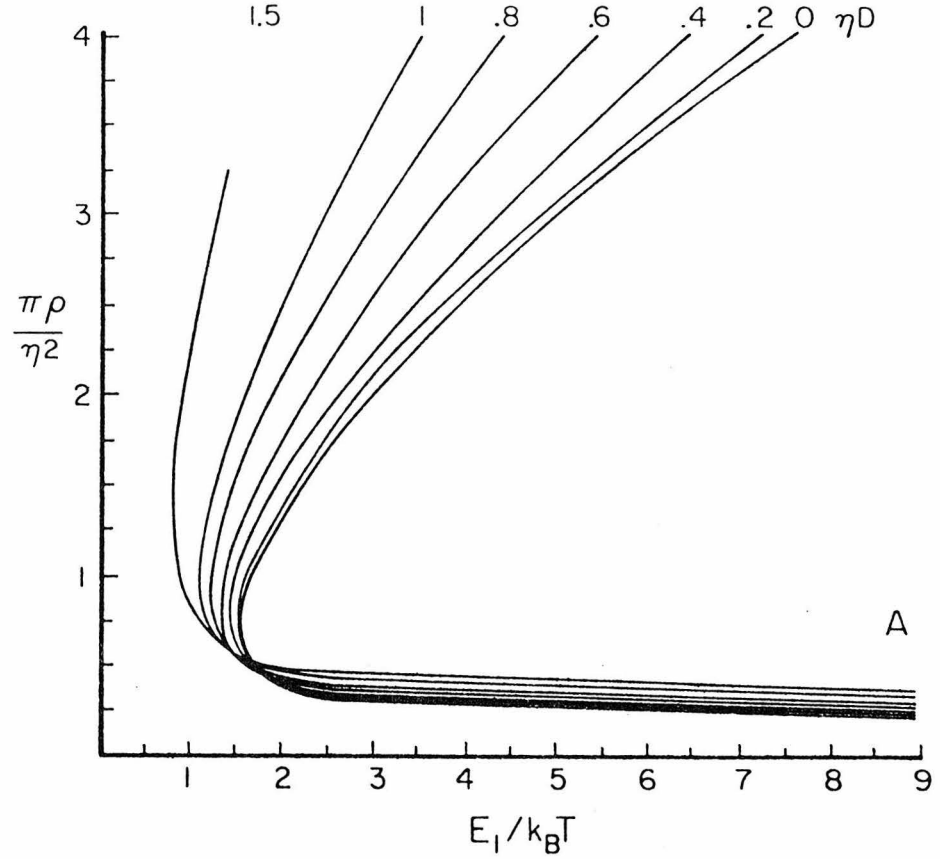
1.5
1
.8
.6
.4
.2
0
ηD
4
3
2
1
πρ/η2
A
1
2
3
4
5
6
7
8
9
E1/kBT

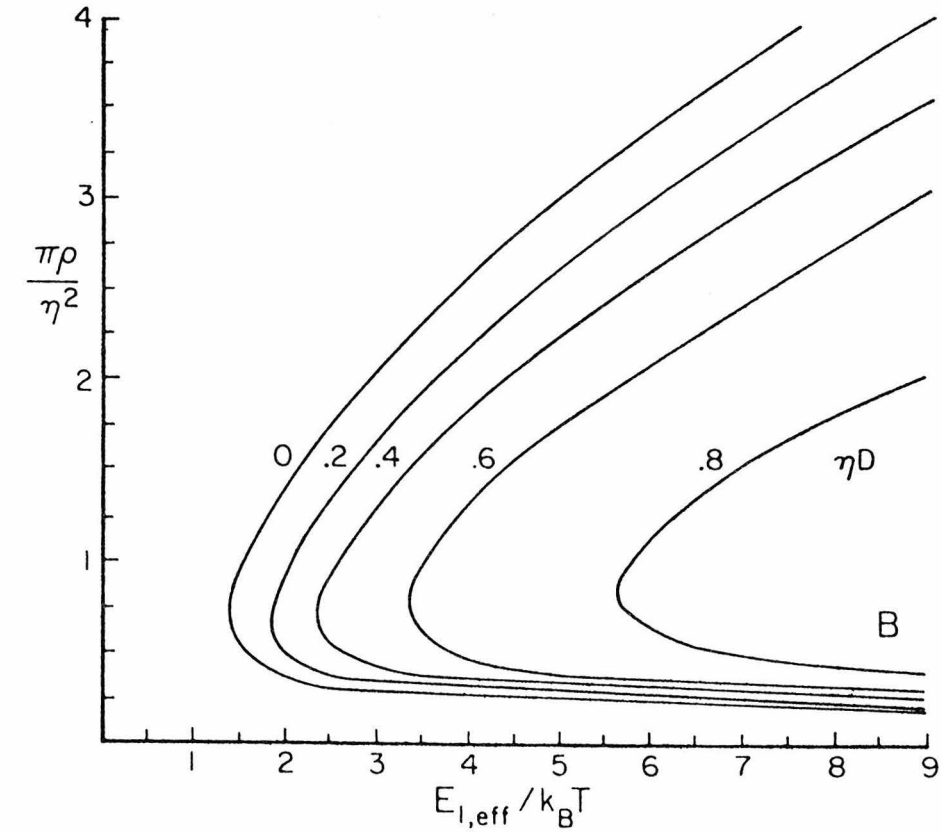
4
3
2
1
πρ/η2
0
.2
.4
.6
.8
ηD
B
1
2
3
4
5
6
7
8
9
E1,eff/kBT

shift of the stability limits.

We will see that ηD is usually between .4 and .6. Then the stability limits are shifted by a factor of roughly 2 in $E_{1,eff}$. Though this effect is significant, we ignore it in section IV.A because of the inaccuracy in present estimates of E_1, η , and D.

REFERENCES FOR CHAPTER II

1. R. Fettiplace, L.G.M. Gordon, S.B. Hladky, J. Requena, H.P. Zingsheim, & D.A. Haydon "Methods in Membrane Biology" 4: 1-95 E.D. Korn, ed. Plenum Press New York 1975
2. K.C. Chu & W.L. McMillan Phys. Rev. A15: 1181-1187 (1977)
3. J.S. Langer Ann. Phys. (N.Y.) 65: 53-86 (1971)
4. S. Marčelja, D.J. Mitchell, B.W. Ninham, & M.J. Sculley J. Chem. Soc., Faraday Trans. II 73: 630-648 (1977)
5. W. Kleemann & H.M. McConnell Biochim. Biophys. Acta 419: 206-222 (1976)
6. S. Marčelja Biochim. Biophys. Acta 455: 1-7 (1976)
7. H. Schröder J. Chem. Phys. 67: 1617-1619 (1977)
8. M.J. Stephen & J.P. Strahley Rev. Mod. Phys. 46: 617-704 (1974)
9. P.G. de Gennes "The Physics of Liquid Crystals" Clarendon Press Oxford 1974
10. P.M. Morse & H. Feshbach "Methods of Theoretical Physics" 2: 1210 McGraw-Hill New York 1953
11. S.A. Rice & P. Gray "The Statistical Mechanics of Simple Liquids" chapter 2 Interscience New York 1965
12. H. Yamakawa "Modern Theory of Polymer Solutions" Harper & Row New York 1971

13. A. Katchalsky & P.F. Curran "Nonequilibrium Thermodynamics in Biophysics" chapter 6 Harvard University Press Cambridge 1965

14. P. Glansdorff & I. Prigogine "Thermodynamic Theory of Structure, Stability, and Fluctuation" chapter 3 Wiley-Interscience London 1971

15. S.R. DeGroot & P. Mazur "Non-Equilibrium Thermodynamics" chapter 11 North Holland Amsterdam 1962

16. M.L. Huggins Kolloid Zeit. Zeit. Polym. 251: 449-455 (1973)

17. D. Branton Phil. Trans. Roy. Soc. London B261: 133-138 (1971)

18. V. Speth, D.F.H. Wallach, E. Weidekamm, & H. Knufferman Biochim. Biophys. Acta 255: 386-394 (1972)

19. Y. Yamanaka & D.W. Deamer Biochim. Biophys. Acta 426: 132-147 (1976)

20. R.B. Gunn & R.G. Kirk J. Membrane Biol. 27: 265-282 (1976)

21. C.R. Kahn J. Cell Biol. 70: 261-286 (1976)

22. Y. Kitajima, T. Sekiya, & Y. Nozawa Biochim. Biophys. Acta 445: 452-465 (1976)

23. A.J. Verkleij, R.F.A. Zwaal, B. Roelofsen, P. Confurius, D. Kastelijn, & L.L.M. Van Deenen Biochim. Biophys. Acta 323: 178-193 (1973)

24. C. DeLisi & A. Perelson J. Theor. Biol. 62: 159-210 (1976)

25. G.F. Schreiner & E.R. Unanue Adv. Immunol. 24: 37-165 (1976)

26. T.L. Steck J. Mol. Bio. 66: 295-305 (1974)

27. G.M. Edelman Science 192: 218-226 (1976)

28. K. Wang & F.M. Richards J. Biol. Chem. 249: 8005-8018 (1974)

29. G.L. Nicholson Biochim. Biophys. Acta 457: 57-108 (1975)

III. PROTEIN CORRELATION FUNCTIONS

A. METHOD OF MEASUREMENT

We next describe a method used for measuring protein pair correlation functions. Our basic goal is to find the mean density of particles at a given distance from a given one, and then average over all particles. The inputs are freeze-fracture pictures, which reveal the positions of protein particles in the plane of the membrane.[1-3]

Pictures are entered into the computer with a Tektronix Graphics Tablet, a device which notes where it is touched with a stylus. The operator places a picture on it, and then touches the stylus to the particles. It can also be used to enter other types of data, such as the membrane boundary and the length standard.

Particles are ignored if they are outside the boundary or less than a threshold distance from another one. The threshold is set at roughly the particle image radius, typically half a millimeter. This prevents particles from being entered more than once.

The program then makes a histogram of interparticle distances. Suppose we wish to measure the correlation function out to some distance D. We divide this distance into N intervals: (d_0,d_1), $(d_1,d_2),\ldots,(d_{N-1},d_N)$ where

$d_n = nD/N$. N is typically 50. B_n, the number of inter-particle vectors in bin n, is the number of particle pairs, (j,k), whose separation, r_{jk}, satisfies: $d_{n-1} \leq r_{jk} < d_n$.

The correlation function is then:

$$g(d_n) = \frac{B_n}{A_n N_T} \qquad (1$$

where N_T is the number of particles and $A_n = \pi(d_n^2 - d_{n-1}^2)$, the area per particle contributing to bin n. For a random particle distribution, g would be $g_r = (N_T - 1)/A_T$, where A_T is the area of the region being analyzed. The deviation from random is thus $C(d_n) = g(d_n) - g_r$.

So far, we have ignored boundary effects. For particles near the border, some of the distance bins include regions beyond the edge. The correlation function would thus be underestimated. This can be corrected as follows. We divide the particles into two classes. Edge particles are ones whose distance from the border is less than D_e, one tenth the width of the region being analyzed. The remaining ones are center particles. When calculating B_n, we include only particle pairs in which at least one is central. We also replace N_T with N_c, the number of center particles. This eliminates edge effects out to a distance of D_e.

If we view the placing of vectors into bins as a Poisson counting process, then the standard error for B_n

is $\sqrt{B_n}$. The length of the error bars on our graphs is twice this, an approximation since particle positions are correlated. However, they are used only to qualitatively show the data's significance.

B. RESULTS

In this section we describe some of the correlation functions so far measured. The basic observation is that they are generally maximal at a distance of 8 to 20 nm, where the particle density is about 1½ to 2½ times the mean. There are sometimes additional peaks near integer multiples of this distance, which decrease in height with increasing distance and fade into noise around 100 nm. For our purposes, the correlation function is not as convenient as its deviation from the mean density. This deviation, expressed as percent of the mean, is what we show on graphs.

We first consider how the correlation function is related to the subjective extent of aggregation. Figure 9 shows a series of pictures of increasingly aggregated membranes, whose correlation functions are shown in figure 10. In the paper these pictures were taken from,[4] they were used as reference standards for subjectively studying the effects of various treatments on protein aggregation. The source of their differences was not specified. It can be seen in table 1 that the height of the first peak increases when the aggregation extent does. There is no obvious trend for the width or location.

Figure 10 reveals an approximately 10 nm ripple in the correlation function. Its origin can

captions

9. Computer representation of the Acholeplasma laidlawii membranes shown in figure 1 of James and Branton.[4]

10. Pair correlation functions for the membranes of figure 9. The deviation from random is shown, expressed as percent of the mean density. These membranes are also shown as points 1-5 in figure 11.

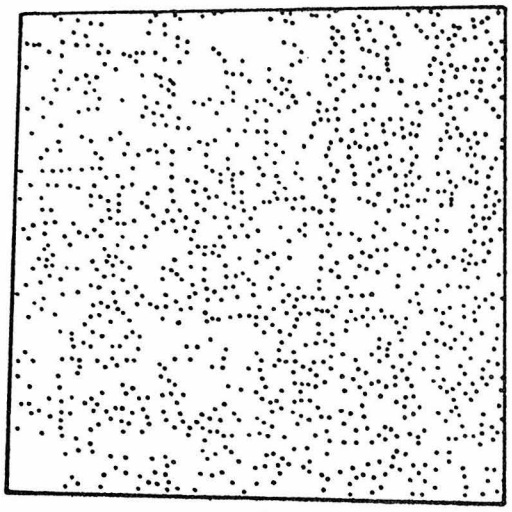

A

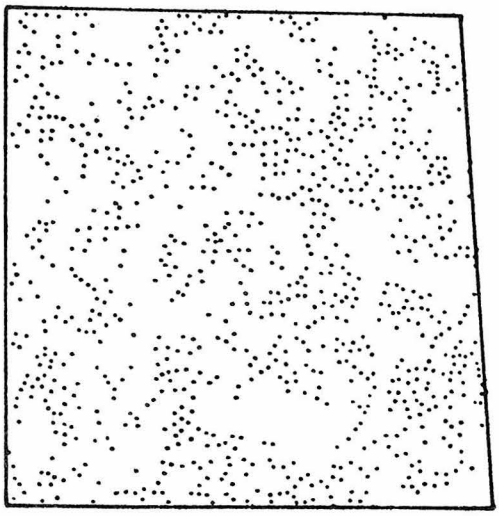

B

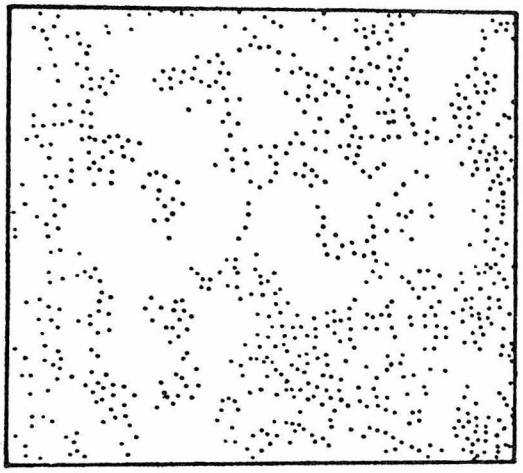

C

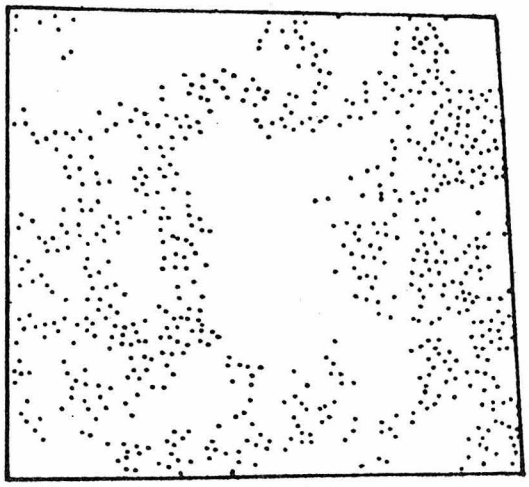

D

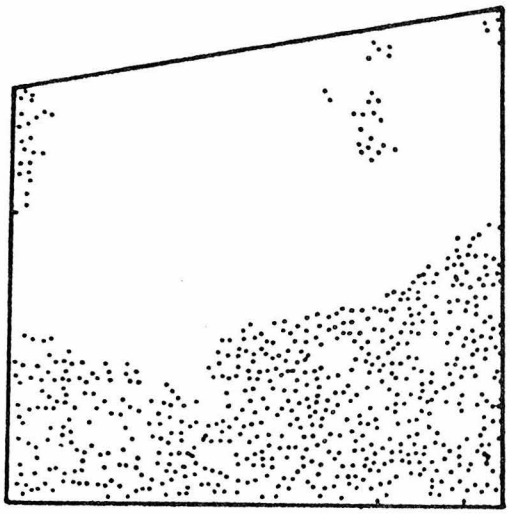

E

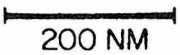

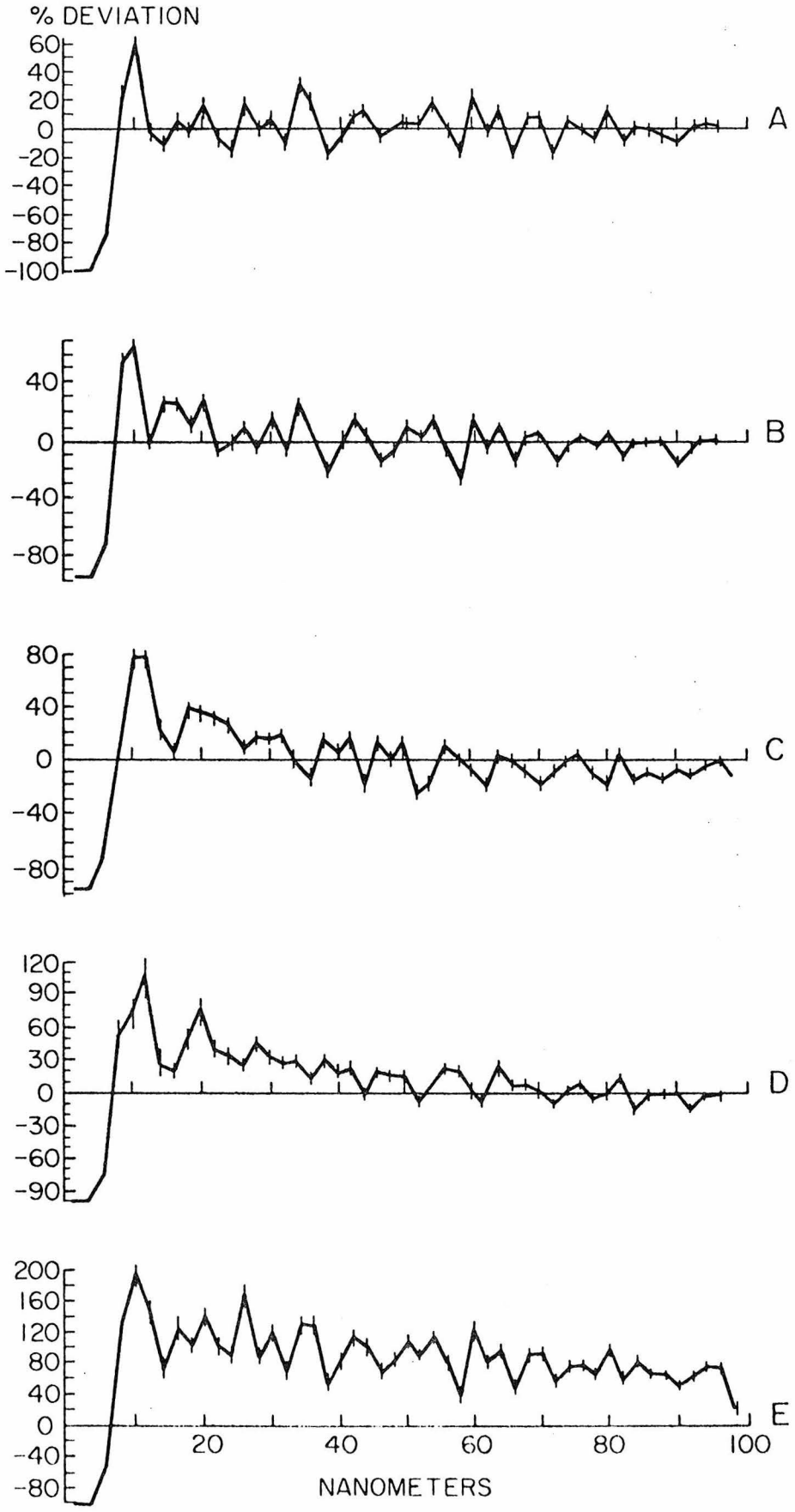
% DEVIATION
60
40
20
0
-20
-40
-60
-80
-100
A
40
0
-40
-80
B
80
40
0
-40
-80
C
120
90
60
30
0
-30
-60
-90
D
200
160
120
80
40
0
-40
-80
20
40
60
80
100
NANOMETERS
E

TABLE 1: SUMMARY OF ACHOLEPLASMA RESULTS

picture	peak			mean density (#/micron^2)
	height(%)	location(nm)	width(nm)	
A	62	10	2.9	2995
B	74	10	3.5	2508
C	79	11	5.3	2302
D	110	12	5.9	2134
E	204	10	5.3	1807

The datawere taken from the graphs in figure 11. "Width" is the width at half maximum height.

be seen in figure 9, especially parts A through C. Many particles are found in strings, in which their spacing is roughly 10 nm. When the aggregation extent increases, as in D and E, the strings are replaced with irregular clusters. In them too, the nearest neighbor spacing is about 10 nm. Ripples would occur whenever the particles form an approximately regular lattice. Then, the correlation function would have a peak corresponding to each lattice vector. Except at small distances though, the spacings between the peaks are less than their widths. The ripples merge into a jumble.

The results of many measurements of correlation functions are summarized in figure 11. This plots the height and location of the first peak versus the mean particle density. It can be seen that there is a rough tendency for the peak height, and perhaps distance, to decrease with increasing density. Since these data were derived from a wide variety of membranes, it is not surprising that there is much scatter. Work with synthetic membranes is needed to determine whether this is a genuine density effect rather than an accidental correlation.

One question is whether the peak location represents close packing of the proteins. If the particles repelled each other only when touching, the peak would be at a distance equal to their diameter. As shown in figure 12,

captions

11. Location and height of the first peak in the pair correlation functions of various membranes. Part A shows the peak location and width at half maximum height. Part B shows the peak height. The membranes are identified by their numbers, which refer to table 2, and by the symbol shapes:

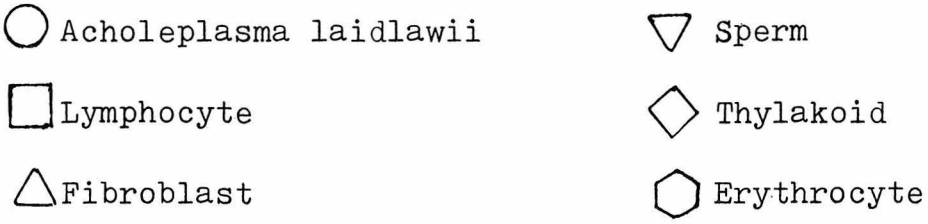

The curve in A shows the mean nearest neighbor distance in a random distribution. It is included only for qualitative comparison: there would be no peak then.

12. Thylakoid correlation function and particle diameter histogram. A shows the correlation function of the particles in figure 10 of Staehlin,[9] also shown as point 17 in our figure 11. B shows a histogram of particle diameters in a similar membrane, copied from figure 18.C of the same paper.

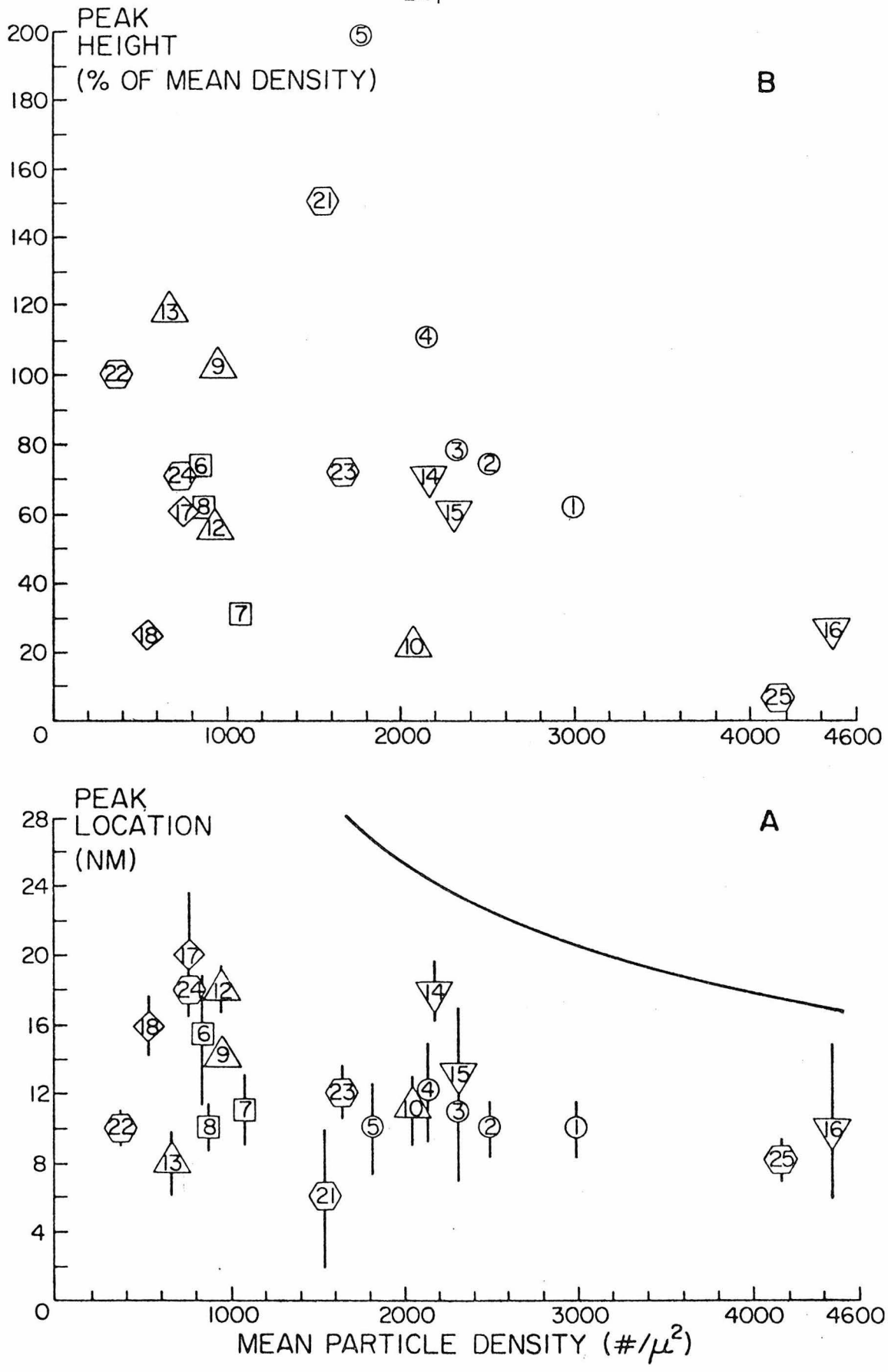
PEAK
HEIGHT
(% OF MEAN DENSITY)
B
200
180
160
140
120
100
80
60
40
20
0
1000
2000
3000
4000
4600
PEAK
LOCATION
(NM)
A
28
24
20
16
12
8
4
0
MEAN PARTICLE DENSITY (#/μ²)

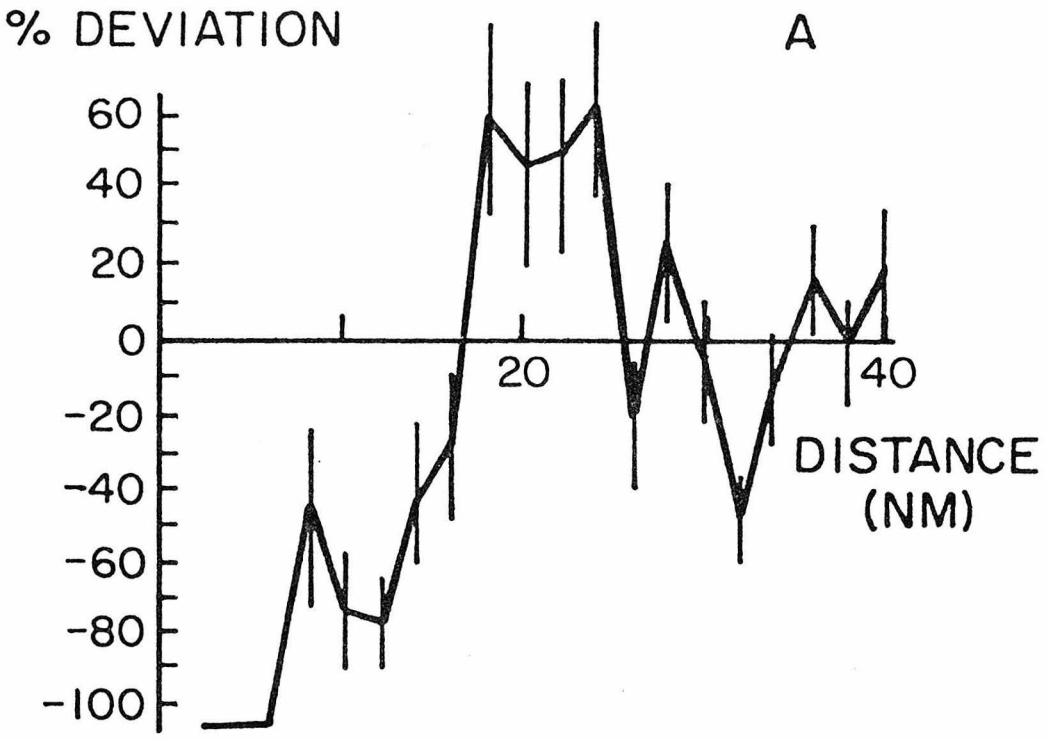
% DEVIATION
A
60
40
20
0
-20
-40
-60
-80
-100
20
40
DISTANCE
(NM)

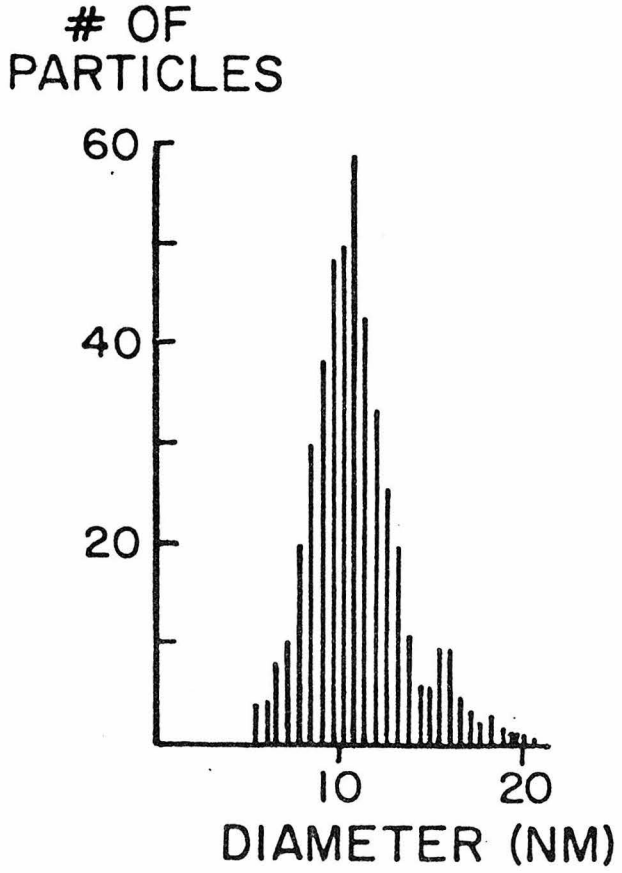
OF
PARTICLES
60
40
20
B
10
20
DIAMETER (NM)

TABLE 2: SOURCES OF MEMBRANE PICTURES

NUMBER	MEMBRANE	REFERENCE
1-5	Acholeplasma laidlawii	James & Branton[4] fig. 1
6	Lymphocyte PM, OF	Wunderlich et al[5] fig. 1
7	Lymphocyte PM, IF	Wunderlich et al[5] fig. 2
8	Lymphocyte PM, IF	Wunderlich et al[5] fig. 3
9	Fibroblast PM, IF	Hasty & Hay[6] fig. 16A
10	Fibroblast PM, IF	Hasty & Hay[6] fig. 16B
12	Fibroblast PM, EF	Hasty & Hay[6] fig. 18B
13	Fibroblast PM, IF	Hasty & Hay[6] fig. 13
14	Sperm nuclear membrane	Friend & Fawcett[7] fig. 18C
15	Sperm flagellar PM	Friend & Rudolf[8] fig. 14
16	Sperm midpiece PM	Friend & Rudolf[8] fig. 18
17	Thylakoid EF	Staehlin[9] fig. 20
18	Thylakoid EF	Staehlin[9] fig. 21
21	Lysed red cell	Seeman[10] fig. 8
22	C' lesions in red cell	Seeman[10] fig. 7B
23	Red cell ghost	Weidkamm et al[11] fig. 2C
24	Red cell	Rothstein et al[12] fig. 7E
25	Red cell	Eitan et al[13] fig. 7 (top left)

Abbreviations: EF, external face; IF, internal face; PM, plasma membrane; C', complement

this is not the case. We have assumed that the diameter seen in pictures is the actual one. It is unknown if this is true. However, the peak distance seems independent of the morphologic diameter. For instance, point 22 in figure 11 represents complement lesions in red cells. Its peak is at about the same distance as that of the endogenous proteins, even though the lesions are about twice their size. We conclude that there is a repulsion between particles, which extends beyond their apparent edges.

REFERENCES FOR CHAPTER III

1. A.J. Verkleij & P.H.J. Th. Ververgaert Ann. Rev. Phys. Chem. 26: 101-122 (1975)
2. S. Bullivant pp. 67-112 in: "Advanced Techniques in Biological Electron Microscopy" J.K. Koehler, ed. Springer-Verlag New York 1975
3. C. Stolinski & A.S. Breathnacii "Freeze-Fracture Replication of Biological Tissues" Academic Press London 1975
4. R. James & D. Branton Biochim. Biophys. Acta 323: 378-390 (1973)
5. F. Wunderlich, D.F.H. Wallach, V. Speth, & H. Fischer Biochim. Biophys. Acta 373: 34-43 (1974)
6. D.L. Hasty & E.D. Hay J. Cell Biol. 72: 667-686(1977)
7. D.S. Friend & D.W. Fawcett J. Cell Biol. 63: 641-664 (1974)
8. D.S. Friend & I. Rudolf J. Cell Biol. 63: 466-479 (1974)
9. L.A. Staehlin J. Cell Biol. 71: 136-158 (1976)
10. P. Seeman Fed. Proc., Fed. Amer. Soc. Exp. Biol. 33: 2116-2124 (1974)
11. E. Weidkamm, D. Brdiczka, D. Pauli, & M. Wildermuth Arch. Biochem. Biophys. 170: 486-494 (1977)
12. A. Rothstein, Z.I. Cabantchik, & P. Knauf Fed. Proc., Fed. Amer. Soc. Exp. Biol. 35: 3-10 (1976)

13. A. Eitan, B. Aloni, & A. Livne Biochim. Biophys. Acta 426: 647-658 (1976)

IV. DISCUSSION

A. ACCURACY OF THE STABILITY LIMITS

1. PRELIMINARIES

Our most basic prediction is that proteins which perturb lipids also tend to bind one another. The strength of this force is controlled by the protein self energy, E_1, and its range, by the lipid correlation length, η^{-1}. Though these conclusions are model independent, the detailed nature of the force is not. Unfortunately, it is not now directly measurable.

Its most obvious consequence is protein precipitation. Determining when it occurs allows us to test the predicted stability limits, shown in figure 7. This requires some way to extract E_1 and η from correlation functions. However, several other factors also influence the correlations. Direct interactions dominate the lipid-mediated ones at sufficiently close approach. Because the latter are weakened by their non-pairwise additivity, this is especially important when the proteins precipitate. We thus need to analyze the direct forces before the lipid-mediated ones. It will be seen that they influence different aspects of correlation functions. The size and shape of protein clusters, and the regularity of particle arrangement within them, also affect correlation functions. However, we will see that this can be ignored for our

purposes.

Most of the adjustable constants appearing in the theory were included only in anticipation of later discussing its molecular basis. From the viewpoint of protein behavior, only E_1 and η matter. All of the others (i.e. φ_o, $\bar{\varphi}$, K_1, K_2) are significant only via their combinations in these two. Both can be determined several ways, which should agree if the theory is valid. In this chapter we obtain E_1 and η only from correlation functions. We later measure them differently, finding consistent results.

The stability analysis shows that membrane proteins can have several qualitatively different behaviors, depending on the magnitudes of E_1 and η. We first need to determine what part of figure 7 corresponds to natural membranes.

We know that $\rho > \eta^2/7\pi$ because membrane proteins often aggregate. ρ must also be well below the upper stability limit: otherwise the precipitate would occupy most of the membrane. It typically covers less than half.

2. QUALITATIVE FEATURES OF CORRELATION FUNCTIONS

One crucial feature of the correlation functions is the short range drop-off: the minimum center to center spacing between particles is typically 5 to 15 nm. This is greater than their morphologic diameter, which shows that the repulsion between them extends beyond their apparent edges. This force is not part of the present model. Its most obvious sources are electrostatic repulsion[1] and steric interference.[2] These could originate in portions of the proteins outside the particles, or even outside the membrane.[3-10] Calculations of the electrostatic forces suggest that their range is too short to account for the observed repulsion.[1] However, present knowledge is inadaquate to evaluate the accuracy of these calculations,[11] or to estimate the steric effects. Because of these difficulties, we simply note that the repulsive forces exist, and characterize their effects.

The simple formula, II.B.1, relating potentials and correlation functions is inaccurate when there are many clusters with more than two particles. If we regard them as droplets of a condensed phase, the nature of the error is suggested by previous studies of simple solids and liquids. Their structure is governed mainly by short range repulsion.[12] Longer range attractions bind the molecules together, but do not control their arrangement.

This is especially true in the present model: non-pairwise additivity weakens the potential within clusters. Lipid-mediated interactions cause them to form, but make only a small contribution to their internal structure.

We are mainly concerned with membranes near the stability limit. In them, many particles remain dispersed, so that the lipid-mediated attraction can still be measured via correlation functions. The inner side of their first peak is very steep, which shows that the repulsion rapidly decreases with distance. That peak thus reflects the range and strength of the lipid-mediated interaction.

Much work has been done on the two dimensional statistical mechanics of particles interacting via hard core[13] or Lenard-Jones[14] potentials. It is known that these systems exhibit solid-liquid transitions,[15] and that their correlation functions have significant ripples only in solids and high pressure liquids.[16] Since this is often the case, we conclude that protein precipitates are under compression, and possibly solid.

These ripples depend on the size of the clusters, and on the regularity of particle arrangement within them. When the particles form a regular lattice, the correlation function has a peak corresponding to each lattice vector. When the particles are disordered, the lattice is still approximately regular over distances of

several particle spacings. The range of this regularity is roughly how far the ripples extend, unless it is larger than the cluster width. Particles near the edge of a cluster give rise to fewer ripples than those near the center. Analyzing this would require knowledge of the cluster size and shape distribution. Here, we are concerned only with the first peak, which contains sufficient information for our purposes.

3. EVALUATION OF E_1 AND n

We first discuss how n can be determined. If one had a detailed model of the direct interactions, they could be separated from the lipid-mediated ones. At low densities then, each could be obtained from the correlation function. Finding n would just be a matter of curve fitting. This approach would be needed to test the theory definitively, but is unfeasable now. We are limited to less accurate measurements. Another way one might get n is to find the stability limits by varying ρ. The threshold density for aggregation would yield n. However, this assumes the validity of the theory. Instead, we will obtain n another way, and then check if the predicted stability limits are accurate.

We measure n by noting where the potential goes through zero. That happens at a distance of $1.2/n$, as shown in figure 3.C. Operationally, we locate this at the first point, beyond the first peak, where the correlation function has its random value. This may be an overestimate because of the direct forces. However, they rapidly decrease with distance, and are thus small there. As two particles within a cluster move apart, they are eventually repelled by their neighbors. This too might shorten the distance to the zero-crossing. It would also make the peak narrower. Due to the lack of

correlation between peak width and aggregation extent, it is probably a minor effect.

The height of the first peak, g_{max}, can be used to estimate E_1. Because E_1 is the binding strength, equation II.B.1 shows that $g_{max}=\rho \exp(E_1/k_BT)$. This is accurate only at low densities and in the absence of direct forces. We now consider the corrections.

The first is non-pairwise additivity, which reduces the effective value of E_1 by a factor of $(1 + 2\pi\rho/n^2)^{-2}$. This is the most important correction, and will be included. We now turn to the others: though possible sources of error, they are small enough to be neglected.

The apparent E_1 is further reduced by clustering. Let g* denote the peak height when all of the particles are contained in large clusters. The proportion of particles in them rises when E_1 increases. g_{max} thus approaches, but never exceeds, g*. The saturation of g_{max} causes it to be less than $\rho \exp(E_1/k_BT)$. However, the error of setting them equal is significant only when the proteins precipitate, which is when E_1 is large. This does not matter near the stability limits.

Finally, short range forces also decrease the peak height. As we discussed in section II.B.5, this effect is partially cancelled by the shift of the stability limit.

In summary, we can evaluate E_1 and κ as follows. The zero-crossing occurs at $1.2/\kappa$, so that κ is readily measurable. We then have: $E_1 = k_B T\ (1 + 2\pi\rho/\kappa^2)^2\ \ln(g_{max}/\rho)$. This is an underestimate when E_1 is much larger than $k_B T$.

The results for many membranes are shown in figure 13. It can be seen that natural membranes lie in a narrow strip. Detailed tests of the stability limit will have to be done in synthetic membranes where E_1 and $\pi\rho/\kappa^2$ can be systematically varied.

κ^{-1} is usually between 10 and 14 nm, so that $\kappa^2/7\pi$ is between 230 and 460 μm^{-2}. The particle density is typically several-fold higher. We thus expect membrane proteins to precipitate for sufficiently high E_1.

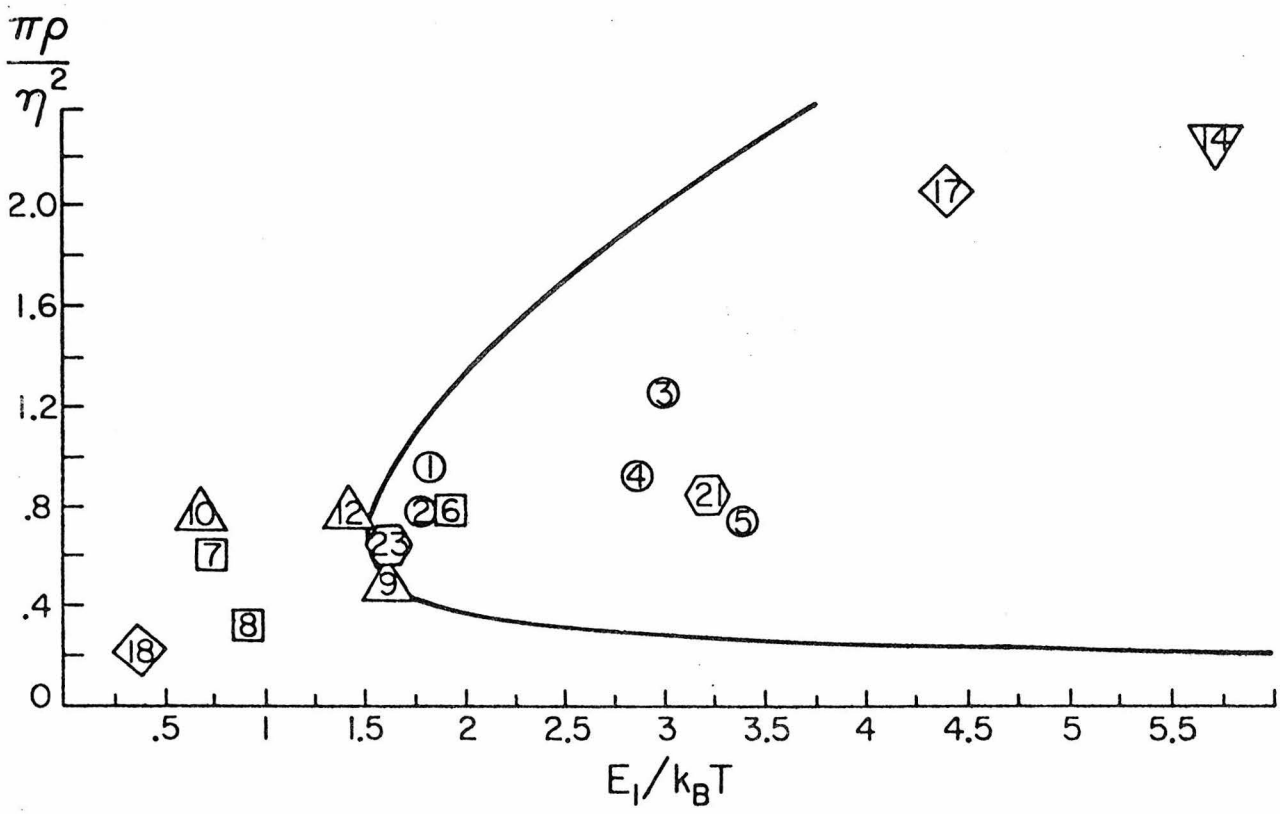

13. Values of E_1/k_BT and $\pi\rho/\eta^2$ in various membranes. The symbols and numbers are the same as in figure 11. The curve is the stability limit.

4. STABILITY LIMITS

Let us first study the Acholeplasma membranes shown in figure 9, and as points 1 to 5 in figure 13. Membrane 1 (figure 9.A) is near the stability limit. Its few clusters are mostly strings, containing only a small proportion of the particles. Membrane 2 (figure 9.B) is farther from the stability limit. In addition to the strings, it also has some blob-like aggregates. Membranes 3 through 5 (figures 9.C - 9.E) are even farther into the unstable region. In them, the clusters become increasingly irregular, and fewer particles remain outside them. The particle-free regions become more extensive. As explained before, E_1 has been underestimated in these membranes. Points 17 and 21 are also deeply into the unstable region. Their particles too have coagulated. Membrane 14 is completely filled by the precipitate.

The other membranes near the stability limit (points 6, 9, 12, and 23) exhibit a slight clustering tendency. This would be expected. Even in stable membranes, clusters are formed by thermal fluctuations; while in unstable ones, not all particles are contained in the precipitate. When calculating the stability limits, we represented the proteins as a continuum. In this approximation, there is a sudden onset of aggregation when the unstable region is entered. This view is accurate

only when membranes are examined with insufficient resolution to see individual particles. On a finer scale, such as ours, the cluster size is seen to increase when the stability limit is crossed. There is no abrupt change of stickiness. The discontinuity results from the coarse graining: the clusters in stable membranes are too small to be seen at low resolution.

Our observations are consistent with the theory: proteins precipitate in unstable membranes, but not in stable ones. However, figure 13 shows that we have tested only part of the stability limit. Curing this requires studies in synthetic membranes. There, E_1 and ρ can be systematically varied.

B. COMPARISON TO OTHER WORK

1. LIPID-MEDIATED INTERACTIONS

We now compare our model of lipid-mediated interactions with two others that have been presented recently.[17,18] They agree with us in predicting that proteins which perturb lipids also tend to aggregate. However, their assumptions, and thus results, differ from ours. In particular, neither of them predicts that the interaction potential has a barrier.

Both models start with statistical descriptions of the OP, seemingly unrelated to ours. They assume that each hydrocarbon segment, i, is characterized by some quantity, φ_i, depending on its orientation. The order parameter is $\langle\varphi_i\rangle$, the expectation value of φ_i. It is also assumed that the energy of each segment, i, has the form $h_i = h_i^o + \sum_j v_{ij} \varphi_i \varphi_j$, where h_i^o is the internal energy, and the second term is the interaction. One can then use the mean field approximation to calculate the OP. Suppose we guess that $\langle\varphi_j\rangle = \Phi_j$, where Φ_j is some number. h_i can then be approximated as $h_i^o + \sum_j v_{ij} \varphi_i \Phi_j$. This decouples the segments from one another, so that they can be studied separately. In particular, $\langle\varphi_i\rangle = \left[\int d\varphi_i \ \varphi_i \exp(-h_i/k_BT)\right] / \left[\int d\varphi_i \exp(-h_i/k_BT)\right]$. Self

consistency requires that $\langle \varphi_i \rangle = \bar{\Phi}_i$. Schröder formally solves this manually;[17] while Marčelja uses a computer to search for the solution.[18] It will later be seen that these descriptions of the OP can often be approximated by ours.

In both models, lipids adjacent to a protein are coupled to it by an additional term, $e_{lp}\varphi_i$, in their energy. This contrasts with our model, in which their OP is fixed at some particular value. Presently, the difference between these boundary conditions is mainly one of convenience. Careful analysis of this remains for the future.

In both models, as in ours, the goal is to calculate the OP energy for various protein arrangements. Subtracting the self energies yields the potential.

Schröder[17] derives an expression for the OP energy which is formally identical to our equation II.A.1. Proteins are then studied in the linear response approximation: it is assumed that their total effect on the OP is the sum of the effects produced by individual particles. In our formalism, this means that equation II.B.4 is replaced with $\vec{c} = \vec{\Delta}$. The justification for this is mathematical simplicitly. However, we avoid this approximation, yet calculate the OP energy more easily than does Schröder. Not only does linear response fail to provide simplicitly,

but it is also invalid. Instability against precipitation arises from the saturation of the protein perturbation, which is ignored by Schröder. The nonlinearity of the two particle case produces the last term of equation II.A.9. Dropping it eliminates the barrier from the potential. Its absence in Schröder's model is an artifact.

The range of the lipid-mediated force is calculated in Marčelja's theory; while it is an adjustable constant in ours. The predicted value is roughly ten-fold smaller than we have observed. We will find in chapter V that the probable source of the discrepancy is that Marčelja picked the wrong OP.

Both models were limited mainly to the two particle case. We have seen that the theory must be generalized to the many particle case to be experimentally testable. There is no practical way to calculate the protein chemical potential in Marčelja's model, while Schröder's approximations eliminate the phenomena needed to test the model. At best, these theories are valid only at densities sufficiently low for the potential to be pairwise additive. This occurs rarely, if ever, in nature.

The best way to resolve the issue of the barrier would be experiment, rather than theoretical arguments. This has not yet been done, however. The barrier remains a prediction of our model.

2. ANALYSIS OF PROTEIN CLUSTERING

Several methods have recently been presented for studying protein clustering.[19-21] We now compare them with ours.

Melhorn and Packer[19] have suggested two schemes: pair correlation functions and histograms showing the proportions of a membrane having various local particle densities. They study only one membrane picture, of a red cell with coagulated proteins. In agreement with us, they find a prominent peak in the correlation function at about 10 nm, where the particle concentration is roughly twice the mean. Unlike us, they find no ripples in the correlation function.

To interpret the clustering, they compare the picture with two hypothetical patterns. One consists of randomly located clusters, each with two to four particles; in the other, particles are excluded from randomly chosen parts of the membrane. The latter is found to be more realistic. This is claimed to prove that proteins precipitate, not because they attract each other, but because they are segregated into certain membrane regions.

Several considerations show this to be unjustified. It is not obvious why they compared those two models: the clusters in their membrane clearly contain many more than four particles. It is not surprising that the first

model failed. The success of the other shows only that there are large spaces between the clusters, and hence, that proteins agglutinate strongly enough to prevent diffusion from redispersing them. This tells us nothing about why they bind.

The absence of peaks beyond the first in their correlation function is explained by examining their picture (their figure 2): the particles are very irregular and poorly resolved. The ripples depend on the regularity of particle arrangement, and would thus be hard to observe. We have used pictures only if the particles were readily distinguishable, with well defined positions. Their picture would have been rejected as unsuitable for accurate analysis.

Finegold[20] has proposed that proteins bind irreversibly upon collision. A computer is used to simulate their Brownian motion. Particles with an initially random arrangement are viewed at various later times. All of them eventually end up in one large cluster. The intermediate stages subjectively resemble a series of pictures of increasingly aggregated red cell membranes. It is concluded that purely kinetic factors normally prevent the proteins from coagulating. Though proteins do diffuse atypically slowly in the red cell,[22,23] it is also known that their precipitation is reversible.[24] The model is thus valid only when E_1 is much larger than

$k_B T$.

Another description of protein clustering is the histogram of nearest neighbor distances.[21] It is less useful than the correlation function, though. With the former, one vector is counted per particle; but with the latter, many. The counting error is thus smaller for the correlation function. Also, the distance distribution is sensitive only to interactions between nearest neighbors, while the correlations reflect all interactions.

C. SPECULATIONS ON MECHANICS

The red cell membrane responds to sufficiently small shear forces, σ, as an elastic solid, but to larger ones as a liquid.[25] The border between these regimes is the yield shear, σ_c=2 to 8 X10^{-2} dy/cm, which is zero in fluids. Since this behavior differs greatly from that of pure lipids,[26] a protein network external to them has been considered the source of solidity. (See section I.A for details.) We will see here that it can also arise from the lipid-mediated force.

When a membrane shears, its proteins rearrange. The lipid-mediated force binds adjacent ones together, with strength roughly E_1. We thus want to know when σ is large enough to pull them apart. Call the separation of two neighbors L. Each can acquire a kinetic energy of σL^2 while traversing this distance: the shear force between them is roughly σL when stresses are resisted only by the lipid-mediated force. We infer that $\sigma_c = E_1/L^2$. On the average, $L^2 = 1/\pi\rho$ if the particles are randomly arranged. We finally conclude that $\sigma_c = \pi\rho E_1$. This estimate is very crude, since we have ignored bond orientation and viscous damping of protein motion.[27]

We can now evaluate σ_c. E_1 is 6.2-12.4 X10^{-14} erg in the red cell (points 21 and 23 in figure 13). Non-pairwise additivity reduces its effective value to 1.5 - 3.1

$X10^{-14}$ erg ($\pi\rho/\eta^2=\frac{1}{2}$; see page 139). ρ is roughly 3 $X10^{11}/cm^2$. This leads to σ_c=1.4-2.9 $X10^{-2}$ dy/cm, close to experiment. The lipid mediated force thus significantly contributes to σ_c, and possibly even dominates it. We see that indirect protein interactions can solidify membranes, whether or not the lipids are fluid. This claim would be more convincing if we could correctly calculate the viscosity and rate of particle collision. The notorious difficulties[28] of two-dimensional fluid mechanics have so far prevented this.

An important supposition is that the proteins are uniformly dispersed. This remains valid within the precipitate when present. Then, however, the deformation occurs mainly in the particle-poor regions, where σ_c is much smaller: zero with our approximations.

D. CONCLUSIONS

So far, our basic goal has been to study the consequences of lipid perturbation by proteins. We first needed to solve several other problems. The standard statistical mechanical approximations destroy those parts of the theory most relevant to us. We thus had to develop appropriate mathematical techniques. On the other hand, there has previously been little quantitative analysis of protein clustering. We thus needed to devise a method for that too. Finally, many different phenomena influence the correlation function, so that we had to disentangle them before extracting any useful information.

Much of our analysis of these functions is model independent. They clearly reveal a repulsive force extending several nm beyond the apparent edges of protein particles, and an attractive one extending about 10 nm more.

The main evidence that the observed attraction coincides with the predicted one is the accuracy of the stability limit. We showed that the behavior of natural membranes qualitatively agrees with the theory. Our comparison has two major limitations. Natural membranes occupy only a small region in plots of $\pi\rho/n^2$ versus E_1/k_BT, so that we tested only part of the stability limit. We can eliminate this problem by making the measurements

in synthetic membranes. The other difficulty is the approximate nature of the stability limit: it is just the boundary of the region where the clusters are large. Thus it cannot be located very precisely. Curing this will require analysis of the cluster size distribution.

Our chief assumptions were that field theory is relevant to membranes, and the particular choice of a field equation. When we began, simplicity was the only justification for this choice. The experimental input was that proteins sometimes aggregate. Though this is not a prediction of the model, its details are. We have seen the predictions to be at least roughly correct. We will study the molecular basis of the model in chapter V, and find that studies of the lipids do support our field equation and evaluation of n.

While presenting the theory, we often speculated about its significance, suggesting mechanisms for protein rearrangement during development, drug action, and physiological responses. Testing these ideas requires measurement of E_1 and n in these membranes. Finding which changes will limit the range of possibilities for how these processes occur.

REFERENCES FOR CHAPTER IV

1. D. Gingell in: "Mammalian Cell Membranes" 1: 198-223 G.A. Jamieson & D.M. Robinson, eds. Butterworths London 1976

2. D.J. Meier J. Phys. Chem. 71: 1861-1868 (1967)

3. H. Saibil, M. Chabre, & D. Worcester Nature 262: 266-270 (1976)

4. R.W. Kensler, P. Brink, & M.M. Dewey J. Cell Biol. 73: 768-781 (1977)

5. C.J. Arntzen, R.A. Dilley, & F.L. Crane J. Cell Biol. 43: 16-31 (1969)

6. W.C. Davis, H.E. Sandberg, & P.H. DeFoor in: "Biomembranes" 8: 1-46 L.A. Manson, ed. Plenum Press New York 1976

7. G.M. Edelman Science 192: 218-226 (1976)

8. R.L. Juliano Biochim. Biophys. Acta 300: 341-378 (1973)

9. T.L. Steck J. Cell Biol. 62: 1-19 (1974)

10. M.S. Bretscher Science 181: 622-629 (1973)

11. C.J. Barnes & B. Davies J. Chem. Soc., Faraday Trans. II 71: 1667-1689 (1975)

12. J.D. Weeks, D. Chandler, & H.C. Anderson J. Chem. Phys. 54: 5237-5247 (1971)

13. B.J. Alder, W.G. Hoover, & D.A. Young J. Chem. Phys. 49: 3688-3696 (1968)

14. F. Tsien & J.P. Valleau Mol. Phys. 27: 177-183 (1974)

15. W.G. Hoover & F.H. Ree J. Chem. Phys. 49: 3609-3617 (1968)

16. W.W. Wood J. Chem. Phys. 52: 729-741 (1970)

17. H. Schröder J. Chem. Phys. 67: 1617-1619 (1977)

18. S. Marčelja Biochim. Biophys. Acta 455: 1-7 (1976)

19. J. Melhorn & L. Packer Biophys. J. 16: 613-625 (1976)

20. L. Finegold Biochim. Biophys. Acta 448: 393-398 (1976)

21. T.P. Copps, W.S. Chelack, & A. Petkau J. Ultrastructure Res. 55:1-3 (1976)

22. V. Fowler & D. Branton Nature 268: 23-26 (1977)

23. M. Edidin Ann. Rev. Biophys. Bioeng. 3: 179-201 (1974)

24. P. Pinto da Silva J. Cell. Biol. 53: 777-787 (1972)

25. E.A. Evans & R.M. Hochmuth Biophys. J. 16: 1-11, 13-26 (1976)

26. M. Joly in: "Surface and Colloid Science" 5: 1-79 E. Matijevic, ed. Wiley-Interscience New York 1972

27. C.E. Chaffey J. Colloid Interface Sci. 56: 495-504 (1976)

28. P.G. Saffman J. Fluid Mech. 73: 593-602 (1976)

V. MICROSCOPIC NATURE OF THE OP

A. INTRODUCTION

We previously described membranes in terms of an order parameter, φ, controlled by its energy density:

$$\mathcal{E} = K_1(\nabla\varphi)^2 + K_2(\varphi - \varphi_o)^2 \qquad (1$$

φ everywhere equals φ_o at equilibrium unless there are constraints on it. For instance, the OP is shifted to some other value, $\bar{\varphi}$, adjacent to proteins. The equilibrium OP then is the solution of:

$$\left(\frac{\nabla^2}{n^2} - 1\right)\varphi + \varphi_o = 0 \qquad (2$$

where $n^2 = K_2/K_1$. This field equation was the basis for our analysis of the lipid-mediated attraction between proteins.

Our discussion of φ was mainly thermodynamic, and ignored its microscopic basis. Here, we examine the latter. In particular, we will find that the behavior of φ coincides with that of membrane thickness. An immediate question is whether its variation is controlled by lipid tilt or conformation. Previous work[1] has assumed the latter. We will see that this is implausible, suggesting that φ measures lipid tilt. We will also derive equation 2 from lipid statistical mechanics, thus revealing the relation of φ to spectroscopic OP's.

B. MEMBRANE THICKNESS ELASTICITY

We first note that the last two equations also describe membrane thickness, h, regardless of whether it is physically the same as Φ. To understand the relation between them, we start by calculating K_1 and K_2 for h.

Consider a unit area of membrane, with thickness h_o. If h is made non-uniform, deviating only slightly from h_o, the area becomes $1+\frac{1}{2}(\nabla h)^2$. This increases the energy density by $\frac{1}{2}\gamma(\nabla h)^2$, where γ is the interfacial tension (of the entire membrane, not of each interface with water). We conclude that $K_1=\frac{1}{2}\gamma$. A typical value[2] for γ is 40 dy/cm, so that $K_1 \sim 20$ dy/cm.

$K_2=\frac{1}{2}\frac{\partial^2 \varepsilon}{\partial h^2}$ can be determined by applying an electric potential difference across the membrane, thus compressing it. This electrostriction increases the capacitance, which can be used to measure the thickness, and hence K_2.[3] As the field increases, the membrane eventually becomes unstable and breaks down.[4,5] The voltage difference, V_c, at which this occurs also reveals K_2, though it is more accurately obtained from the dependence of V_c on the pressure difference across the membrane.[6] These experiments are consistent with the force law: $dP=-Y\, dh/h$, where P is the stress normal to the membrane and Y is the Young modulus. If we are concerned with membranes near the

equilibrium thickness, h_o, we can integrate this to get $P=-Y(h-h_o)/h_o$, or $\mathcal{E} = \frac{1}{2}Y(h-h_o)^2/h_o$. We see that $K_2=Y/2h_o$. Typical values for Y are 2-6 $X10^7$ dy/cm^2 and for h_o, 5 $X10^{-7}$ cm, so that K_2 is 2-6 $X10^{13}$ dy/cm^3. It should be noted that the value of Y we used is that of lipid bilayers. There has recently been controversy concerning its much smaller value in black lipid films.[7] However, Y is controlled there by solvent extrusion from the membrane. This relaxation can be avoided by measuring Y on a millisecond time scale[8] or in low solvent films.[3] Then the result agrees with that in natural membranes.

Collecting these results, we obtain the thickness correlation length: $\pi^{-1} \sim$ 8-14 nm. By analyzing protein clustering, we measured $\pi^{-1} \sim$ 10-14 nm. The agreement between these estimates suggests that φ may be h, though of course it could be fortuitous. For now, we will assume that φ is h, and explore the consequences.

We first check if the predicted protein effect on h is plausible. Obviously, it cannot decrease by more than the initial thickness, or increase by more than the final one. The magnitude of the change is fixed by the self energy, E_1, the shift in OP energy caused by one protein particle. We showed that $E_1=\pi K_1(\bar{\varphi} - \varphi_o)^2$, and measured $E_1/k_BT \sim$ 1-4. We thus find $\bar{\varphi} - \varphi_o \sim \frac{1}{4}$-$\frac{1}{2}$ nm, which is less than a tenth of the membrane thickness. This supports our approximation that $\bar{\varphi}$ is close to φ_o.

Most work on membrane order parameters has been concerned with spectroscopic ones: $S_\nu = \langle P_2(\cos\nu)\rangle$, where $P_2(x)=\frac{1}{2}(3x^2-1)$, ν is some angle, and brackets denote averaging.[9,10] ν is often γ_i, the angle between the mean hydrocarbon chain axis and C-C bond "i". The length, L, of a hydrocarbon chain may often be approximated by:[11]

$$L = \tfrac{1}{2}\, l\, (n' + \sum_i S_{\gamma_i}) \qquad (1$$

where l=.125 nm and the sum is over the n' C-C bonds in the chain. If it is perpendicular to the membrane surface, then $h=2L+h^*$, where h^* is the thickness of the polar regions and the space (if any) between the terminal methyl groups. With these assumptions, h is controlled by S_γ, so that Φ can also be identified with S_γ. We will later see that this leads to ridiculous values for η and K_2.

The resolution of this contradiction is suggested by recent work of Petersen and Chan.[12] They showed that S_γ by itself is inadaquate for describing the dynamics of chain reorientation. One needs an additional OP, S_α, where α is the angle between the chain axis and the director (local symmetry axis). Before examining the implications of this, we will study S_γ in greater detail.

C. STATISTICAL MECHANICS

Consider a protein-free membrane described by the Hamiltonian:

$$H = \sum_i h_i = \sum_i \left(h_i^o - \sum_k V(d_{ik}) \varphi_i \varphi_k + \varphi_i \lambda_i\right) \quad (1$$

This expression is very general: special cases of it have underlain most previous work on lipid statistics. The φ's are quantities whose expectation values are the order parameters. The indices i and k refer to molecules or monomers. In Marčelja's model,[17] $\varphi_i = P_2(\cos \gamma_i)$. h_i^o is the portion of the energy of segment i which is independent of φ_k for $k \neq i$: for instance, conformational energy and φ-independent interactions. $V(d_{ik})$ is the coupling between φ_i and φ_k, where d_{ik} is the distance between i and k. It is presently controversial whether V represents the anisotropy in dispersion or in steric interactions.[13] However, this does not matter for our purposes. Finally, the λ's are auxiliary variables which are zero in the membrane, but useful for theoretical purposes. Any physical terms linear in φ are included in h^o.

For simplicity, we assume that the molecules have fixed positions. Without this, the derivation is much more complicated, but yields an identical result.

The basis of our analysis is the mean field approximation:

we decouple the φ's from one another by replacing φ_k with $\Phi(\vec{r}_k)$, where Φ is some function of $\vec{r}_k$, the position of k. Self-consistency requires that $\Phi(\vec{r}_k)=\langle\varphi_k\rangle$, where the brackets denote an ensemble average with $\lambda=0$. The goal is to find some criterion, a field equation for Φ, which insures self-consistency. Comparison with equation V.A.2 then reveals the lipid correlation length.

We first assume that there exists a constant, Φ_o, such that $\Phi = \Phi_o$ is self-consistent. In the absence of external constraints on φ, this is its equilibrium value. Our task is to find the dependence of the partition function on $\Phi - \Phi_o$. Once we have that, we can calculate $\langle\varphi\rangle$, and thus test for consistency.

We start by expanding Φ in a Taylor series:

$$\Phi(\vec{r}_k) = \Phi(\vec{r}_i) + (\vec{r}_k-\vec{r}_i)\cdot\vec{\nabla}\Phi(\vec{r}_i) + \tfrac{1}{2}((\vec{r}_k-\vec{r}_i)\cdot\vec{\nabla})^2\Phi(\vec{r}_i) \quad (2$$

where $((\vec{r}_k-\vec{r}_i)\cdot\vec{\nabla})^2$ is short for $\sum_{\mu,\nu}(\vec{r}_k-\vec{r}_i)_\mu\,(\vec{r}_k-\vec{r}_i)_\nu\,\nabla_\mu\nabla_\nu$. We will later examine the error of ignoring the higher order terms. We then find:

$$\sum_k \varphi_i\,\Phi(\vec{r}_k)\,V(d_{ik}) = \varphi_i\,\Phi(\vec{r}_i)\sum_k V(d_{ik}) + \tfrac{1}{2}\varphi_i(\nabla^2\Phi(\vec{r}_i))\sum_k V(d_{ik})d_{ik}^2$$

$$\equiv \varphi_i\,\Phi(\vec{r}_i)\,W_{0,i} + \tfrac{1}{2}\varphi_i(\nabla^2\Phi(\vec{r}_i))W_{2,i} \quad (4$$

We dropped the linear term because it vanishes when we average over particle positions. Also, $((\vec{r}_k-\vec{r}_i)\cdot\vec{\nabla})^2$ becomes $d_{ik}^2\nabla^2$ during this averaging. Strictly speaking, these changes should not be made until equation 9. However,

it simplifies the notation to include them here. These arguments assume that V is isotropic or uniaxial. Generalization to the biaxial case is straightforward.

If we set:

$$S_i = (\Phi(\vec{r}_i) - \Phi_o) W_{0,i} + \tfrac{1}{2}(\nabla^2 \Phi(\vec{r}_i)) W_{2,i} \qquad (5$$

and: $$h_i^+ = h_i^o - \varphi_i \Phi_o W_{0,i} + \varphi_i \lambda_i \qquad (6$$

then $h_i = h_i^+ - \varphi_i S_i$. The partition function, which depends on Φ and the λ's, is thus:

$$Z(\Phi, \lambda) = \Sigma^* \exp(-\beta \sum_j h_j) \qquad (7$$

$$\sim \Sigma^* \exp(-\beta \sum_j h_j^+)\ (1 + \beta \sum_j \varphi_j S_j) \qquad (8$$

Σ^* denotes summation over all discrete states and integration over all continuous ones. β is $1/k_B T$. In the second step, we have expanded the exponential as a series in the deviation from unconstrained equilibrium. We can rearrange this as:

$$Z(\Phi, \lambda) = Z(\Phi_o, \lambda)\ (1 + \beta \sum_j \langle \varphi_j S_j \rangle_\lambda) \qquad (9$$

where $\langle\ \rangle_\lambda$ denotes the expectation value with non-zero λ.

Finally, we impose self-consistency:

$$\Phi(\vec{r}_i) = \langle \varphi_i \rangle = -\frac{1}{\beta} \left. \frac{\partial \ln Z(\Phi, \lambda)}{\partial \lambda_i} \right|_{\lambda=0} \qquad (10$$

$$= \Phi_o - \frac{1}{\beta} \frac{\partial}{\partial \lambda_i} \ln(1 + \beta \sum_j \langle \varphi_j S_j \rangle_\lambda) \qquad (11$$

Expanding ln in a Taylor series, this becomes:

$$\Phi(\vec{r}_i) - \Phi_o = -\frac{\partial}{\partial \lambda_i} \sum_j \langle \varphi_j S_j \rangle_\lambda \qquad (12$$

$$= \beta \sum_j \left(\langle \varphi_i \varphi_j S_j \rangle - \langle \varphi_i \rangle \langle \varphi_j S_j \rangle \right) \qquad (13$$

The φ's are independent of S, so that we can average them separately. Also, $\langle \varphi_i \varphi_j \rangle = \langle \varphi_i \rangle \langle \varphi_j \rangle$ for $i \neq j$. The sum is thus trivial, and we find:

$$\Phi(\vec{r}_i) - \Phi_o = \beta \left(\langle \varphi_i^2 \rangle - \langle \varphi_i \rangle^2 \right) \langle S_i \rangle \qquad (14$$

From the definition of S, we have:

$$\langle S_i \rangle = X_1 (\Phi(\vec{r}_i) - \Phi_o) + \tfrac{1}{2} X_3 \nabla^2 \Phi(\vec{r}_i) \qquad (15$$

where: $$X_q = \sum_k d_{ik}^{q-1} V(d_{ik}) = 2\pi \int_0^\infty V(s) g_1(s) s^q \, ds \qquad (16$$

and g_1 is the lipid pair correlation function. Inserting this into equation 14, and setting $M_2 = \langle \varphi^2 \rangle - \langle \varphi \rangle^2$, we finally obtain:

$$\Phi(\vec{r}) - \Phi_o = \frac{\frac{1}{2} X_3}{\frac{k_B T}{M_2} - X_1} \nabla^2 \Phi(\vec{r}) \qquad (17$$

Comparison to the field equation yields the correlation length:

$$\xi^{-1} = \left(\frac{\frac{1}{2} X_3}{\frac{k_B T}{M_2} - X_1} \right)^{\frac{1}{2}} \qquad (18$$

We now transform this into a more useful form. First consider M_2. The equipartition theorem tells us that:

$$\frac{k_B T}{M_2} = \frac{\partial^2 E_i(\Phi_o)}{\partial \Phi^2} \equiv E^{(2)} \qquad (19$$

$E_i(\Phi)$ is the mean value of h_i when φ_i is constrained at Φ. This is independent of i when the monomers are identical.

We next consider X_1 and X_3. In most models, the molecules are fixed on a regular lattice, with interactions limited to nearest neighbors. If we call the nearest neighbor number and spacing n and d respectively, then: $X_i = d^{i-1} V_d n$, where $V_d = V(d)$.

Combining these results, we obtain:

$$\xi_d = \left(2\left(\frac{E^{(2)}}{nV_d} - 1\right)\right)^{\frac{1}{2}} = \left(2\left(\frac{k_B T}{nV_d M_2} - 1\right)\right)^{\frac{1}{2}} \qquad (20$$

An equivalent equation has recently been derived by very different means.[14]

We first show that the square root is meaningful. Thermodynamic stability requires that $E^{(2)} > nV_d$. In the definition of $E^{(2)}$, the derivatives were taken with respect to the OP of one particular monomer. When the OP undergoes the same variation on all of them, the derivative becomes $E^{(2)} - nV_d$. This must be positive for the state $\Phi = \Phi_o$ to be stable. When it is zero, for instance at a second order phase transition or a critical point of a first order one, there is no restoring force for OP fluctuations. They, and their correlation length, diverge.

These ideas can be made more precise as follows. A calculation very similar to the preceding one yields the susceptibility:

$$\left.\frac{\partial \langle \varphi_i \rangle_\lambda}{\partial \lambda}\right|_{\lambda=0} = \left(X_1 - \frac{k_B T}{M_2}\right)^{-1} \qquad (21$$

where $\lambda_k = \lambda$ for all k. One sees that when $\mathcal{N}^{-1}$ diverges, so does the susceptibility. The membrane is then unstable to small perturbations. Our conclusions also apply to the Maier-Saupe model of the nematic-isotropic transition.[15]

The order-disorder transition of membranes is first order,[16] so that $\mathcal{N}^{-1}$ remains finite. Both phases are metastable at the transition, hence $E^{(2)} - nV_d > 0$ in each.

Before applying these results, let us examine our approximations. The two major ones were the Taylor series used to calculate Φ and ln Z. If the higher order terms are included in the series for Φ, the field equation becomes:

$$\Phi - \Phi_o = \frac{1}{\frac{k_B T}{X_1 M_2} - 1} \sum_{m=1}^{\infty} \frac{X_{2m+1}}{X_1 (2m)!} \nabla^{2m} \Phi \qquad (22$$

With nearest neighbor interactions, $X_i = d^{i-1} X_1$. The m-th term is thus small when $\frac{d^{2m}}{(2m)!} \nabla^{2m} \Phi \ll \Phi - \Phi_o$. This refines our earlier statement that we only consider cases where the variations in Φ and $\nabla^2 \Phi$ are significant only over distances large compared to a molecular spacing. In

particular, this requires that $\kappa^{-1} \gg d$, or $E^{(2)} < \frac{3}{2} nV_d$.

The other crucial series expansions were those used in equations 8 and 12. The higher order terms are small when $\beta \langle V(d_{ik}) \varphi_i (\Phi(\vec{r}_k) - \Phi_o) \rangle \ll 1$ for all i and k. This means that the deviation of the interaction from unconstrained equilibrium is small compared to $k_B T$. When this is not satisfied, the derivation can be generalized to include the higher order terms. One would obtain a non-linear field equation, which would be useless with present experimental knowledge.

In Marčelja's analysis,[1,11,17] $nV_d = V_o (n_t/n')^2$, where V_o=680 cal/M and n_t/n' is the fraction of trans bonds in the hydrocarbon chain. h^o has two parts: the conformational energy, calculated in the discrete rotational isomer approximation, and the steric interaction, PA, where P is the two dimensional pressure and A is the area of the chain (projected onto the membrane surface). Proteins are assumed to change the configurational potential of adjacent lipid molecules. The protein effect is found to extend for several molecular spacings, which means that $1/\kappa$ d is 3 or 4. This compares to an experimental value of 20 to 30. We now try to account for this discrepancy.

First consider equation 20. If κ^{-1} is really as small as calculated, our version of the mean field approximation is inaccurate. However, we will use it to

estimate what nV_d would have to be to account for the observed η. When $1/\eta d \gg 1$, we also have $k_BT/M_2nV_d \sim 1$. Marčelja calculated that $P_t = \langle n_t/n' \rangle \sim .7$, so that $nV_d \sim$ 340 cal/M. From table 1 of reference 12, we calculate $M_2 = \frac{81}{64} P_t(1-P_t) \sim \frac{1}{4}$. (Our γ is their "p orbital γ".) We finally obtain $k_BT/M_2nV_d \sim 8$, which is too large. One might try increasing V_o or eliminating the $(n_t/n')^2$ factor. This is probably not the solution, however, because the model does provide an excellent description of protein-free membranes, at least in the disordered phase.

Since the experimental tests all examined single molecule properties, it could also be argued that the error lies in the mean field approximation. The energy of single gauche bonds is vastly underestimated in Marčelja's model.[18] Their energy is lowered when they form clusters:[19-21] association of a gauche$^+$ bond with a gauche$^-$ bond on the same chain or a gauche$^+$ one on another decreases the intermolecular repulsion. The mean field approximation ignores this effect, so that it predicts too small a correlation length. Marčelja obtained V_o from the vaporization enthalpy of n-alkanes, so that the potential implicitly assumes the gauche bonds to be clustered. Though this effective V_o compensates for the neglect of correlations when studying single molecules, it also precludes accurate study of the correlations. However, this is probably not

the important error, as we will next see.

A crucial assumption of Marčelja's is that S_γ is the order parameter mediating protein interactions; S_α was implicitly fixed at 1. However, the available evidence suggests that S_α is the relevant one. In particular, we will see that: 1) the claim that S_γ controls membrane thickness leads to an extreme overestimate of the Young modulus; 2) among polymers and liquid crystals in general, Y is comparable to that in membranes when it is controlled by molecular orientation, but not when by conformation; 3) S_α cannot be ignored in descriptions of membrane structure and dynamics; and 4) in the only case where a protein effect on membrane thickness has been examined, the change is controlled by hydrocarbon tilt.

D. WHAT CONTROLS THICKNESS?

We first calculate the Young modulus, Y, on the assumption that S_γ controls the thickness, h. We showed earlier that:

$$\frac{Y}{h} = \frac{\partial^2 E_t}{\partial h^2} \quad \text{and} \quad \frac{k_B T}{M_2} - nV_d = \frac{\partial^2 E_\gamma}{\partial S_\gamma^2} \qquad (1$$

where E_t is the thickness energy per unit area and E_γ is the OP energy per C-C bond. Using equation V.B.1, we find:

$$Y = \frac{2h_o}{l^2 n' a^*} \left(\frac{k_B T}{M_2} - nV_d \right) \qquad (2$$

where a* is the area per hydrocarbon chain. This formula neglects the variation of S_γ along the chain. Taking $a^* = 20$ Å^2 and $n' = 15$, we calculate $Y = 1.5 \times 10^{10}$ dy/cm^2, much larger than the observed 5×10^7 dy/cm^2. We conclude that changes in S_γ do not underlie the thinning caused by compression.

Among polymers in general, Y is in the range 10^{10}-10^{11} dy/cm^2 when length changes arise from rotation around bonds[22-25] (i.e. between the primary and secondary relaxations in polyethylene); Y is even larger when bond bending or stretching is involved (i.e. before the secondary relaxation). When Y is controlled by molecular rearrangement (i.e. after the primary relaxation) Y becomes orders of magnitude smaller. In smectic liquid crystals, where changes in

layer thickness are known to reflect tilt changes,[26] $Y \sim 5 \times 10^7$ dy/cm^2. (Our Y is half their $B_\perp$.) Tilt changes are thus a prime suspect for the mechanism of compression-induced thickness changes in membranes.

Most work on membrane statistics has assumed that the hydrocarbon chains are perpendicular to the membrane surface. However, x-ray[27-29] and electron[30] diffraction studies reveal them to be tilted in many lipid phases. In the disordered phase, which was Marčelja's main concern, the average tilt is zero. Even then, its fluctuations are important though. Interpretation of spin relaxation, both of lipid nuclei[12,31] and spin label electrons[32-34], requires consideration of two types of motion: rotational diffusion about an axis, and reorientation of that axis. The former, caused by rotational isomerization, is much faster than the latter, probably tilt fluctuations.[12,32] The amplitude of the latter depends on temperature,[32,33] chemical composition,[34] and curvature.[12] Though we do not yet understand what controls tilt, this work shows its neglect to be unjustified. Indeed, electron microscopic and x-ray diffraction analysis of the interaction of poly-l-lysine with fatty acid bilayers shows that it increases their thickness, via a decrease of hydrocarbon tilt angle.[35] The change in h is roughly .5 nm, consistent with our estimate from E_1.

E. CONCLUSIONS

We have seen that protein interactions and thickness elasticity lead to consistent estimates of n, thus suggesting that our OP is membrane thickness. We also found that the thickness change estimated from E_1 agreed with the one experimental measurement. However, these results refer to such different systems that the conclusion is not definitive. Proof that φ is h would require doing both measurements on the same membrane.

If φ is h, the next question is whether h is changed via lipid conformation or tilt. We showed that the former leads to an implausible prediction for the Young modulus. Work on membrane-like systems also suggests that tilt is the relevant variable. In molecular terms this means that φ is S_α, the tilt OP.

This raises the question of what tilt is. A single gauche bond in a hydrocarbon chain tilts the more distal portion of the chain. Our elasticity analysis implicitly assumed that all gauche bonds occur as parts of kinks (gauche$^+$-trans-gauche$^-$ sequences). If this is incorrect, our calculated Y is an overestimate. It is commonly believed that chain repulsion limits gauche bonds to kinks. However, work on membrane-like systems suggests that this repulsion can be avoided by clustering gauche bonds on adjacent chains[19](i.e. cooperative bending).

If thickness changes did originate this way, Y would be smallest if the bending occurred near the polar region. Repeating the earlier derivation, one finds that Y is multiplied by a factor of roughly 1/n': each gauche bond affects all the other bonds in its chain, not just the adjacent one. A given thickness change thus requires only 1/n' as many gauche bonds as before. Y is still thirty-fold too large, however. We conclude that cooperative bending is not the mechanism of the thickness response to compression. This suggests that the relevant tilt is of entire lipid molecules, rather than of portions.

Our conclusions do not necessarily apply to thickness changes caused by agents other than proteins or compression. Indeed, the accuracy of Marčelja's calculation of membrane thermal expansivity[17] suggests that it is controlled by chain isomerization, at least in the disordered phase.

Our conclusions also do not preclude protein effects on the conformation of adjacent lipids. This too should produce a lipid-mediated interaction. However Marčelja's calculations suggest that its range is less than that of the direct interactions between proteins.

In the interpretation of nuclear spin relaxation, it is controversial whether tilt fluctuations represent cooperative bending, or tilting of entire molecules.[12,31]

Our arguments show that the restoring force for the latter is smaller, so that its amplitude is larger. This is not necessarily relevant, however. The most important fluctuations have a correlation time of about 10^{-7} sec (in the disordered phase of unsonicated lecithin membranes). The issue becomes whether the rigid tilting is this fast. Studies of dielectric breakdown in natural membranes suggest that the electrostrictive time constant is less than a μsec;[5] while measurements of displacement current decay in oxidized cholesterol films reveal one of several msec.[36] If the former is taken as more relevant to synthetic phospholipid bilayers, this suggests that the rigid motions are fast enough to affect NMR spectra, and thus dominate bending.

REFERENCES FOR CHAPTER V

1. S. Marčelja Biochim. Biophys. Acta 455: 1-7 (1976)
2. S. Ohki & C.B. Ohki J. Theor. Biol. 62: 389-407 (1976)
3. O. Alvarez & R. Latorre Biophys. J. 21: 1-17 (1978)
4. J.M. Crowley Biophys. J. 13: 711-724 (1973)
5. H.G.L. Coster & U. Zimmerman J. Membrane Biol. 22: 73-90 (1975)
6. U. Zimmerman, F. Beckers & H.G.L. Coster Biochim. Biophys. Acta 464: 399-416 (1977)
7. J. Requena, D.A. Haydon, & S.B. Hladky Biophys. J. 15: 77-81 (1975)
8. D. Wobschall J. Colloid Interface Sci. 40: 417-423 (1972)
9. J. Seelig Quart. Rev. Biophys. 10: 353-418 (1977)
10. O.H. Griffith & P.C. Jost pp. 453-523 in: "Spin Labelling: Theory and Applications" L.J. Berliner, ed. Academic Press New York 1976
11. H. Schindler & J. Seelig Biochem. 14: 2283-2287 (1975)
12. N.O. Petersen & S.I. Chan Biochem. 16: 2657-2667 (1977)
13. R.E. Jacobs, B.S. Hudson, & H.C. Andersen Biochem. 16: 4349-4359 (1977)
14. H. Schröder J. Chem. Phys. 67: 1617-1619 (1977)

15. R. Blinc, S. Lugomer, & B. Žekš Phys. Rev. A9: 2214-2219 (1974)

16. D. Chapman Quart. Rev. Biophys. 8: 185-235 (1975)

17. S. Marčelja Biochim. Biophys. Acta 367: 165-176 (1974)

18. P.E. McMahon, R.L. McCullough, & A.A. Schlegel J. Appl. Phys. 38: 4123-4139 (1967)

19. G. Lagaly Angew. Chem. Int. Ed. Engl. 15: 575-586 (1976)

20. W. Pechold, E. Liska, H.P. Grossmann, & P.C. Hägele Pure Appl. Chem. 46: 127-134 (1976)

21. M.B. Jackson Biochem. 15: 2555-2561 (1976)

22. L. Holliday & J.W. White Pure Appl. Chem. 26: 545-582 (1971)

23. G.E. Roberts & E.F.T. White chapter 3 of: "The Physics of Glassy Polymers" R.N. Haward, ed. John Wiley & Sons New York 1973

24. N. Saito, K. Okano, S. Iwayanagi, & T. Hideshima in "Solid State Physics" F. Seitz & D. Turnbull, eds. 14: 344-502 Academic Press New York 1963

25. N.G. McCrum, B.E. Read, & G. Williams "Anelastic and Dielectric Effects in Polymeric Solids" John Wiley & Sons New York 1967

26. R. Ribotta & G. Durand J. de Phys. 38: 179-204 (1977)

27. R.P. Rand, D. Chapman, & R. Larsson Biophys. J. 15: 1117-1124 (1975)

28. A. Tardieu, V. Luzzati, & F.C. Reman J. Mol. Biol. 75: 711-733 (1973)

29. G.W. Brady & D.B. Fein Biochim. Biophys. Acta 464: 249-259 (1977)

30. S.W. Hui Chem. Phys. Lipids 16: 9-18 (1976)

31. M.P.N. Gent & J.H. Prestegard J. Mag. Res. 25: 243-262 (1977)

32. H. Schindler & J. Seelig J. Chem. Phys. 59: 1841-1850 (1973)

33. J. Israelachvili, J. Sjösten, L.E. Eriksson, M Ehrström, A. Gräslund, & A. Ehrenberg Biochim. Biophys. Acta 382: 125-141 (1975)

34. M.A. Hemminga J. Mag. Res. 25: 25-45 (1977)

35. T.J. McIntosh, R.C. Waldbillig, & J.D. Robertson Biochim. Biophys. Acta 466: 209-230 (1977)

36. D.F. Sargent J. Membrane Biol. 23: 227-247 (1975)

the transition,[31] Δ should be different in the two phases. The aggregation tendency is Δ-dependent, so that it too can change at the transition. Furthermore, proteins shift the mean OP from φ_o towards $\bar{\varphi}$, thus decreasing its difference between the phases. This weakens and shifts the transition. These effects clearly resemble nature at least superficially. We will see, however, that the agreement is also quantitative.

It is sufficient for our purposes to describe the transition in general thermodynamic terms. Previously, the Gibbs free energy density of each phase was $g=g^o+\epsilon(\varphi)$, where $\epsilon=0$ when $\varphi=\varphi_o$. However, there are two possible equilibrium states near the transition: ordered, "O", and disordered, "D". We henceforth distinguish between them with the subscripts O and D when appropriate.

The transition in protein-free membranes occurs when $g_t=g_D^o-g_O^o=0$. Near there:

$$g_t \sim \frac{\partial g_t(T_t)}{\partial T}(T-T_t) = g'(T-T_t) \qquad (1$$

where T_t is the transition temperature. The O phase is the low temperature one, so that $g'<0$.

In the presence of proteins $\langle\epsilon\rangle \neq 0$ at equilibrium, where brackets denote an average over protein arrangements. We showed in section II.B.2 that:

$$\langle\epsilon\rangle = 2K_2 m\Delta^2 \qquad (2$$

with:

$$m = \frac{1 + \eta^2/8\pi\rho}{(1 + \eta^2/2\pi\rho)^2} \qquad (3$$

The transition now occurs when $g_t + \xi_t = 0$, where $\xi_t = \langle\xi_D\rangle - \langle\xi_0\rangle$. Solving this yields T_p, the transition temperature in the presence of proteins.

We are also interested in $\varphi_p = \langle\varphi\rangle_D - \langle\varphi\rangle_0$, where $\langle\varphi\rangle_x$ is the mean value of φ in a protein-containing phase x. We showed in section II.B.3 that:

$$\langle\varphi\rangle_x = \varphi_x + \frac{\Delta_x}{1 + \eta_x^2/2\pi\rho} \qquad (x="0","D") \quad (4$$

where φ_x is φ_0 in phase x. φ_p is the discontinuity of $\langle\varphi\rangle$ across the transition. We will see that φ_p is roughly proportional to the transition enthalpy, the usually measured quantity. This equation will be used to predict protein effects on the transition extent.

The effect of proteins on the transition is generally complicated by their aggregation. It is necessary to repeat our analysis separately for the protein-rich and -poor regions.

This theory allows us to obtain η from calorimetry. We will find that the result agrees with previous measurements.

We will also see that our predictions about T_p are consistent with experiment. The theory

allows us to predict the phase diagrams of protein-lipid mixtures.

Protein segregation between coexisting lipid phases is controlled by the self energy, E_1. The free energy change when a particle is transferred between phases roughly equals the change in E_1. We showed in equation II.A.5 that:

$$E_1 = \pi K_1 \Delta^2 \qquad (5$$

We can use this to calculate protein partition coefficients.

B. PROTEIN EFFECTS

We start by studying how proteins affect the transition when they are stable against precipitation. Combining equations A.1 through A.3, we find:

$$T_p - T_t = -\frac{2}{g'}\left(K_{2,D}\, m_D\, \Delta_D^2 - K_{2,0}\, m_0\, \Delta_0^2\right) \quad (1$$

$$= D_s\, \varphi_t^2\, m_0\, \delta \quad (2$$

where $\varphi_t = \varphi_D - \varphi_0$, $D_s = -2K_{2,0}/g'$, and

$$\delta = 1 - \frac{2\Delta_0}{\varphi_t} + \left(\frac{\Delta_D}{\varphi_t}\right)^2\left(\frac{K_{2,D}\, m_D}{K_{2,0}\, m_0} - 1\right) \quad (3$$

We first make the approximation, justified only by the success of the theory, that the change of $\langle\varepsilon\rangle$ across the transition is controlled by the change in Δ . We thus assume that $K_{2,D}=K_{2,0}$ and $m_D=m_0$, so that:

$$\delta = 1 - 2\Delta_0/\varphi_t = -1 - 2\Delta_D/\varphi_t \quad (4$$

An important result is the sign of T_p-T_t. When it, and thus δ, are negative, $\bar{\varphi}$ is closer to φ_D than to φ_0. T_p is thus lowered by proteins which force the OP closer to its disordered value than to its ordered one. One would expect this even without the mathematics.

m becomes $\pi\rho/2\pi^2$ when $\rho \ll \pi^2/2\pi$, so that $T_p-T_t = D_s\varphi_t^2\pi\rho\delta/2\pi^2$. We thus predict that the transition shift is proportional to ρ for small ρ , but saturates as it is

raised. However, other factors complicate this behavior: the transition can be eliminated by proteins, and it occurs at different temperatures inside and outside protein aggregates.

We first consider the observability of the transition. Experimentally,[10,12,13] proteins are known to broaden it, thus obscuring it. This is controlled by thermal fluctuations of the OP, which we are ignoring. Proteins can also eliminate the transition by reducing the OP discontinuity there. This jump is φ_t in the absence of proteins, but becomes φ_p when they are present. Equation A.4 shows that:

$$\varphi_p = \frac{\varphi_t}{1 + 2\pi\rho/n^2} \qquad (5$$

It can be seen that proteins have little effect when $\rho \ll n^2/2\pi$, but reduce the discontinuity at higher densities.

When the proteins form a precipitate, lipids within it behave differently than those outside. The analysis depends on whether aggregation occurs in both phases or only in one, so that we first need to predict which happens.

The aggregation tendency is controlled by $\pi\rho/n^2$ and E_1/k_BT, as discussed in section II.B.4. When $\pi\rho/n^2 > 1/7$, there exists some E_s such that proteins precipitate if $E_1 > E_s$, or equivalently, if $|\Delta| > \Delta_s = \sqrt{E_s/\pi K_1}$. We have assumed that the protein effect on the transition arises

entirely from the difference between φ_0 and φ_D, so that Δ_s is the same in both phases. The criteria for aggregation take the simple form shown in figure 14. The most common behavior, precipitation only in the ordered phase, means that $\bar{\varphi}$ is closer to φ_D than to φ_0.

We now study the lipid phase behavior in each of the regions of figure 14. Suppose that the protein concentration is ρ_e within the clusters, and that its mean is ρ , with $\rho < \rho_e$. The clusters thus occupy ρ/ρ_e of the membrane. We assume they contain all the proteins, so that m=0 outside them, but $m \sim 1$ within them.

Equations 2, 4, and 5 remain valid when the clusters are present in both phases. If we ignore propagation of protein effects away from the clusters, then $T_p = T_t$ and $\varphi_p = \varphi_t$ outside them. The transition is thus unperturbed there. On the other hand, $\varphi_p \sim 0$ within the clusters: the transition is eliminated there. One typically measures the ρ-dependence of F, the fraction of the unperturbed transition remaining. F is thus the proportion of the lipids outside the precipitate.

Next consider the case where the proteins precipitate only in one phase, say the ordered one. As the aggregation state changes, the protein concentration at each point does too. Equation 4 thus becomes an invalid approximation for δ. Instead, $m_0 \sim 1$ and:

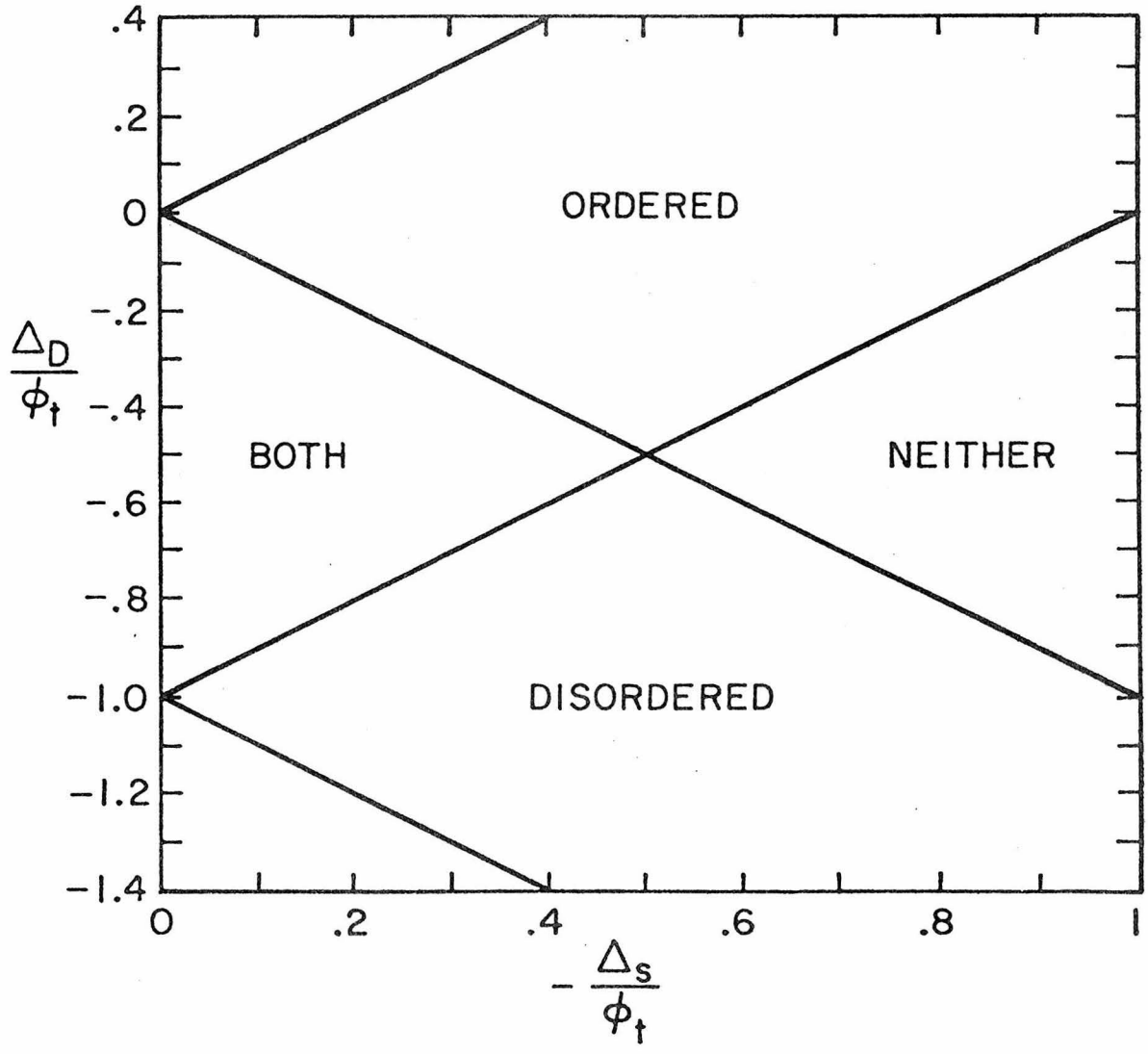

14. Which phases the proteins precipitate in. Note that Δ_d/φ_t is -1 when $\bar{\varphi} = \varphi_0$, and 0 when $\bar{\varphi} = \varphi_D$. Also, membranes with dilute proteins lie to the right.

$$m_0 \delta \sim 1 - \frac{2\Delta_0}{\varphi_t} + \left(\frac{\Delta_D}{\varphi_t}\right)^2 (m_D - 1) \qquad (6$$

within the clusters. However, $\Delta_D = \Delta_0 - \varphi_t$ and $m_D \ll 1$, so that equation 2 becomes:

$$T_p - T_t = -D_s \Delta_0^2 \qquad (7$$

In contrast, $m_0 = 0$ outside the clusters:

$$T_p - T_t = D_s m_D \Delta_D^2 \qquad (8$$

there.

We know that $\Delta_D^2 < \Delta_0^2$ because the proteins precipitate only in the ordered phase, while $m_D < 1$ by definition. We thus find that the transition is split into perturbed and unperturbed ones, the former occuring at lower temperature. The shift of the unperturbed transition is less than its width,[12] which accounts for its misleading name. The signs of the shifts reflect the change of protein concentration at each point during the transitions. Opposite signs would be found if aggregation were limited to the disordered phase.

We next study the OP discontinuity across the unperturbed transition:

$$\langle \varphi \rangle_D - \varphi_0 = \varphi_t + \frac{\Delta_D}{1 + \pi^2/2\pi\rho} \qquad (9$$

When $\rho \ll \pi^2/2\pi$, this becomes φ_t, its value in the absence of proteins. It becomes Δ_0 when $\rho \gg \pi^2/2\pi$. This too

would be expected: it means that the OP goes from Φ_0 below the transition to $\overline{\Phi}$ above, since the proteins are then everywhere. One similarly finds the OP discontinuity of the perturbed lipids:

$$\langle\Phi\rangle_D - \langle\Phi\rangle_0 = \frac{-\Delta_D}{1 + 2\pi\rho/\eta^2} \qquad (10$$

This is tiny when $\rho \gg \eta^2/2\pi$. On the other hand, the clusters occupy only a small fraction of the membrane unless $\rho \sim \rho_e$. When $\rho_e \gg \eta^2/2\pi$, it will thus be difficult to see the perturbed transition, except with techniques which respond primarily to the proteins or lipids adjacent to them.

Let us now unify these various cases. We are interested in the dependence of the transition behavior on protein concentration. We assume that the experimental technique for measuring F is sensitive to the OP discontinuity times the proportion of lipids involved. The amount of transition is Φ_t in the absence of proteins. When they are very dilute, it is given by equation 5, roughly $\Phi_t(1 - 2\pi\rho/\eta^2) = \Phi_t F$. Both the amount of transition and its temperature thus depend linearly on ρ. An important prediction is that F depends on the number of protein particles, but not on any other property of them.

As ρ grows, the stability limit of the ordered phase is eventually reached. The observed transition then arises

from the protein-poor regions. They contain $1-A\rho/\rho_e$ of the lipids, where A is the area fraction of the clusters occupied by lipids. Using equation 9, we find:

$$F = \left(1 + \frac{\Delta_D/\Phi_t}{1 + \eta^2/2\pi\rho}\right)(1 - A\rho/\rho_e) \qquad (11$$

Its numerical value is shown in figure 15.

With further increases of ρ, the proteins may precipitate in both phases. Then the transition is truly unperturbed in the protein-poor regions, so that F is just the second factor of equation 11.

The transition is most strongly perturbed when there is no aggregation. This would be expected: all the lipids are then affected because the proteins are everywhere. Precipitation confines them to part of the membrane, thus decreasing their effect.

So far we have assumed that the aggregation tendency is greater in the ordered phase. When it is greater in the disordered one, F is still given by equation 11, except that Δ_D is replaced with $-\Delta_0$.

We seek to determine η from experimental measurements of F. This requires evaluation of the other parameters in equation 11, which we next do.

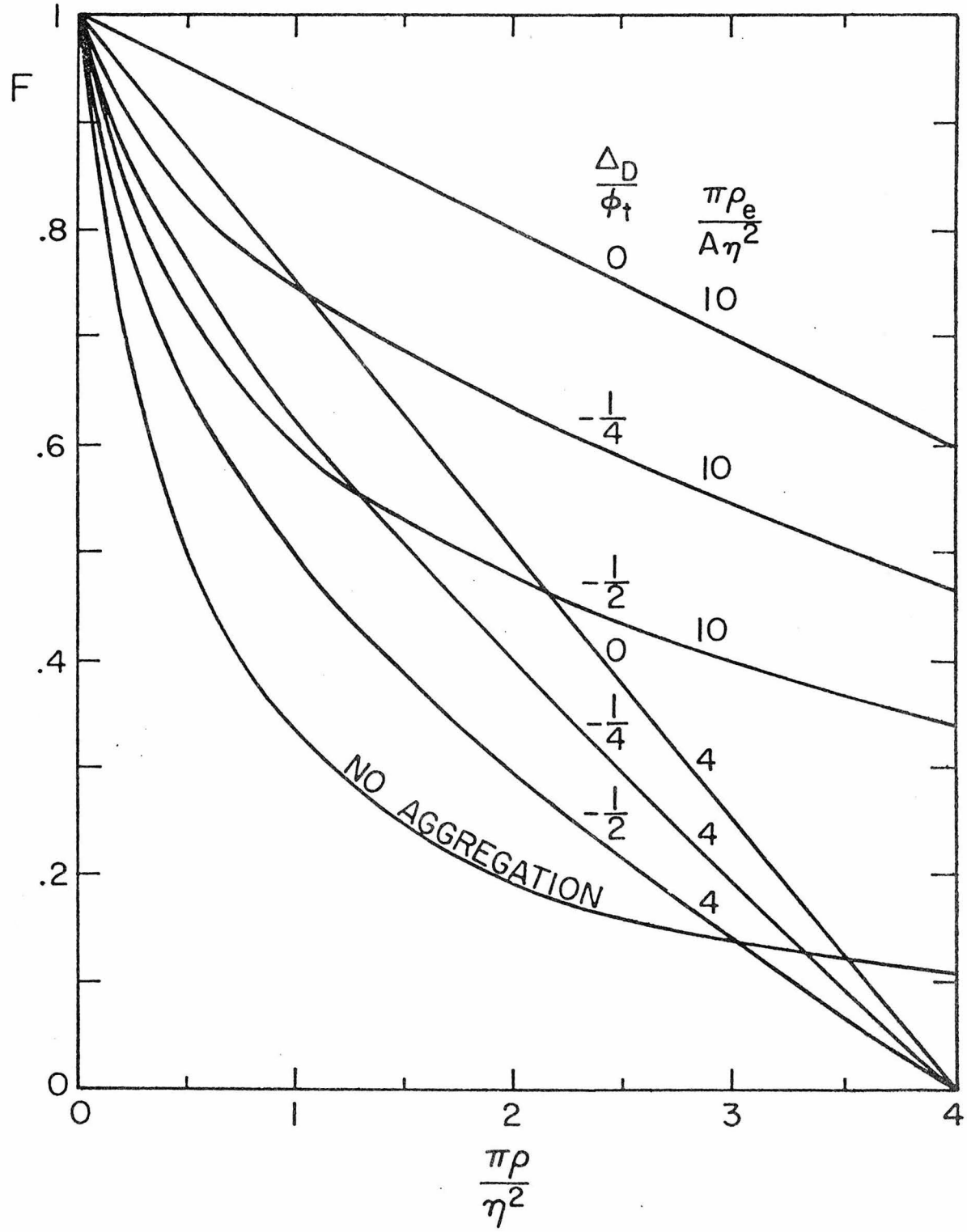

15. Dependence of F on $\pi\rho/\eta^2$.

C. MEASUREMENT OF η

Graphs of F versus ρ are usually thought to show that each protein particle eliminates the phase transition in a region of area $M=-\partial F/\partial \rho$. Its width, roughly $(M/2\pi)^{\frac{1}{2}}=w$ is commonly called the range of the protein effect. Equation B.5 shows that $w=\eta^{-1}$ in the absence of aggregation, but we will see that $w<\eta^{-1}$ when there is. This justifies our earlier claim that w is only a lower bound for η^{-1}.

Using equation B.11 to evaluate M at $\rho=0$, we find:

$$M = \frac{A}{\rho_e} - \frac{\Delta_D}{\varphi_t}\,\frac{2\pi}{\eta^2} \qquad (1$$

so that:

$$\eta^{-1} = \left(\frac{M - A/\rho_e}{-2\pi\,\Delta_D/\varphi_t} \right)^{\frac{1}{2}} \qquad (2$$

We will determine the right hand side from experiment, and check if the result is consistent with our earlier measurements of η^{-1}.

Most workers have measured not M, but rather m, the number of lipid molecules perturbed by each protein molecule. $M=nma^*$, where a^* is the area per lipid molecule, and n is the number of protein molecules per particle. Particle formation has usually been neglected, however, so that M is underestimated. Unfortunately, n is generally unknown, so that we cannot correct this error.

This problem was avoided by Romans and Segrest[36] in work on proteolytic fragment T(is) of glycophorin: both ρ and F were measured.[36] One can calculate from their data that M=250 nm^2. A/ρ_e is harder to get. However, they[36] assembled membranes with ρ at least $6000/\mu m^2$, which is thus a lower bound for ρ_e. A=3/4 at that density if the apparent edges of particles in freeze-fracture pictures are the actual ones. φ_t is roughly -1 nm if the OP is membrane thickness.[31] In chapter V, we estimated that Δ_D is $\frac{1}{4}$ to $\frac{1}{2}$ nm. Substituting into equation 2, we find $\pi^{-1} \sim$ 6.5-8.2 nm. This compares to the previous values, 8-14 nm and 10-14 nm. Our assumed ρ_e is an underestimate, so that the present value of π^{-1} is too. We conclude that all three appraisals of π^{-1} agree, despite the use of different membranes for each. This strengthens confidence that the theory is more than mere curve fitting.

We have assumed that T(is) aggregates in the ordered phase, and only there. This claim is based on studies of glycophorin,[37] which does behave that way. If T(is) does not aggregate, then π^{-1} would be 6.5-7 nm. Figure 15 shows why the correction would be minor: T(is) corresponds to the case $\pi\rho_e/A\pi^2 \sim 1.2$. F is determined mainly by the protein perturbation of the disordered phase, so that it is not very important what happens in the ordered one.

The arguments used in chapter V to estimate Δ_D are insensitive to its sign. We assumed it to be positive,

however. The justification can be seen by studying equation 1: A/ρ_e is 125 nm^2, which is smaller than M. Δ_D and Φ_t must thus have opposite signs. This means that $\bar{\Phi}$ is between Φ_0 and Φ_D.

Figure 15 might lead one to expect that graphs of F versus ρ should be curved. The result is generally linear though. This is not surprising when one notes that $\pi\rho/\eta^2$ is generally less than two; in the T(is) study, it was less than one. The curvature is thus slight.

We have neglected any dependence of particle structure on protein concentration. For instance, T(is) is not multimeric when there is sufficiently little of it.[38] F then depends more strongly on the amount of protein than when it is multimeric. This is expected, because there are more particles per amount of protein in the former case. It is unknown if T(is) is oligomeric then, so that we considered only the latter case. Without microscopy, the bend could have been mistaken for the predicted curvature.

This problem is illustrated by a recent study of gramicidin perturbation of the phase transitions of various lecithins.[13] It was found that F depended non-linearly on ρ, qualitatively resembling the curves of figure 15. This result was believed to show the onset of aggregation: a reasonable conclusion if there were a sharp border between the perturbed lipids and the rest. However, gramicidin

is much smaller than genuine proteins, so that ρ could become much larger than with the latter. Even without aggregation, saturation of the perturbation would yield curvature. Unfortunately, gramicidin does not form visible particles. The question of its aggregation remains unsolved.

D. THERMODYNAMIC ASPECTS

We now return to several topics previously glossed over. We start with a quantitative discussion of the perturbed transition. We next discuss the phase diagrams of protein-lipid systems. Finally, we reconsider several of our approximations.

We seek to calculate the transition temperatures, given by equations B.2, 7, and 8. Our first task is to evaluate D_s. g' is the transition entropy, $\Delta s = s_0 - s_D$, if we neglect the difference between the heat capacities of the two phases. A typical value[18] for Δs is -28 cal/K°-M. Combining this with our earlier estimate, $K_2 = 2\text{-}6 \times 10^{13}$ dy/cm^3, we find $D_s = \frac{1}{2}\text{-}2$ K°/nm^2.

Typically, $0 < m < \frac{1}{2}$, $-\frac{1}{2} < \delta < 0$, and $\varphi_t \sim -1$ nm. Equation B.2 thus shows that the transition temperature changes less than a degree unless there is aggregation. When there is, equations B.7 and B.8 show that the unperturbed transition moves even less, while the perturbed one shifts several degrees. These are only crude estimates, due to the inaccuracy of our values for Δ_D and Δ_0. We will see, however, that they are consistent with nature.

We previously assumed that the observed transition was entirely the unperturbed one. If the total transition is measured, without separation of its components, misleading results will be obtained unless the perturbation eliminates

the transition, rather than just shifting it. The discussion of equation B.10 shows that this occurs when $\Delta_D/\Phi_t \ll 1$ or $2\pi\rho_e/n^2 \gg 1$.

This point is demonstrated by recent work with myelin proteolipid apoprotein (PLA). Early calorimetric studies suggested that each protein perturbed m=15 lipid molecules.[10] However, later higher resolution work showed that the transition split into two components, about 2 degrees apart.[12] When only the unperturbed transition is included, the result is m=142. The perturbed one occurs at higher temperature. Our model thus predicts that PLA aggregates preferentially in the disordered phase. This remains untested, though.

More typical behavior is shown by sarcoplasmic reticulum (SR) ATPase, which precipitates only in the ordered phase. Only an unperturbed transition is found when bulk lipid behavior is examined, while measurements of enzyme activity reveal a perturbed one about 10° C lower.[2] A phase diagram of SR ATPase and lipids has been presented.[39] It qualitatively agrees with our predictions about the splitting of the transition. The membrane consists of a single disordered phase at temperatures above the upper transition. Between it and the lower one, there is an ordered, protein-poor phase and a disordered, protein-rich one. The latter becomes ordered when cooled through the lower transition.

There seems, at first sight, to be a conflict. Kleemann and McConnell[39] claim that the upper transition temperature is more ρ-dependent than the lower one, while we predict the opposite. Their own analysis, however, shows their phase diagram to be misleading. They measured f', the partition coefficient of a spin label between the membrane and water. Transitions were assumed to occur at bends in graphs of f' versus temperature. They showed that their results are explicable as an increase of n^{-1} near the transition. This enlarges the annulus, thus producing a bend in f' versus T. This occurs near, but not at, the transition temperature. The ρ-dependence is thus only apparent, as is the conflict with our predictions or with the previous measurements.[3]

Studies of membrane enzyme kinetics in Escherichia coli have shown that lipids adjacent to proteins undergo their transition at temperatures below that of the rest.[5] As would be expected from our model, those proteins aggregate only in the ordered phase. This shows that they have greater affinity for disordered than for ordered lipids. The enthalpy change when a protein particle is transferred between the phases is $E^*=E_{1,D}-E_{1,O}=\pi K_1 \delta \varphi_t^2$. We have ignored the ρ-dependence of the effective E_1. The error affects mainly $E_{1,D}$, because the proteins are mostly in the disordered phase. $E_{1,D}$ is small, however, so that the error

is too. Using the previous estimates, K_1=20 dy/cm and φ_t=-1 nm, we have E*=9δ kcal/M (of particles). We also estimated that $-\frac{1}{2} < \delta < 0$, so that -4.5 kcal/M < E* < 0. The experimental results[5] have been expressed as a partition coefficient, k=exp(-E*/RT), typically between 2 and 10. Thus -E* is .4-1.4 kcal/M, consistent with the theory.

We have assumed that E* is the Gibbs free energy of transfer. This ignores the ideal entropy and OP-independent interactions. The former is unimportant when E* is large compared with RT, clearly a marginal assumption. Present knowledge is insufficient to estimate the latter. However, the measurements of E* are so crude that it is not obvious whether the errors matter. They would affect our predictions about T_p-T_t and E*, but not F.

We have also assumed that the transition enthalpy is proportional to the OP discontinuity. This is reasonable if there is only one independent OP. In general though, there is no reason to expect any simple relation between the OP and the enthalpy. The success of the theory is the only reason to believe this approximation.

E. CONCLUSIONS

We have seen that studies of protein effects on lipid phase transitions reveal much about the structure of the perturbed annulus. We now review this, and then consider what it says about our model.

Most basic is the size of the annulus. Though it has no sharp boundary, η^{-1} is a rough estimate of its width, w. As shown earlier, w is underestimated when particle formation and clustering are ignored. Further error may result from the assumption that the transition is eliminated in the annulus. Calorimetric determinations of w are thus highly suspect unless the particle concentration and aggregation state are measured, and only the unperturbed transition is included in F. Avoiding these errors, we found that w or η^{-1} is 6-8 nm. This is much larger than commonly believed, roughly 1 nm, but consistent with our earlier measurements.

Another prevalent notion is that the annulus is frozen in the ordered state. We have shown this to be ruled out by the observations that proteins have greater affinity for disordered lipids and that the perturbed transition is observable, though weakened. Proteins constrain the nearby lipids to some state between the ordered and disordered ones, closer to the latter.

The ability of the model to unify seemingly unrelated

phenomena is shown by the agreement between measurements of n based on calorimetry, protein clustering, and elasticity. Furthermore, the successful estimation of E^* and $T_p - T_t$ from information about elasticity supports the identification of our OP with membrane thickness. Though many aspects of the model remain untested, these results show it to be at least approximately correct.

REFERENCES FOR CHAPTER VI

1. H.K. Kimelberg & D. Papahadjopoulos J. Biol. Chem. 249: 1071-1080 (1974)
2. C. Hidalgo, N. Ikemoto, & J. Gergely J. Biol. Chem. 251: 4224-4232 (1976)
3. T.R. Hesketh, G.A. Smith, M.D. Houslay, K.A. McGill, N.J.M. Birdsall, J.C. Metcalfe, & G.B. Warren Biochem. 15: 4145-4151 (1976)
4. A. Stier & E. Sackmann Biochim. Biophys. Acta 311: 400-408 (1973)
5. L. Thilo, H. Trauble, & P. Overath Biochem. 16: 1283-1290 (1977)
6. J.M. Boggs, W.J. Vail, & M.A. Moscarello Biochim. Biophys. Acta 448: 517-530 (1976)
7. M.A. Hemminga & J.F.M. Post Biochim. Biophys. Acta 436: 222-234 (1976)
8. Y.S. Chen & W.L. Hubbell Exp. Eye Res. 17: 517-531 (1973)
9. C.F. Fox pp.279-306 in "Biochemistry of Cell Walls and Membranes" C.F. Fox, ed. Butterworths London 1975
10. D. Papahadjopoulos, W.J. Vail, & M. Moscarello J. Membrane Biol. 22: 143-164 (1975)
11. H. Trauble & P. Overath Biochim. Biophys. Acta 307: 491-512 (1973)

12. W. Curalto, J.D. Sakura, D.M. Small, & G.G. Shipley Biochem. 16: 2313-2319 (1977)

13. D. Chapman, B.A. Cornell, A.W. Eliasz, & A. Perry J. Mol. Biol. 113: 517-538 (1977)

14. W. Kleemann & H.M. McConnell Biochim. Biophys. Acta 345: 220-230 (1974)

15. E. Schechter, L. Letellier, & T. Gulik-Krzywiki Eur. J. Biochem. 49: 61-76 (1974)

16. F. Wunderlich, D.F.H. Wallach, V. Speth, & H. Fischer Biochim. Biophys. Acta 373: 34-43 (1974)

17. V. Luzzati & A. Tardieu Ann. Rev. Phys. Chem. 25: 79-94 (1974)

18. D. Chapman Quart. Rev. Biophys. 8: 185-235 (1975)

19. H. Schindler & J. Seelig Biochem. 14: 2283-2287 (1975)

20. R.E. Jacobs, B.S. Hudson, & H.C. Andersen Biochem. 16: 4349-4359 (1977)

21. G.W. Brady & D.B. Fein Biochim. Biophys. Acta 464: 249-259 (1977)

22. A. Tardieu, V. Luzzati, & F.C. Reman J. Mol. Biol. 75: 711-733 (1973)

23. F. Caron, L. Mateu, P. Rigny, & R. Azerad J. Mol. Biol. 85: 279-300 (1974)

24. J.L. Ranck, L. Mateu, D.M. Sadler, A. Tardieu, T. Gulik-Krzywicki, & V. Luzzati J. Mol. Biol. 85: 249-277 (1974)

25. P.N. Yi & R.C. McDonald Chem. Phys. Lipids 11: 114-134 (1973)

26. H. Trauble & D.H. Hayes Chem. Phys. Lipids 7: 324-335 (1971)

27. R. Mendelson, S. Sunder, & H.J. Bernstein Biochim. Biophys. Acta 413: 329-340 (1975)

28. N. Yellin & I.W. Levin Biochem. 16: 642-647 (1977)

29. M.J. Janiak, D.M. Small, & G.G. Shipley Biochem. 15: 4575-4580 (1976)

30. B.P. Garber & W.L. Peticolas Biochim. Biophys. Acta 465: 260-274 (1977)

31. R.P. Rand, D. Chapman, & K. Larsson Biophys. J. 15: 1117-1124 (1975)

32. S.H.-W. Wu & H.M. McConnell Biochem. 14: 847-854 (1975)

33. S. Mabrey & J.M. Sturtivant Proc. Nat. Acad. Sci. USA 73: 3862-3866 (1976)

34. P. Overath & H. Trauble Biochem. 12: 2625-2634 (1973)

35. D.L. Melchoir, H.V. Morowitz, J.M. Sturtivant, & T.Y. Tsong Biochim. Biophys. Acta 219: 114-122 (1970)

36. A.Y. Romans & J.P. Segrest pp.191-197 in "Cellular Neurobiology" Z. Hall, R. Kelly, & C.F. Fox, eds. Alan R. Liss, Inc. New York 1977

37. C.W.M. Grant & H.M. McConnell Proc. Nat. Acad. Sci. USA 71: 4653-4657 (1974)

38. J.P. Segrest, T. Gulik-Krzywicki, & C. Sardet
Proc. Nat. Acad. Sci. USA 71: 3294-3298 (1974)

39. W. Kleemann & H.M. McConnell Biochim. Biophys. Acta
419: 206-222 (1976)

VII. THE BIG PICTURE

We originally set out to explain why membrane proteins sometimes precipitate. We picked the simplest plausible field theory, and found its predictions reasonable. This would not be very convincing by itself, given the many steps separating our assumptions from their experimental tests. Though modelling lipids, we looked only at the proteins. The order parameter thus remained a hypothetical construct. We even lacked reason to believe that it described lipids, rather than water or proteins outside particles.

We next saw that the predicted OP behavior coincides with that of membrane thickness. This shows the model to be not just an explanation of protein aggregation, but also a consequence of our knowledge about thickness elasticity.

It has previously been assumed that hydrocarbon conformation underlies lipid-mediated forces. This leads, however, to a serious underestimate of their range. We showed that the membrane Young modulus is vastly too small for compression-induced thinning to arise from conformational changes. Lipid tilt is the only other obvious possibility. Though proteins might affect lipid conformation, it is tilt which mediates their interactions.

We next supplemented the model with a general thermodynamic description of lipid phase transitions.

Protein rearrangement near them and influence on them followed from the model. The predictions appear reasonably consistent with nature, though the murkiness of present experimental knowledge prevents definitive comparison. Despite this, we showed that the perturbed annulus surrounding proteins is far larger than commonly believed. Furthermore, its lipids resemble the disordered state more than the ordered one. The experiments typically thought to prove the opposite actually show only that the ordering increases there.